OUKA
Osaka University Knowledge Archive

Title	VSION-BASED ON-CHIP CELL MANIPULATION
Author(s)	Uvet, Huseyin
Citation	大阪大学, 2010, 博士論文
Version Type	VoR
URL	https://hdl.handle.net/11094/23494
rights	
Note	

Osaka University Knowledge Archive : OUKA

https://ir.library.osaka-u.ac.jp/

Osaka University

工學 1430A

VISION-BASED ON-CHIP CELL MANIPULATION

HUSEYIN UVET

MARCH 2010

VISON-BASED ON-CHIP CELL MANIPULATION

A dissertation submitted to

THE GRADUATE SCHOOL OF ENGINEERING SCIENCE

OSAKA UNIVERSITY

in partial fulfillment of the requirements for the degree of

DOCTOR OF PHILOSOPHY IN ENGINEERING

BY

HUSEYIN UVET

MARCH 2010

OSAKA UNIVERSITY

ABSTRACT

VISION-BASED ON-CHIP CELL MANIPULATION

By HUSEYIN UVET

Chairperson of the Supervisory Committee: Professor TATSUO ARAI
Department of System Innovation

On-chip miniaturized system technology and its applications are extensive. It has significant advantages bringing the benefits of miniaturization, integration and automation to biotechnology related studies. Microfluidic or the Lab-on-a-chip has emerged as a new study area as a result of the increasingly important role of biotechnology in medical science. Microfluidic-based technology offers a novel platform for cellular analyses of biological systems, as the small scale of micro-channels and devices allows producing scalable system architecture. Therefore, microfluidic systems have a major potential for improving the efficiency of techniques applied in cellular based analyses.

Conventional hybrid microfluidic systems have many functions such as separation, sorting and filtering of biological particles. These hybrid systems are required for delivering particles into microfluidic chips and for their dexterous on-chip manipulation. Successful realization of these functionalities requires visual sensing of particles. However, only a limited number of studies are available on on-chip visual sensing techniques as well as on retrieving of living cells into microfluidic devices and their manipulation thereafter.

On-chip manipulation tasks of living cells associated with visual sensing techniques using numerous computer vision methods have vital importance for microfluidic devices. Key requirements in successful implementation of such tasks are real-time cell detection and tracking which are also essential parts of any micro-robotic application. Integration of cell treatment steps with micro-robotics provides a unique platform for single cell analysis and for the study of vital concepts such as cell supply and transportation, cell fusion and nuclear

transplantation. The project "Automated Mammalian Cell Cloning" provides novel approach to overcome difficulties (e.g., expensive and highly inefficient) encountered in cell cloning process. In this project, several manipulation tasks are performed by different on-chip modules accommodated in one single chip. Two important tasks associated with this project are single cell transfer noninvasively and on-chip cell coupling.

In this thesis, two main concepts, i.e. on-chip visual sensing "MicroVision Systems" and on-chip manipulation, and the challenging issues in their realizations are studied. New on-chip MicroVision systems and manipulation techniques with their key applications are reported. The vision-based on-chip cell manipulation technique is applied on several microfluidic tasks. Its efficiency and advantages are shown by testing with different microfluidic cell operations. The novel "vision-based single cell loading &supply" and novel "cell coupling" modules are presented in terms of "Automated Mammalian Cell Cloning" project.

TABLE OF CONTENTS

LIST OF FIGURES

LIST OF TABLES

ACKNOWLEDGMENTS

First of all, I would like to express my sincere gratitude to my supervisor Prof. Tatsuo ARAI for his patience, wise advices, ideas and suggestions and for his strong insistence and high pressure to achieve better work. He has helped me to the utmost of his ability and patient and understanding at all times. I am proud of working under his capable supervision during 5 years. I would like to thank to Prof. Kosuke SATO and Prof. Fumio MIYAZAKI for critical review of my dissertation. I would like to also express my gratitude to Prof. Yasuyuki OKAMURA, Prof. Tadashi ITOH and Prof. Fumihito ARAI from Tohoku University, for their technical assistance and useful discussions.

The work presented in this thesis has been realized with help of number persons, whom I gratefully would like to acknowledge: Asist. Prof. Yoko Yamanishi from Tohoku University who teaching me all clean room processes and micromachining technology. Asist. Prof. Kenichi Ohara for all help and fruitful discussion for my theoretical and experimental works. Hasegawa Akiyuki for the great effort of preparation microfluidic systems and introducing me to microbiology area. Ebubekir Avci, Amr Amdallah and all other Arai Laboratory members for their supports.

This work is supported by the Bio-oriented Technology Research Advancement Institution under the Research and Development Program for New Bio-industry Initiatives.

Dedication

I would like to dedicate this dissertation to my parents who supported and encouraged me throughout my academic career. I would like to also thanks to Mr. Ali Atlamaz for showing infinite patience and the will to always listen to me in the most troublesome moments during my PhD study. The words are too little to describe my thanks to my family and Mr. Ali Atlamaz for their endless support to withstand the challenges of life and work.

Chapter 1: Introduction

1.1 On-chip Biotechnology Applications

1.1.1 Development of Biotechnology and Microfluidic Devices

Technical developments in recent years have proved the biotechnology as one of the fastest growing areas of science. Biotechnology has found applications mostly in medical filed, cell engineering, food science and agriculture field.

In these research fields, high speed high precision, and manipulation of micro-nano size objects are demanded. Conventional robotics applications on biotechnology area became a potential breakthrough. Integration of biotechnological techniques and robotics created a new technology field, so called BioRobotics. Essentials of BioRobotics filed are manipulation technology, micro system technology, sensing techniques and human interface. The history of Biotechnology advancements related with BioRobotics field is given in Figure 1.

Microfluidic technology and its applications are extensive and have made significant advantages bringing the benefits of miniaturization, integration and automation to biotechnology related studies over the past several decades [1][2][3]. Microfluidic-based technology offers a convenient platform for cellular analyses of biological systems, as the small scale of micro-channels and devices allows producing scalable system architecture [4]. Their inexpensive composition makes them a potential candidate for large scale production. Microfluidic technology covers not only the material phenomena but also the technology for manipulating and controlling the components as micro size particles in micro size artificial capillaries. Therefore, microfluidics systems provide a real potential for improving the efficiency of techniques applied in cellular analyses and manipulation.

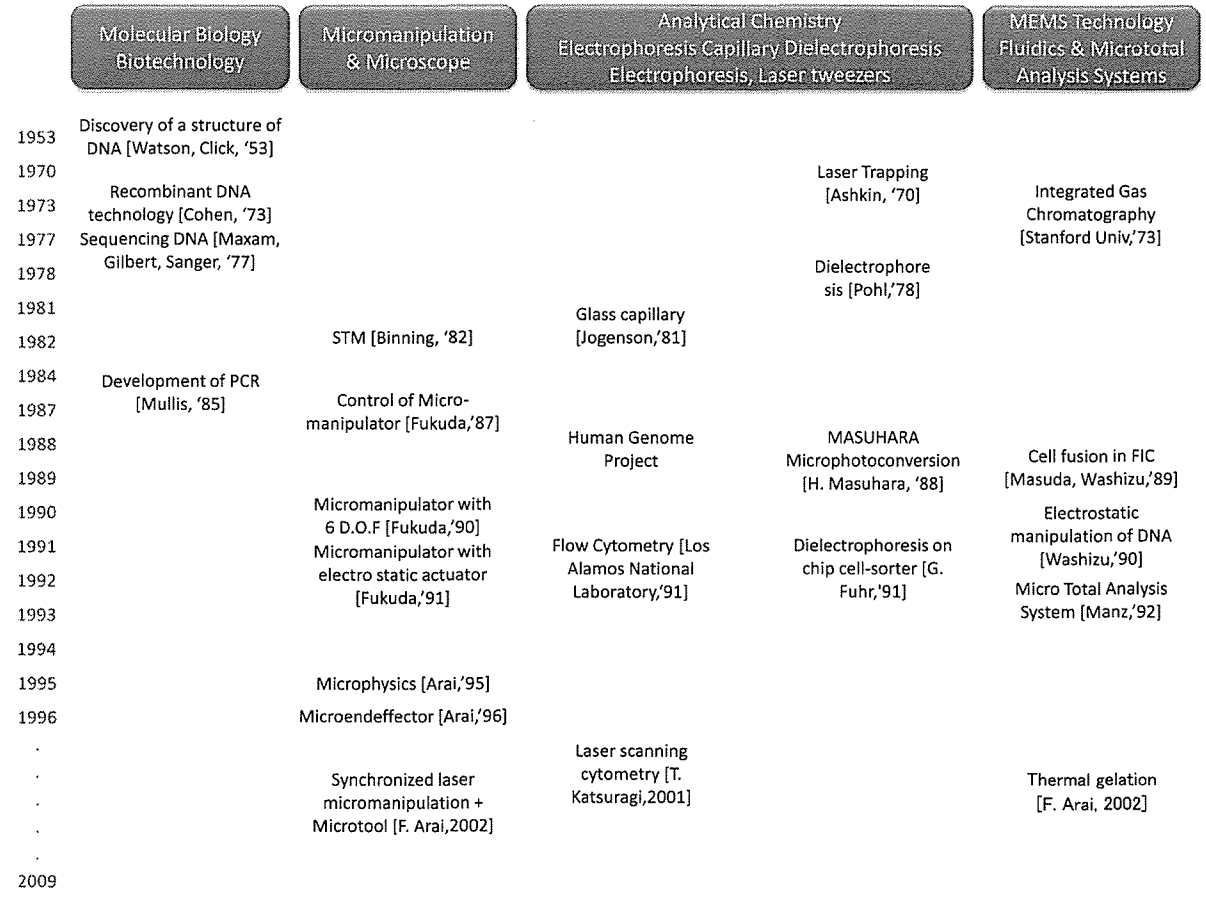

Figure 1, History of the development of the biotechnology and its applications

1.1.2 PDMS-based (Polydimethylsiloxane) Microfluidic Devices

R Recent advancements in micro system technology for biomedical related products such as biosensor, biochip and microfluidic devices may bring adequate solution for the automation of biotechnology. Micro-fabrication techniques on microfluidics structures have already shown to significantly enhance the manipulation of cells [3][4][5]. Especially, soft lithography has been successfully applied to produce microfluidic channel structures in which biological particles can be observed and manipulated. One of the most common elastomer used in soft lithography for biological applications is PDMS (Polydimethylsiloxane), which is non-toxic to living cells and

impermeable to water. Furthermore, cured PDMS has low surface energy preventing specimens in the PDMS microfluidic channel from interacting with it. Besides, optical properties of the PDMS (transparent down to 300nm of wavelength) have key functionality for several kinds of cell monitoring applications [6][7][8]. Therefore, the PDMS has remarkable advantages for prototyping and fabricating a variety of microfluidic mechanisms, which have been used in Lab-on-a-chip (LOC), existed for almost a decade (Figure 2).

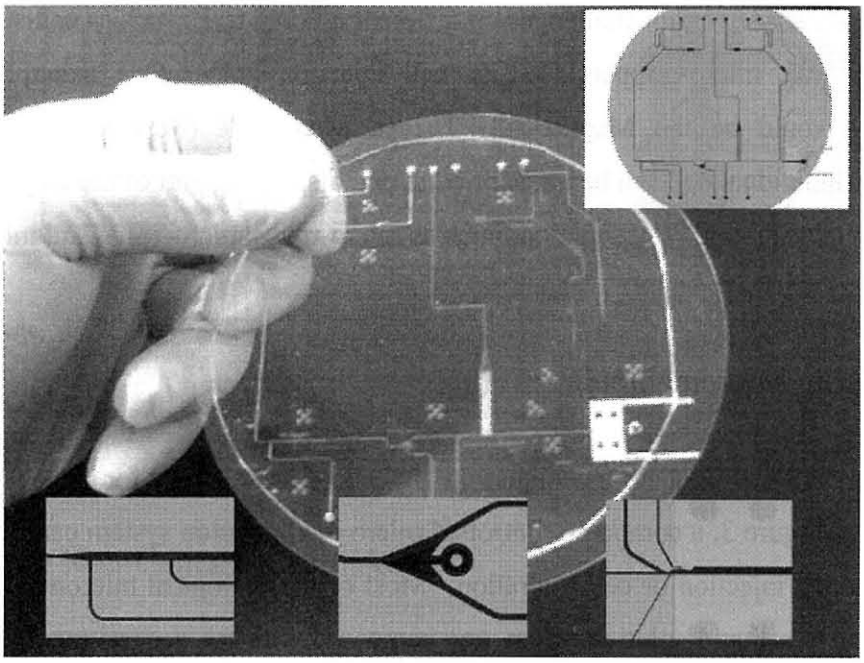

Figure 2, Example of a PDMS Microfluidic chip for Automatic Somatic Cell Cloning

1.2 On-Chip Manipulation

Manipulation task is an important part of BioRobotics applications. The well-known applications are manipulation of a DNA molecule, animal or plant cells. However current research works are not potentially enough to support these tasks. Manipulation techniques can roughly be classified as contact and non-contact types [9][10].

1.2.1 On-chip Contact Manipulation

Conventional microfluidic chips have many functions such as separation, sorting and filtering biological particles. With these systems, biological or chemical particles can be delivered into a chip to required positions for further operations. However limited studies are available on retrieving of the manipulated cells from the chip systematically. Mechanical manipulation of cells on a microfluidic chip must cope with the complex physical properties of biological cells. These properties cause certain challenges on different on-chip tasks such as cell separation [11], cell filtering [12], micro-grippers [13] or cell injection [14]. One example for contact manipulation would be the Magnetically Driven Microtools (MMT) [15]. In this novel technique, an individual cell can be transported to cell dispensing part of the chip. The produced soft MMT provide a number of functions such as micro-rotor, micro-valve and micro-sorter and so on.

1.2.2 Off-chip Micromanipulators

Conventional micromanipulator techniques are the one of the example for contact manipulation. As it shown in Figure 3, a computer-controlled micro manipulation system can perform several tasks such as cell injection or cell aspiration. Most of the biological micromanipulation tasks are performed in a liquid solution. Thus, one compared with the general manipulation task in the air, we have to consider much different kind of forces effecting on the liquid solution which contains biological cells such as the gravity, buoyancy, resistance force from viscosity of the fluid, Brownian motion and interactive forces in the micro/nano world.

Since a size of biological cell is in micro level, it is quite difficult to manipulate freely. Automation of micromanipulation is also quite difficult, thus skilled operator are required in most tasks such as microgripper or the use of a suction tip. In addition, if there is flow in a solution, fluid force relative to flow direction may disturb both cell and suction-tip. And also, if we operate the micromanipulator while observing biological cells under a microscope, it is a hard-task to handle cells sequentially.

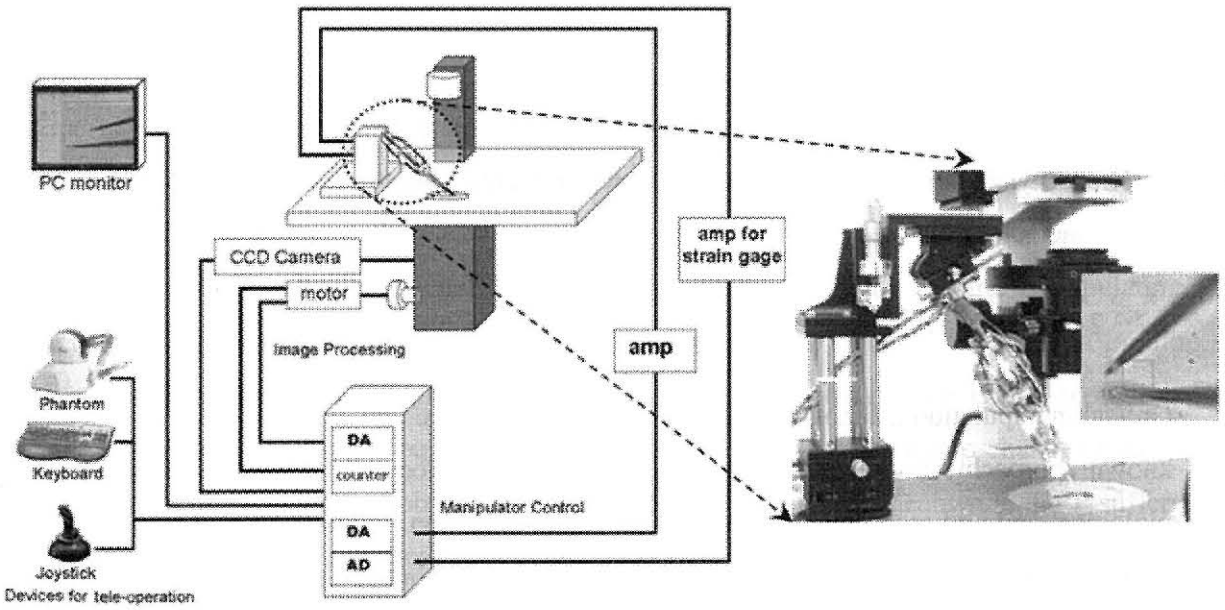

Figure 3, Micromanipulation with a microgripper connected to computer to provide automation

1.2.3 On-chip Non-Contact Manipulation

1.2.3.1 Magnetic Manipulation

The manipulation of micro-nano size magnetic particles attached to cells is referred as magnetic manipulation. This method commonly used for cell separation or purification in microfluidic devices.

All techniques for magnetic manipulation of cells are required to employ inhomogeneous magnetic fields in different manners. By applying magnetic field gradients generated by various methods, cells are captured or trapped, using magnetic particles which can be bonded to specific antibodies. These magnetic particles sizes vary from 5nm to 1um and they are made of material that cannot be oxidized easily. Because of the small size of magnetic particles, single DNA

molecule manipulation can be efficiently performed [16]. Micromanipulation of single DNA molecule allows precise study of the proteins which process DNA. Another usage technique is in obtaining rare cell types, especially in handling red blood cells [16].

Even though this method employs very small size micro beads which do not affect cell functionality, in some specific biological cell application such as somatic cell fusion, it is not viable and is harmful on fused cell.

1.2.3.2 Optical Manipulation

Optical manipulation is a non-contact and contamination-free manipulation process. It is a well-known approach that optical trapper, or optical tweezers, focuses laser beam on a particle or biological cell and manipulate them with very high precision. A momentum that is transferred through tightly focused laser beam hits an object and traps it in the direction of the laser beam.

Due to microfluidics optical properties such as transparency, this method can be easily adapted with microfluidic systems. Optical tweezers is the most commonly used optical manipulation method in microfluidic devices [18][19].

A microscope unit for optical tweezers has a high numerical aperture to focus a high resolution laser beam. Due to this high numerical aperture, it has a limited manipulation area. The particle range for the optical manipulation varies from a few Angstrom up to 10μm. On the other hand, because of the usage of high laser energy, long handling time causes heating problem that can be harmful for biological objects. Even though optical manipulation has numerous advantages; its applications in microfluidics require complicated optical setup and expensive microscopic instrumentation.

1.2.3.3 Electrical Manipulation

Dielectrophoresis (DEP) technique is first reported and named by Pohl in 1951. It is defined as the movement of uncharged particles affected by a non-uniform electric field [20][21]. DEP has

been widely used in different biological applications. It has been also applied on microfluidic devices successfully in order to detect, separate, manipulate, characterize living cells and biological objects such as viruses, DNA molecules, yeast and mammalian cells [22][23][24][25][26].

In microfluidic chips, DEP filed is provided by fabricating and placing parallel electrodes on the bottom surface of a micro-channel. As a result of this, the biological particles can be manipulated along the micro-channel under the DEP force. The trapping and manipulating capability of Dielectrophoresis force make it a good option for cell based microfluidic application. In chapter 4, DEP force was used where the flow drag force is not enough to provide cell coupling. Nickel barriers patterned on side walls of the micro-channel pushed fibroblast cells through the immobilized oocyte to complete coupling. Meanwhile, DEP suffers from low survival rate of biological cells in electrical field. Because of that, DEP force must be applied for a short period of time.

1.2.3.4 Ultrasound Manipulation

T he on-chip manipulation of particles and cells via ultrasound is a well studied topic in the last decades. Ultrasound waves have been used for manipulating as well as separating, sorting…etc., of biological cells. Ultrasound field will disturb the environment with fluid flow and cells which is subject to this field move to another location [27]. Moreover, ultrasound force can be used for stirring and mixing of liquids in microfluidic chips. In some applications, flow-free manipulation and cell transport has been studied [28]. Force generated frequency-modulation was utilized in two modulation techniques for stabilized particle alignment and particle transport in microfluidic chips. The particle speed is controlled by modulation frequency.

The thermal control in this method has a vital importance to maintain the viability of manipulated cells. During the absorption of ultrasound energy, a temperature may increase. Several studies have investigated these aspects, the effect on culture medium or cell can be

evaluated via on-chip thermocouple or fluorescence technique. Moreover, heating is a limiting factor for application of acoustic force [29].

1.2.3.5 Fluid-Flow Manipulation

Fluid-flow manipulation commonly referred as non-contact manipulation is commonly used for single cell applications and cell injections. It is a non-invasive method for biomedical field. Gentle movement can be successfully done with this way. Some cell operations, such as cutting of mammalian cell can be implemented with this technique [28]. There are drawback associated with conventional flow manipulation techniques, such as requirement of high accuracy micro-pumps and differences between speed of particles and liquid. While control system is adapted to flow speed, particles speed may exponentially change.

1.2.3.6 Summary of On-chip Manipulation Techniques

Table 1, Methods of Controlling energy field of bio-manipulation

	Application	Control Method	Selectivity
Magnetic Manipulation	Transportation Separation	Magnetic Field utilizing permanent magnets and electromagnets	Magnet Density and Sizes
Electric Manipulation	Transportation Separation	High Frequency Electric Filed	Difference of Dielectirc Properties of Particles
Optical Manipulation	Trapping of Single Object	3D Confocal Scanning of Laser Beam with mirror	Trapping Particles is larger than the wave length of laser beam
Ultrasonic Manipulation	Filtaration Fixation	Configuration of Micro Resonator	Difference of Size and Density of Particles

Table 1 shows the method and characteristic of above manipulating methods. Among of these systems, optical, fluid-flow and ultrasonic manipulations require position information of the cells and sensing system is needed for automation. When we consider precise and non-invasive handling of micro-objects, optical beam is suitable. However, it has heating problem on living cells as well as it requires high magnification on microscoping images so that it is considerably not efficient to use micro objects over 50 micrometers.

Table 2, Comparison of the Energy Field

Manipulation Technique	Transportation	Selectivity	Controllability	Resolution	3D operability	Healthy
Electric	Fair	Good	Good	Fair	Good	Poor
Optical	Poor	Poor	Good	Good	Fair	Poor
Ultrasound	Poor	Fair	Fair	Poor	Poor	Poor
Magnetic	Fair	Good	Fair	Fair	Fair	Fair
Fluid-Flow	Good	Fair	Fair	Fair	Fair	Good

Ultrasound may disturb the environment. Table 2 shows the comparisons of the manipulation techniques according to their classifications. In this table, we can see that fluid-flow technique is the best way to manipulate cells in damaging-free method, particularly, when we consider mammalian oocyte cell around 100um. On the other hand, for the cell fusion process we need to use DEP force in brief time period which is required for cell trapping and coupling.

1.3 Optical Sensing

In the sensing system, the detection issues will arise when sensing systems are miniaturized. The reduced analysis volumes mean a reduction in detection volumes, decreasing the number of

analytes available for detection make it more difficult to be detected. Thus, the two main factors that affect the choice of the detection method for microfluidic devices are sensitivity and scalability to smaller dimensions. Electro- chemical detection (e.g. conductivity, potential) does not satisfy all these conditions, where sensitive portable systems are required. Hence, there is a developing interest to couple and integrate optical components into microfluidic devices. The optical components used in these detectors are mainly light-emitting diodes (LEDs) or laser diodes as light sources, optical fibers, gradient refractive index lenses, and diffractive elements. These parts are assembled into compact detectors to develop a portable instrumentation based on microfluidic devices.

1.3.1 Off-chip Optical Sensing

Macro-scale optical detection, especially spectrometric detection is common because there is a wide range of applications, i.e. absorbance, fluorescence and chemiluminescence. In order to couple these macro-scale detection into micron-sized detection areas, the use of pinholes at focus points along the optical path or optical fiber is commonly called as "off- chip approach". The advantages of this approach are very low levels of background signal that can be combined with very sensitive photon detection techniques, such as photomultiplier tubes (PMTs) and charge-coupled devices (CCD) which in turn, result in very low detection limits. However, the reduction in path length within the device could also decrease the sensitivity of the method, in particular for absorbance measurements. Currently, the development of a wide range of intense light-emitting diodes and photodiodes that can be well coupled directly to microfluidic devices to provide a miniaturized technique of on-chip detection can easily be realized. The existing devices in the "off-chip approach" are generally well developed either as homemade detection system or commercial instrument system such as Shimadzu MCE-2010,Hitachi SV1100, and Agilent Bioanalyzer 21000.

1.3.2 On-chip Optical Sensing

The integration of optical components or functions in a microfluidic platform that should be able to perform all chemical functions and detection in a single device, requires increased integration of not only fluidic elements, but also electrical or other types of elements. This method can be classified as "the on-chip approach". The microelectromechanical systems (MEMS) world has demonstrated the integration of mechanical and electrical functionalities into small structures for diverse applications. Micromachining technologies have traditionally been silicon-based, since it makes the combination of mechanical and electrical functions in single devices possible. Recent effort has in fact focused on the fabrication of mechanical devices with passive optical functions, such as movable mirror arrays, refractive microlenses, and optical filters [31]. The term micro-optical electromechanical systems (MOEMS) have been considered as a branch of MEMS. It drives the development of micro-optical technologies to replace bulky, large and expensive macroscopic optical systems.

1.3.3 Summary

Monitoring techniques associated with numerous visual detection methods are readily implemented to microfluidic channels by employing big bulky microscopes [32]. Due to high cost and big sizes, those microscopic systems are not appropriate to be used with LOC devices effectively. Thus, integration of optical components with microfluidic devices accompanied by light sources and sensors can be an efficient alternative. Hence, compact vision systems become crucial in order to accommodate image processing for microfluidic applications. So far, several researches have been reported to miniaturize conventional optical devices to make portable LOC systems. J. Koschwanez et al. applied fiber optic bundle onto microfluidic channel to identify single yeast cells [33]. Even though separation of vision system has been done, microscope objective and body is still needed. Webster JR et al. developed a fluorescence optical detector in a PDMS chip for DNA analysis [34]. Roulet JC et al. developed a microfluidic chip integrated with circular or elliptical microlenses for fluorescence detection by means of biochemical analysis [35]. In a recent integrated optics application, Jeffrey R.

Krogmeier et al [36] has built a detection system consisting of an on-chip objective, a fiber optic illuminator and a collection mirror, and placed it on both sides of a microfluidic chip for the detection of single DNA molecules. Although there have been a wide range of applications using integrated optics on fluorescent techniques, there are no widely-known integrated camera ready optical devices coupled with a light source for the purpose of image analysis capable of acquiring the required information such as size and position to manipulate cells in a micro channel.

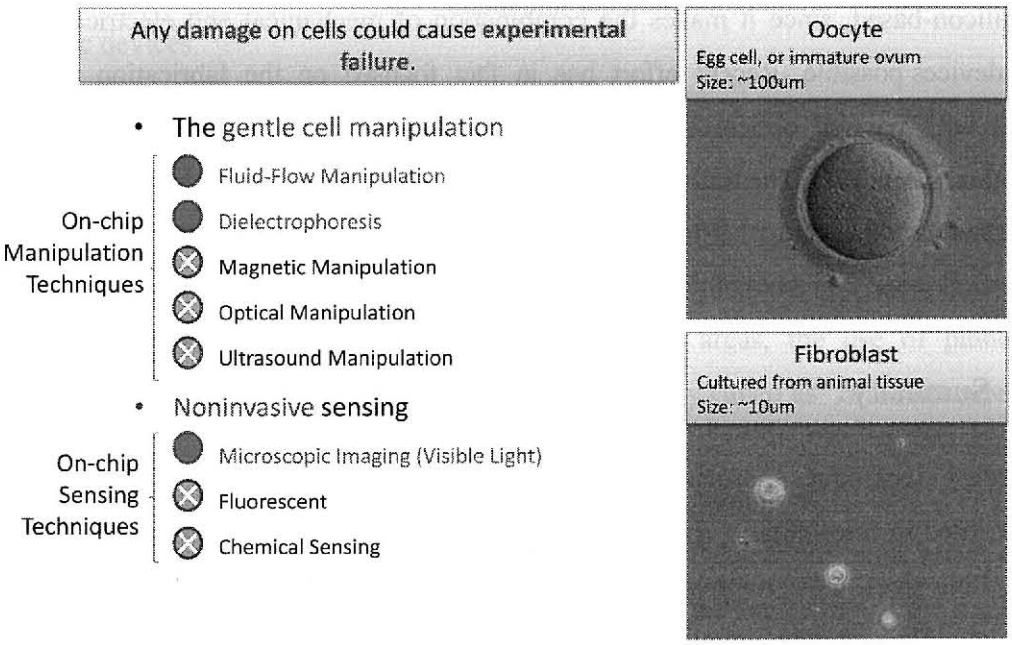

Figure 4, The gentle cell handling and manipulation are required most of biological experiments such as cell cloning. On the other hand, the most of the sensing techniques use labeling which is invasive method. The alternative way may be microscopic imaging under the visible light spectrum.

1.4 Motivation

1.4.1 Automated Mammalian Cell Cloning

Technical developments in recent years have proved biotechnology as one of the fastest growing areas of science. Biotechnology has found applications mostly in medicine, food

science and agriculture. Especially, the highly accessible "nuclear transplantation" technique, known also as nuclear cloning, plays important roles for a broad range of fields including regenerative medical techniques, pharmaceutical technology, stock breeding and fertility treatment. In the commonly used method of "somatic cell nuclear transfer" cloning is achieved by transferring the genetic material from a donor cell (fibroblast) into an enucleated oocyte whose genetic material has been removed in advance. Although it is frequently used, the procedures are not automated and all the steps have to be performed manually under a microscope.

The core technology is the micromanipulation in which an expert operates a micromanipulator manually to accomplish the steps of nuclear transplantation including the removal of genetic material of unfertilized oocyte and its replacement with the donor. This process due to the high number of critical steps to be performed with utmost care usually leads to high loss and takes long time to be completed even by operators with sophisticated skills. In other words, the efficiency of generated cloned cells from adult donor cells is low in most species. In general, only 1-3% of the cloned embryos create viable embryos. These fundamental limitations of cloning may be addressed by using micro-robotics with analyses of the underlying cellular mechanisms.

Integration of cell treatment steps is crucial to develop microfluidic devices for analysis of cell constituents, cell lysis and cell culture [37][38]. For example, experimental results show that microfluidic technology provides a significant advantage in the production of mammalian embryos. Besides these vital concepts, cell fusion and nuclear transplantation [39][40] are also important topics. Our project "Automated Cell Cloning Using Micro Robotics" is a novel approach for finding a solution to overcome difficulties in the nuclear transplantation process. In this project, several cell manipulation tasks such as positioning, cutting, sorting, filtering, and fusion are performed by different interconnected modules, by a so-called "Desktop Bioplant" [41]. This Desktop Bioplant, which includes micro channels and micro wells on a chip with appropriate sensors and actuators, is increasingly in demand for nuclear transplantation operations in biotechnology (Figure 5)

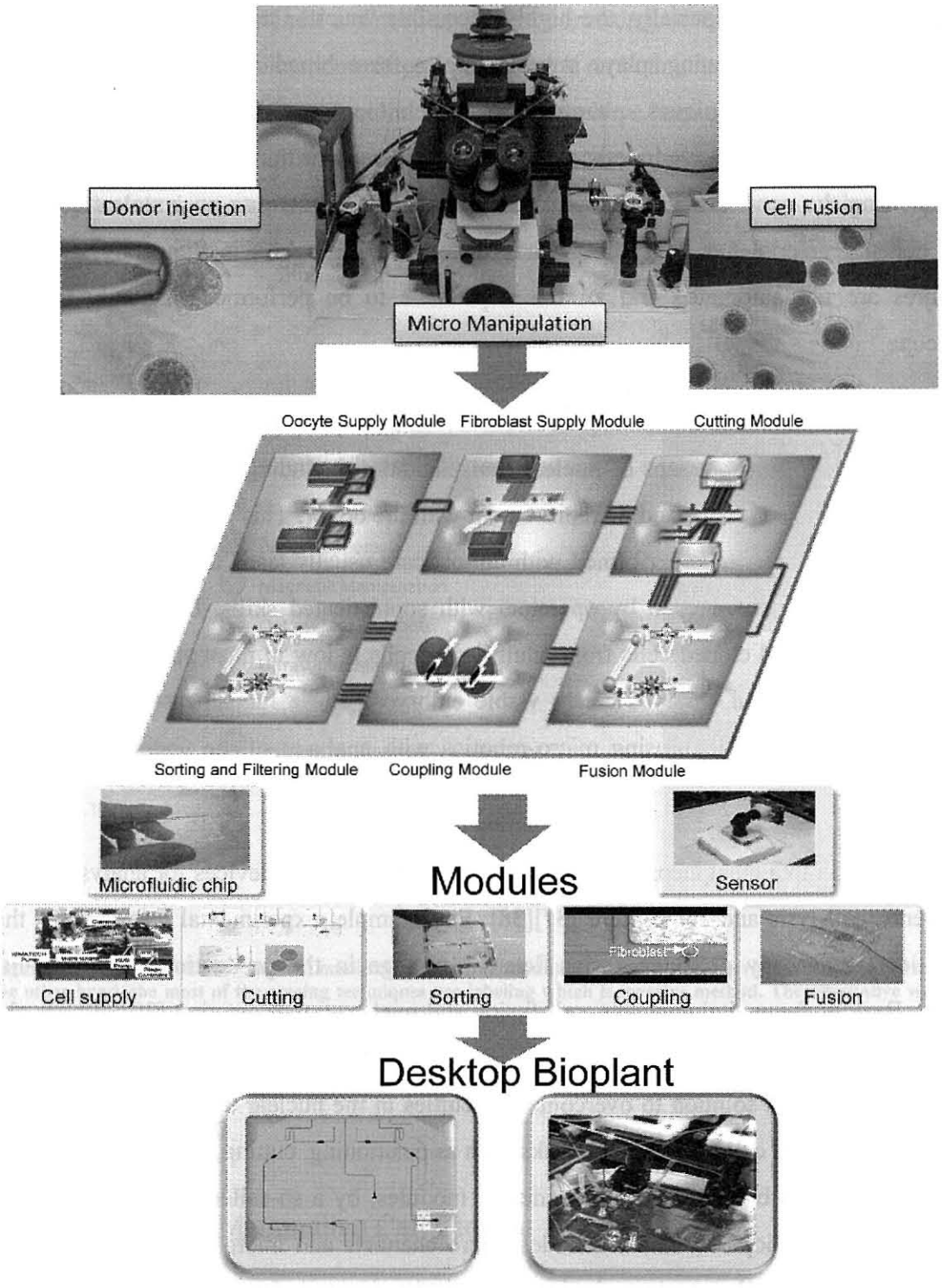

Figure 5, Illustration of "Automatic Mammalian Cell Cloning" Project.

There are two kinds of nuclear transfer methods, microinjection and cell fusion. The bud of the mammalian cloning technique development was seen in the middle of the 20th century [42]. Briggs and King first demonstrated that cell nuclei could be reprogrammed to a zygotic state and could generate early cleavage embryos when transplanted into enucleated oocytes by using nuclei from frog blastomeric in 1952 [43]. In 1962, Gurdon succeeded in generating cloned frogs from differentiated tadpole stage cells [44], but adult donor cells have not produced cloned frogs. In 1983, nucleus transplant method and fertilized egg nucleus substitution was developed by a method to be transplanted zygotic nuclei into previously enucleated zygotes using cell fusion. Several cloned individuals (lambs [45], cattle [46], and pigs [47]) were bone in the subsequent years, and all clones were derived by nuclear transplantation using nuclei from blastomeres as donor cells. In 1997, the first cloned mammal from somatic cell nuclei was sheep, called "Dolly", generated by "cell fusion method" [48]. Subsequently, "microinjection method" was developed to clone mice by selective nuclear transfer [49]. By using these nuclear transfer methods with adult donor cells, various mammalian species have been produced live born clones, cattle [50], pig [51], and so on.

Here, we consider to cell fusion method about somatic cell cloning. The conventional scheme of the fusion nuclear transfer procedure is illustrated in Figure 6.a; (1) the zona pellucida of an oocyte is cut by applying piezo-driven at the tip of an enucleation pipette and its nucleus is drawn into small glass pipette and removed. (2) The fibroblast cells are injected one by one directly into the enucleated oocyte. (3) The cells are fused by the application of an electrical current with small electrodes. After the nuclear transfer, fused oocyte is activated by chemical treatment or electric pulse (in Figure 7, electric pulse activation was applied at the same time). When this oocyte begins to develop as an embryo, it is implanted into mother's uterus after culture. In this work, we have to manipulate oocytes and fibroblast cells one by one with small glass pipette or other tool. So, we have proposed automation of somatic cell cloning process based on a novel protocol as illustrated in Figure 6.b [52]; (1) the zona pellucida is removed from an oocyte by chemical treatment. (2) The oocyte is cut into two parts and half part with nucleus is removed. (3) The remaining half part without nucleus is coupled with a fibroblast

cell. (4) They are fused by the application of an electrical current with electrodes. After nuclear transfer process is same as conventional method.

1.4.2 Why Microfluidic Systems for Cell Cloning Technology

As it summarized in the section "1.1.2 PDMS-based Microfluidic chips", the advantages of using microfluidic chips include the ability to fabricate disposable structures rapidly and inexpensively and to provide non-toxic environment for living cells.

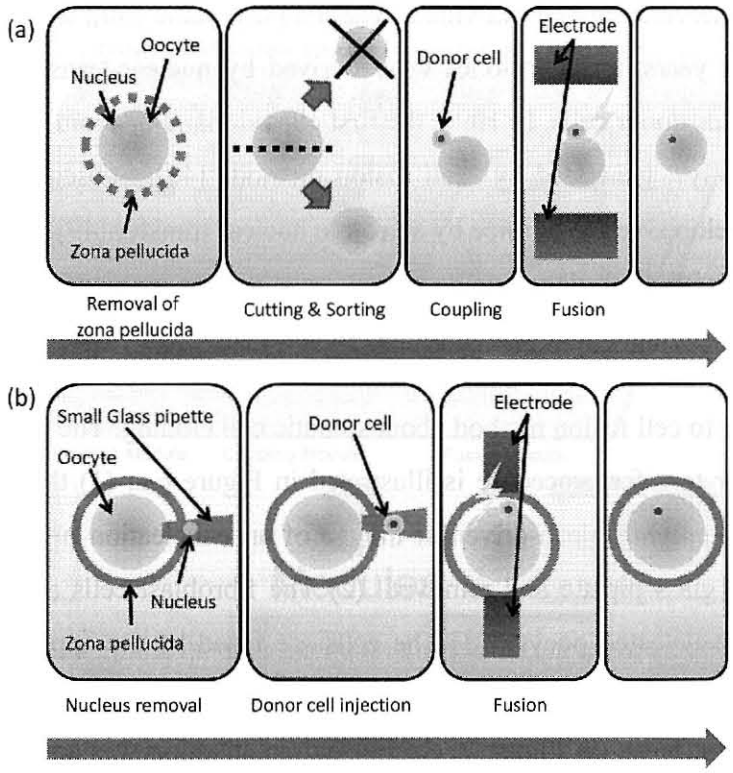

Figure 6, The scheme of the fusion nuclear transfer procedure (a) New protocol for automation of somatic cell cloning process (b) Conventional method

Here, first thing come into mind is automation of current off chip manipulation techniques to perform cell cloning. Effective manipulation of mammalian cells can be grasp in place and

injected with a fibroblast cell contains genetic information, by operator through a vision and force feedback interface. Although there are considerable efforts to automate off-chip manipulation techniques with feedback control mechanism, the drawbacks associated with conventional contact manipulation, based on holding and microinjection pipette techniques, motivated us to focus on microfluidic methods.

Microfluidic chips present a great environment for our project. The advantages of microfluidic chips for cell cloning as follows:

1. Hybrid systems

   Conventional laboratory techniques can be successfully miniaturized and integrated on microfluidic chips including micro-pumps, micro-manipulators, and micro-mixers.

2. Small liquid volume consumption

   Manipulating very small sample volume brings an advantage on fast diagnosis and high-throughput analysis.

3. Contamination-free environment

   In conventional methods, a labor uses mineral oil droplets to cover up the cell culture. Microfluidic capillaries cut off the interaction with atmosphere so that bacterial contamination may be minimized or stopped. Moreover, we can perform the biological cell operations in room temperature.

4. Change solutions easily

   During the experimental phase of cell cloning, we need different solutions such as changing M2 solution to ZFM (details described in following chapters). State-of-the-art microfluidic structures allow us shifting micro level liquids easily.

5. Inexpensive structure

   Conventional cell cloning techniques are expensive and bulky. Its inexpensive structure allows us to fabricate in mass production.

6. Dielectrophoresis

   As it is explained previous section, conventional methods for DEP based manipulation has been readily implemented on chip. Using AC or DC electric field energies, we can apply this approach to perform cell coupling or cell fusion.

1.4.3 Novel On-chip Mammalian Cell Coupling Process

Because of the advantages of microfluidic chips for the automation of the cell cloning, the new protocol (Figure 6.a) may build in a microfluidic chip which is shown in Figure 7. Considering the idea of "Automatic Mammalian Cell Cloning Project" (Figure 5), we designed a new microfluidic chip. The new protocol was integrated in this microfluidic module with each step. The total process carry on the chip with following three steps; (1) an oocyte supplied into micro chip is captured in narrow a micro channel, (2) a fibroblast is fused with the immobilized oocyte by dielectrophoresis, and then (3) the new oocyte and fibroblast couple are released.

Obviously, the new cloning protocol (Figure 6.a) is suitable for the automation cell cloning process with microfluidic technology. Cell coupling is one the critical application of this multifunctional microfluidic chip. In coupling process, two cells, a fibroblast and an oocyte, have to be brought into very close contact. The on-chip cell coupling can be accomplished in three steps; (1) an oocyte supplied into micro chip is absorbed and captured in narrow micro channel. (2) A fibroblast is contacted with fixed oocyte by dielectrophoresis. (3) The pair of oocyte and fibroblast cell is released from micro channel. In the chapter 4, I present the whole process of cell coupling system using microfluidic chip with system construction and the results for future automatic mammalian cell coupling.

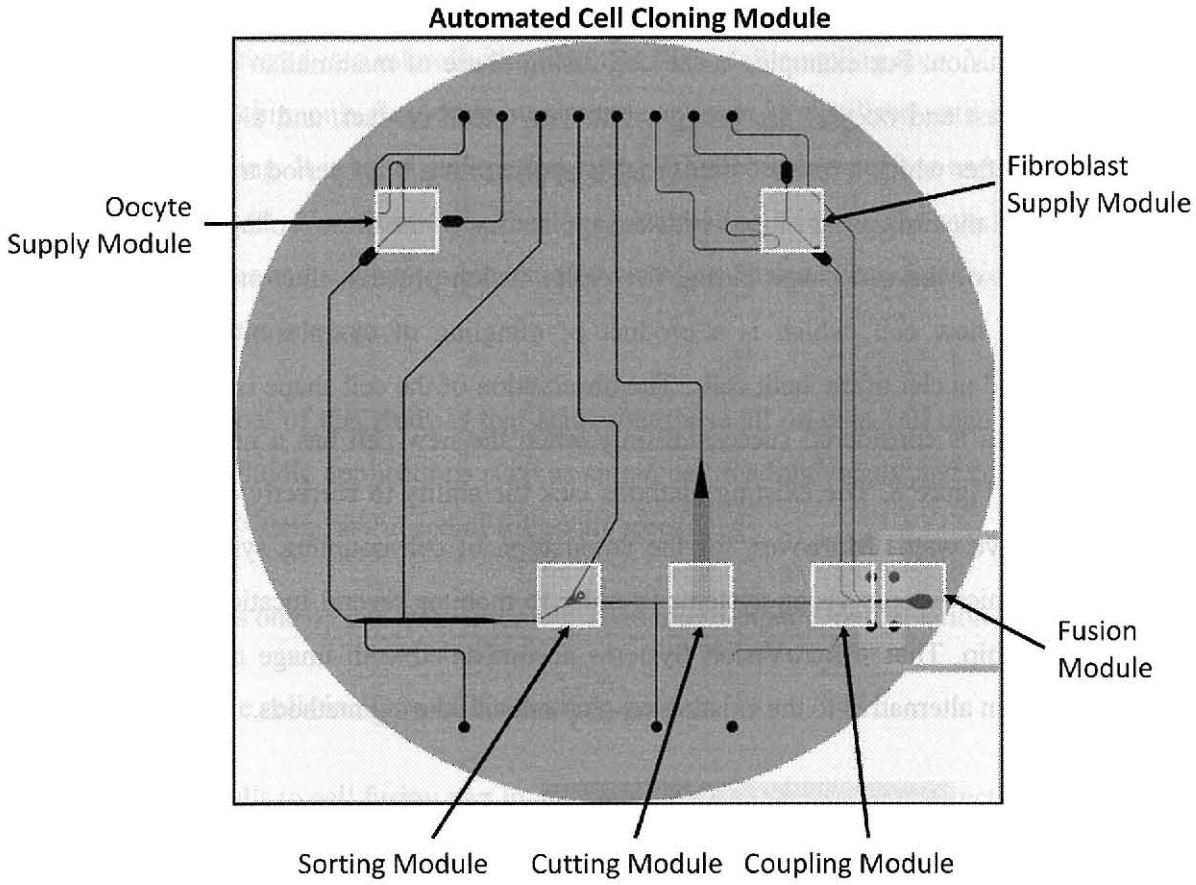

Figure 7, One-chip Microfluidic Cell Cloning Chip. With the permission of Tohoku University, AIST (Advanced Institute of Sci. and Tech.), Fujihira Industry and Kawasaki Heavy Industry

1.4.4 The Goal of This Study

I propose vision-based on-chip cell manipulation technique for cell based microfluidic applications in terms of "Automated Mammalian Cell Cloning Project". The MicroVision Systems associated with on-and-off chip manipulation techniques are center of this study.

On-chip micro vision systems are design and implementation of miniaturized microscopic systems accompanied with real-time cell detection, tracking and sizing. Current embedded lab-on-a-chip sensors utilizing light scattering, electrical resistance, and sound method technologies,

are not sufficient to extract desired information about a cell through steps of the cell coupling as well as cell fusion. For example, in the cell-fusing phase of mammalian cloning process, two cells (fibroblast and oocyte) are brought into very close contact, and aligned via alternating current (ac) after which a direct current (dc) is applied for a brief period to complete the fusion [53][54]. Cell membranes are fused with the application of the direct voltage without observing the evolution of the cell shape during the entire fusion process, thus one cannot be sure of formation of new cell, which is a product of mingling of cytoplasmic contents including organelles and nuclei of the both cells. The observation of the cell shape is important because a fusion process is considered successful only when the new cell has a near circular shape as illustrated in Figure 8. The existing methods lack the ability to correctly detect the shape in a non-destructive way. Moreover, for the automation of cell coupling system, it is crucial to miniaturize microscopic vision systems in order to monitor several locations at the same time on a same chip. Thus, MicroVision Systems accompanied with image analysis methods are proposed as an alternative to the existing on-chip optical sensing methods.

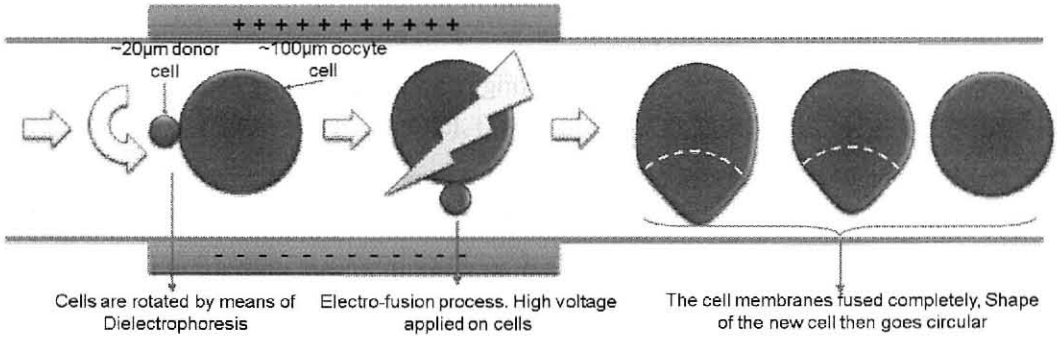

Figure 8, Cell Coupling and Fusion Process

The gentle cell handling and loading into a microfluidic chip one by one and transporting them to a coupling module are challenging issues for a successive application of cell cloning. Because of the fact that any damage on oocyte or fibroblast cells could cause experimental failure, I used an off-chip manipulation technique with micro-glass pipette (suction tip) attached on a micromanipulator. With this method, the cells can be aspirated from a cell-container, in

which needs accurate positioning of the micro-glass pipette with target cells. A desired number of cells can be transferred into microfluidic chip and then, cell coupling area. Moreover, in the PDMS microfluidic chip, only fluid-flow manipulation (Table 2) is utilized until introduction of DEP force for coupling. It is an advantage that cured PDMS has low surface energy preventing the cells in the PDMS microfluidic channel from interacting with it. The synchronization of pumps, PDMS-valves and suction tip are handled via MicroVision Systems, which provide full automation and system integration.

In conclusion, the goal of this study is that achieving those all on-chip cell manipulation tasks for important microfluidic applications such as single cell loading/supply and cell coupling by using MicroVision Systems at the end of following steps:

1. Loading cells one by one from a container via micro-pipette manipulation
2. Storing single cells in microfluidic docking area
3. Supplying cells to cell fusion part by valve manipulations and pump direction control
4. Immobilizing oocyte cells with fluid-flow manipulation
5. Bringing fibroblast cells close contact with oocyte cells
6. Applying DEP force to finalize coupling process

As it shown in Figure 9, there are two main concepts for successful application of single cell loading/supply and coupling systems as visual sensing and manipulation. Visual sensing techniques of living cells associated with numerous computer vision methods and automatic manipulation tasks have great importance for this project. For the best of our knowledge, there is no automated single cell loading/supply and coupling systems for microfluidic chips.

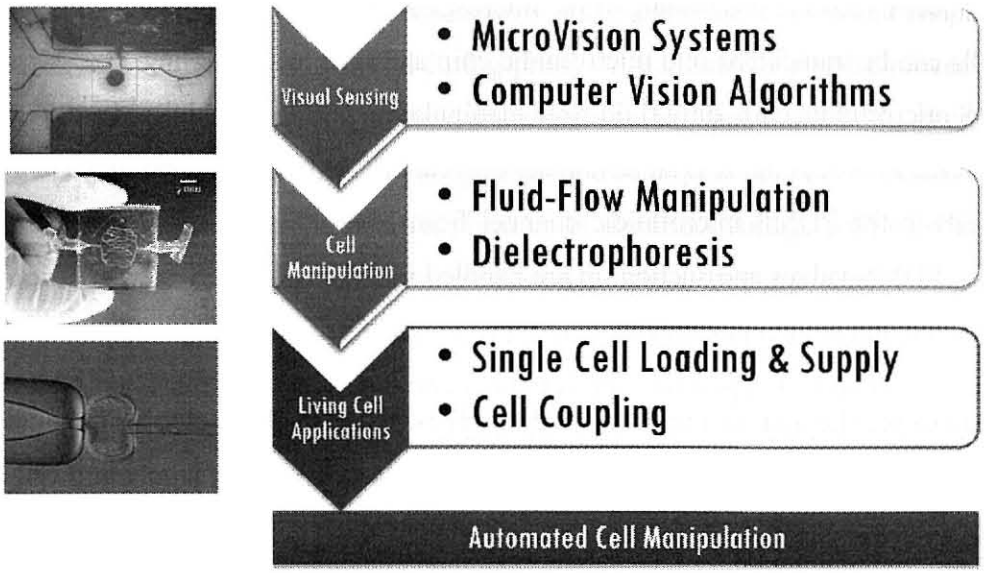

Figure 9, Requirements of successful application of the Single Cell Loading/Supply and Cell Coupling processes

Chapter 2: MicroVision Systems

One of the biggest obstacles for lab-on-chip devices is the miniaturization of large-scale devices and its methodologies. Miniaturization of the current microscopic technologies combined with image processing may bring significant advantages for the lab-on-chip devices in dynamic process of sizing, positioning, flow-control, cell-manipulation at different time scales. Here, MicroVision systems are proposed boarded on a PDMS-based microfluidic chip, which can be utilized in a complex microfluidic network for continuous monitoring of mammalian oocyte and fibroblast cells of sizes in the range of 10 to 100 micrometer. The developed prototype system has sufficient resolution and is accompanied with a robust detection method for cell-based microfluidic applications. To assess its performance, the image processing algorithm was applied, and the capability of detection method was evaluated using 11 μm and 26 μm particles. The results show that the proposed optical system of monitoring and illumination can be effectively incorporated into PDMS structures aiming at lab-on-chip devices.

In this section, I describe 3 types of MicroVision systems, which can be integrated into every module of Desktop Bioplant such as electro-fusion module. The prototype essentially was designed for an all-in-one Cell Cloning microfluidic chip and it was boarded within required dimensions of a PDMS chip.

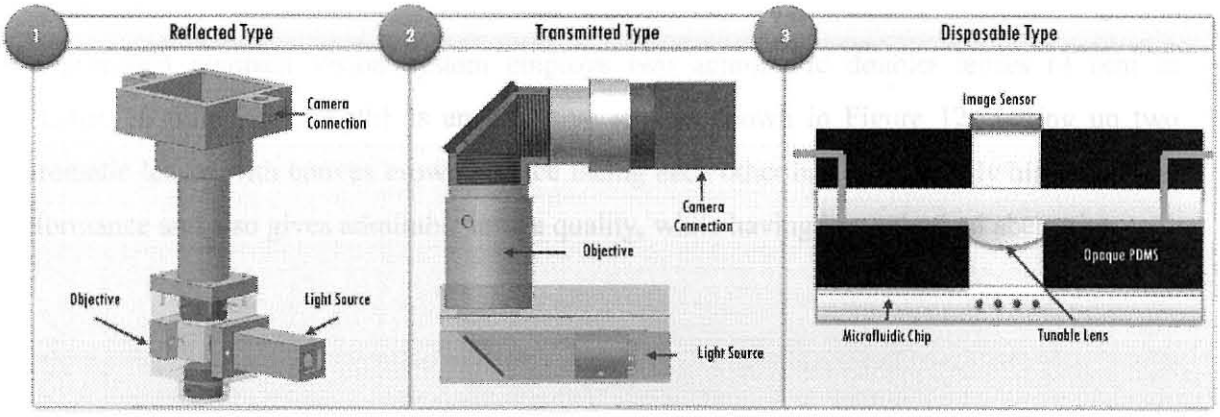

Figure 10, The MicroVision Systems

Table 3, Comparison of 3 MicroVision Systems. Because of easy installation and high resolution value, reflected type vision system has been used in experiments.

	1. Reflected Type	2. Transmitted Type	3. Disposable Type
Sensor Type	CMOS/CCD	CMOS/CCD	CMOS/CCD
On-chip Dimension	10mmX10mm	Φ11 mm	Sensor -Dimension
Light Position	Reflected	Transmitted	Transmitted
Integration	Easy	Hard	Hard
Optical Lens	Solid	Solid	Liquid
Resolution	125lp/mm (4um)	125lp/mm (4um)	24lp/mm (20um)

2.1 First Prototype based on Transmitted Illumination

The first prototype allocated 11 mm area on the chip that allows connecting multiple vision systems onto different locations on a chip (Figure 11). It provides sufficient magnification, and is driven by a motion based imaging algorithm to detect single cell in a capillary. The integration technique of the prototype vision system onto a PDMS chip is reported and listed the step-by-step procedure. The resolving power under the desired field of view dictated by pre-defined requirements such as minimum image extraction limits were depicted in the experimental results section. In this section, the performance of the complete system for cell sizing and accurate positioning are also briefly summarized.

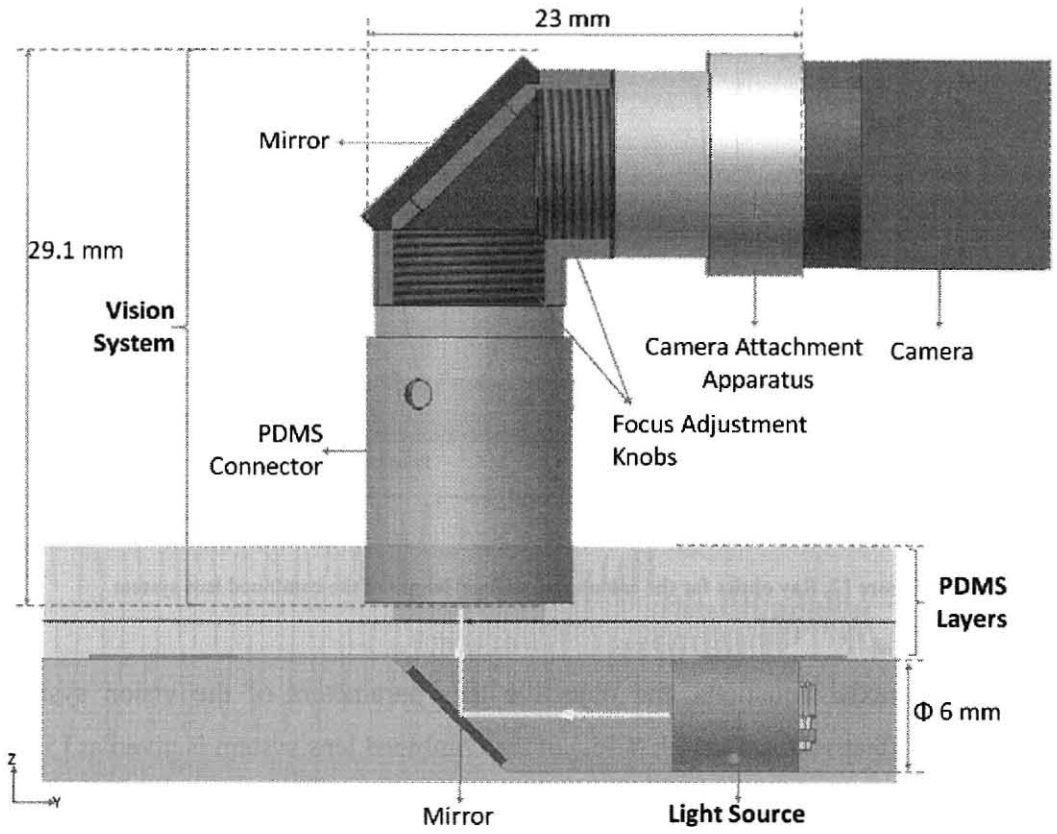

Figure 11, The illustration of the prototype system, which includes illumination and camera units

2.1.1 Optic Design

The proposed compact vision system employs two achromatic doublet lenses (4 mm in diameter, 10 mm focal length) as an objective lens as shown in Figure 12. Setting up two achromatic lenses with convex crown surface facing each other has considerably higher optical performance and also gives admirable image quality, while having low spherical aberration.

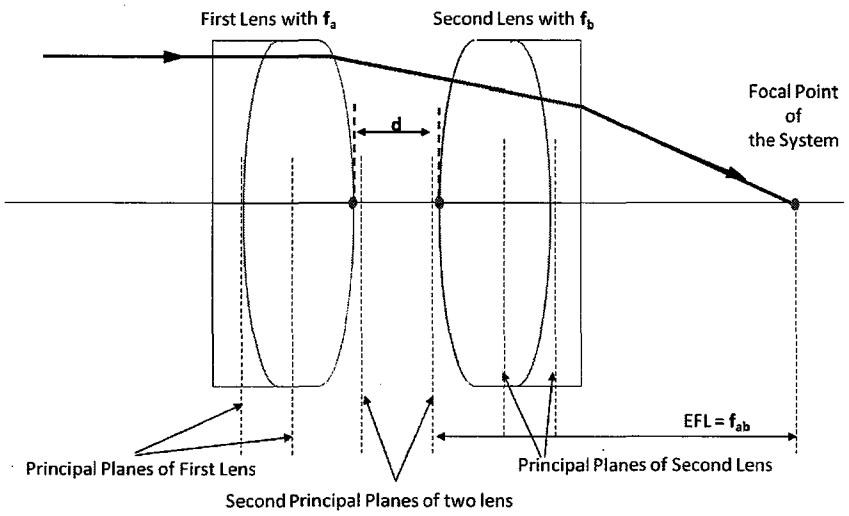

Figure 12, Ray optics for the calculation of focal length of the combined lens system

Using set of paraxial equations, the objective lens parameters of the vision system were calculated. The effective focal length (EFL) of the combined lens system is given as [55]

$$f_{ab} = \frac{f_a f_b}{f_a + f_b - d} \qquad (1)$$

where d is the distance between two achromat lenses, and f_a and f_b are the focal lengths of the two lenses in the system. In the scheme, f_a = 10 mm, f_b =10 mm and d is taken as 0.5 mm resulting in $EFL = 5.12\ mm$.

Another critical point that must be considered is the light gathering capability of the system. This is usually referred to as the f number (f/#) which is calculated as

$$f/number = \frac{f}{\gamma} \qquad (2)$$

where f is focal length of the lens and γ is diameter of the effective aperture. For the system γ is 1 mm, thus the $f/\#$ becomes $f/5.12$. Using this value, the lens was tested system

employing transmission sinusoidal target pattern (Edmund Optics M-19-80, 2 to 256 lp/mm) for $f/5.12$.

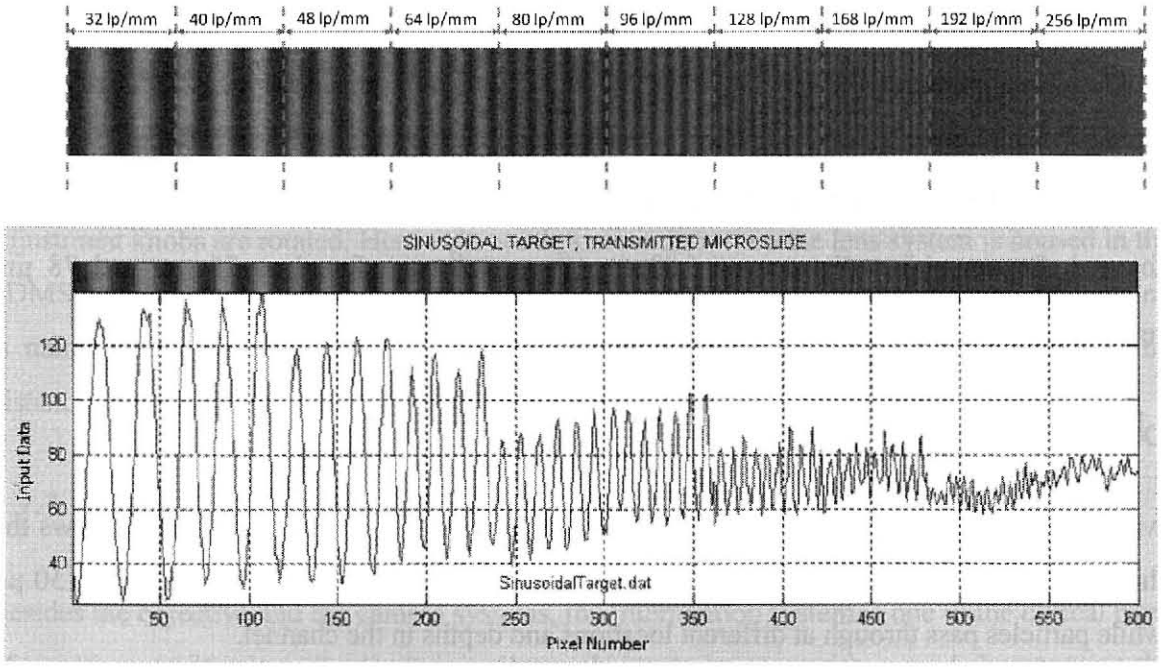

Figure 13, Optical performance of the imaging system at . The test results are taken by each of the ten different frequency patterns sampled using 60 pixels laterally.

As expected with the increasing density of lines per length, contrast between dark and bright lines decreases. From Figure 13, one can conclude that the imaging system could resolve patterns of 96 lp/mm (one line pairs about the 10 μm) or less with an acceptable level of contrast.

Distance wherein objects are in focus (Depth of field - DOF) is computed to find acceptable sharpness when zooming into the channel. The DOF is computed using

Near focus (d_1): $$\frac{\delta x N x \eta^2}{f^2 + \delta x N x \eta} \qquad (3)$$

Far focus (d_2): $$\frac{\delta x N x \eta^2}{f^2 - \delta x N x \eta} \qquad (4)$$

where δ refers to circle of confusion (permissible circle of confusion was taken as 0.011 mm for 1/3inch CCD), N is f/number of the objective, and η is distance at which the objective is focused. For an object distance of 6.00mm, d_1 and d_2 are found as 76 μm and 78 μm, respectively. The DOF is calculated as the sum of d_1 and d_2

$$\text{DOF} = d_1 + d_2 \qquad (5)$$

which gives 154 μm distance to acquire nearly sharp image. This theoretical result shows that the experimental system can be operated on micro channels with depths of 100 μm to 150 μm while particles pass through at different locations and depths in the channel.

2.1.2 Monitoring System

The optical structure detailed in the previous section was designed for easy integration with different camera systems. In order to focusing camera systems, Variety of knobs, which are also promising different addition options for camera systems, was employed on a chip. In the studies, three types of compact camera were used with particular arrangement as (i) Pointgrey Firefly MV camera (60, 30, 15, 7.5 frames per sec.) with 1/3 inch CMOS-752 X 480 pixels, (ii) Misumi SSX-1870 camera (NTSC) with 1/4 inch CCD -768 X 494 pixels and (iii) Plumnet HandyMini camera (NTSC) with 1/7 inch CCD-710 X 480 pixels. The first two cameras (SSX-1870 and Handy Mini) are analog and the third is a digital camera. While the analog cameras have smaller size and lighter weight, the digital solution enjoys the advantage of higher frame rate and better image quality. The mirror used in the apparatus (see Figure 14) is used to change the direction of the incoming light, so that camera unit can be oriented 90° relative to the normal

of the PDMS surface. This helps to avoid the unwanted horizontal growth of the system to provide compactness. To focus the camera, one should move the objective housing the lens system near to or further from the sample surface. All the focusing apparatuses (see Figure 14) in the monitoring system are of the single shaft coarse movement type in which a coarse adjustment knob (PDMS connector) and fine adjustment knobs (lens carrier and camera attachment apparatus) are disposed coaxially with each other. Thus, when a quick focusing is needed, the coarse adjustment knob is rotated, and when a precise focusing is necessary, the fine adjustment knobs are rotated. Here, it is worth to note that when the lens system is housed in the PDMS connector, the lens stays 2.5mm above the lower surface of the connector. This spacing is named as "opto-hole" and its depth was determined considering the range of focusing distance. The reason for opto-hole will become clear in the following sections.

2.1.3 Illumination System

Besides the objective and the camera systems, the illumination system is one of the critical parts of experiments. If it is well adjusted, it allows objects to be seen with a good sharpness on the image plane, otherwise scattered light will confuse fine details of the image. For illumination, I employed the light radiated by a Toyoda-Gosei" SMD (surface mounted device) type light emitting diode (LED) (Type No: E1SM1-0W0M5-05) which has 3.5 X 6.0 X 1.9 (mm) package size and emits highly intensive white light spectrum in the range of 400 nm to 650 nm. A "Heavy Frosted" filter ("%47.1 transparency" Calamel Company) was placed in contact with the LED to expand the illuminating field and to reduce high intensity throughout the cell manipulation and detection area. Oblique rays of light from the source are transmitted through the filter, which decreases the intensity level. The amount of decrease in the intensity depends on the density of the frosted filter. Level of incident light was smeared equally over the filter front face yielding an almost uniform illumination. A plano-convex lens (2 mm) was positioned right after the frosted filter to provide a collimated light illumination on the micro-channel. This avoids problems due to short-range lens adjustment after the light source. Finally the light

source was placed under the PDMS chip and aligned with the camera system. The final setup of illumination system is illustrated in Figure 15.

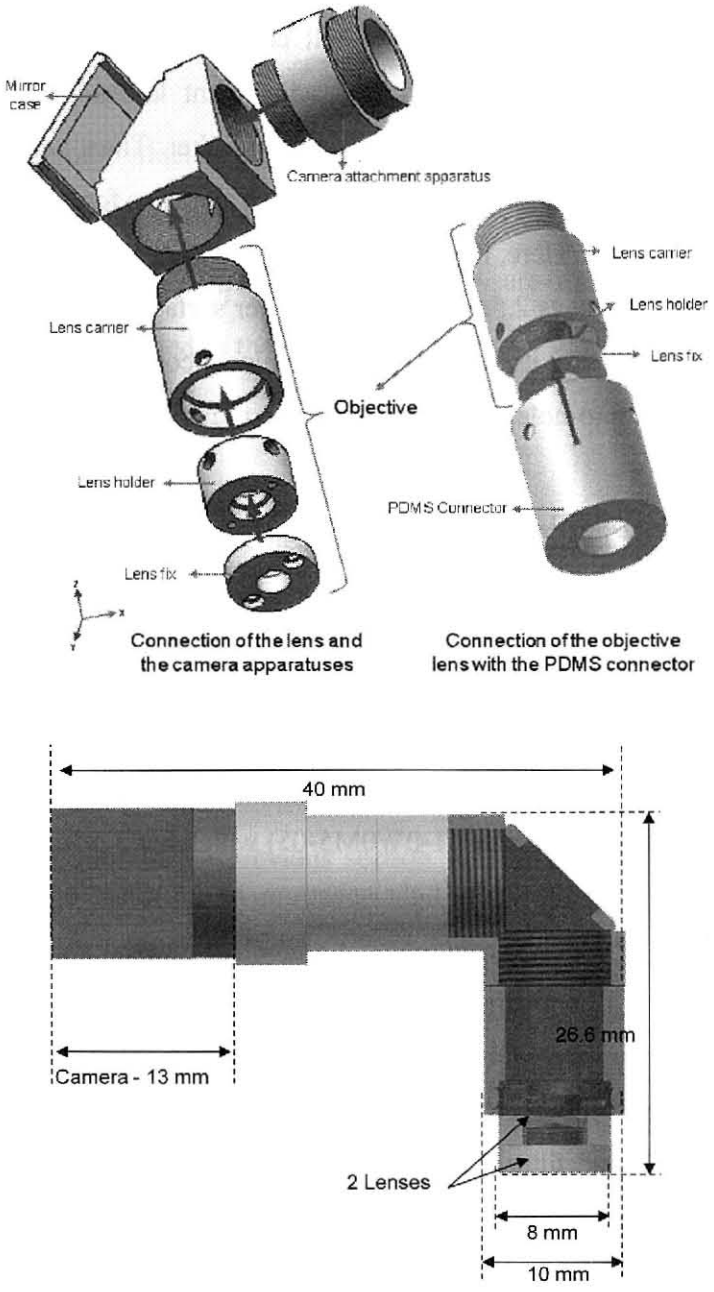

Figure 14, Structure of the miniaturized vision system

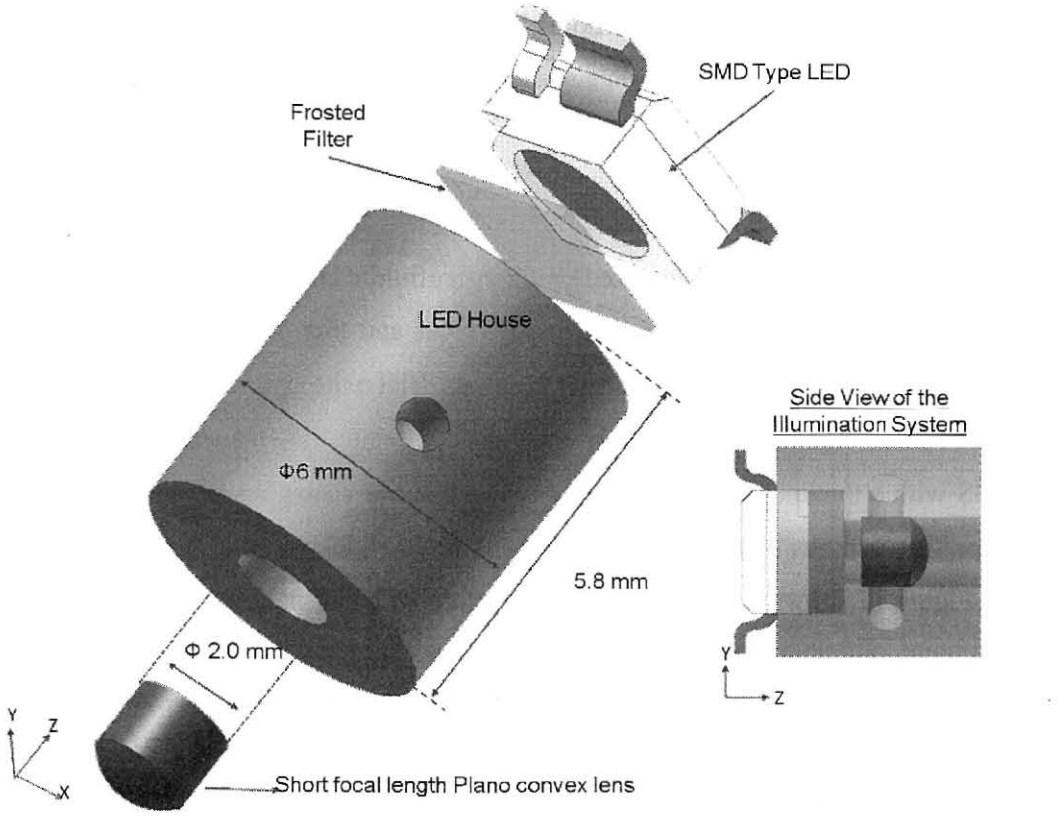

Figure 15, Schematics of the illumination system

2.1.4 PDMS Integration

The PDMS preparation and integration of the imaging system are depicted in Figure 16.First, an initial PDMS layer (depicted as the first layer in Figure 17) including micro channels was prepared. The micro-channels were patterned on negative mold master by pouring PDMS mixture, which was degassed in vacuum conditions. Prosthesis with a thickness of ~2 mm was cured for less than 20 min at 100°C in an oven. Then, it was peeled from the mold and treated by air plasma using expanded plasma cleaner for 1 minute together with a slide-glass rinsed in ethanol. The slide-glass was placed on the prosthesis and a pressure was applied until they bind firmly to each other. Then, the inlet and outlet were connected to silicon tubes before mounting.

This constitutes the first layer of the whole chip. The thickness of this layer was chosen as 2mm to allow fine adjustments of the vision system so that the channel is kept within the focusing range.

After each of the optical component is aligned properly and fine adjustments of the connectors are done, the vision system is integrated to the microfluidic chip in two essential steps: First, the PDMS connector is placed on the first PDMS layer and then decant another layer of PDMS until it exceeds the level of connector about 1 mm. Since the opto-hole has a depth of 2.5mm, the liquid PDMS flooding into the hole does not cling onto the lens surface. Then a third layer of PDMS with a thickness of ~7mm is poured to jam the vision system into the polymer-based structure. This ensures that the vision system is fixed rigidly so that it will not shift or move around. Figure 17 shows a photo of the finished chip with the integrated vision system.

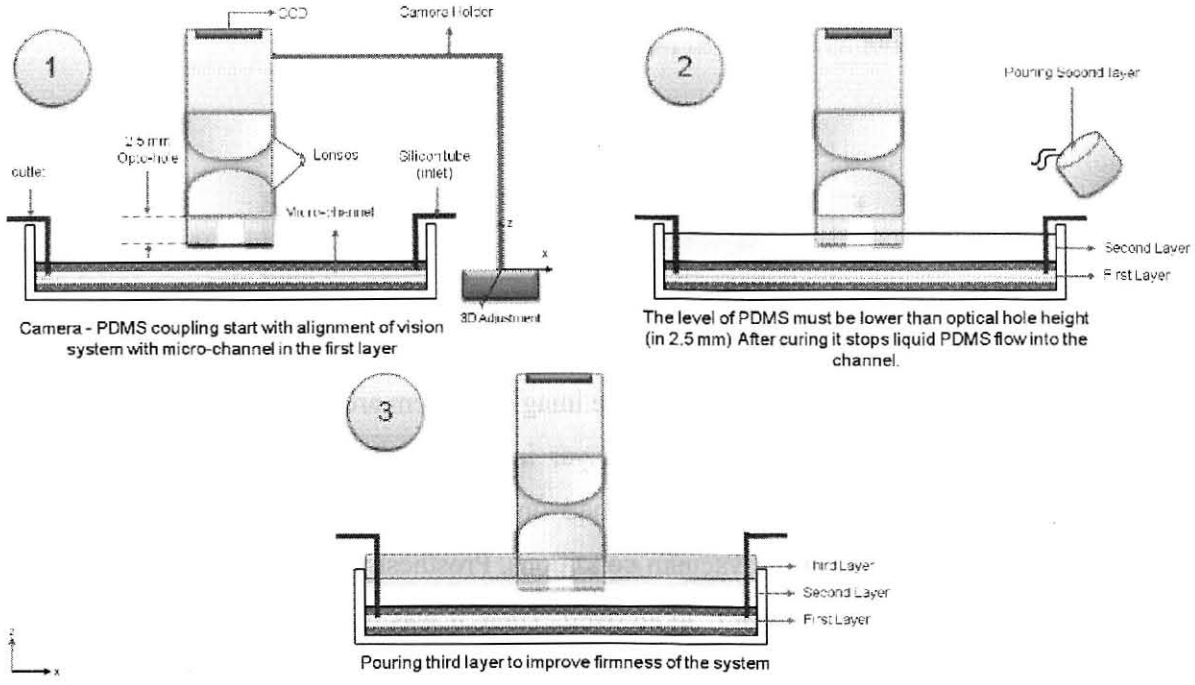

Figure 16, A schematic illustration of PDMS chip making and the integration of the vision system.

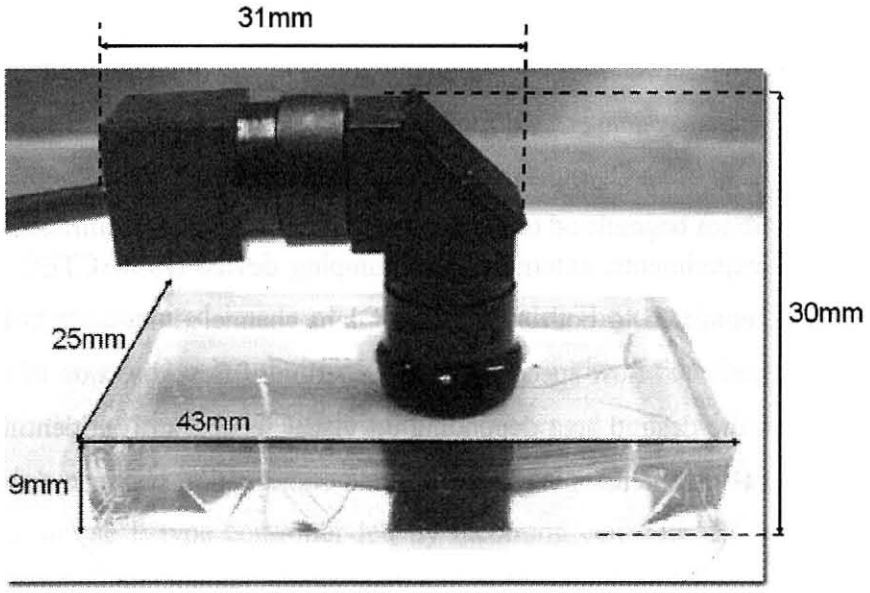

Figure 17, Miniaturized Vision system coupled with SSX-1870 camera on a PDMS chip. Although the micro channels and other two PDMS layers are disposable, the first prototype of current vision system itself does not engage with any disposable components according as its expensive structure.

2.1.5 Experimental Results

Automatic detection and tracking are the critical functions for the accomplishment of a well-controlled manipulation of cells and particles. Every real time detection algorithm must identify the object to be tracked according to environmental parameters. In the system, cell deformation may change the accuracy of the detection task in some cases due to limited depth of field, i.e., the cell may escape out of the fine range of focusing. The background subtraction algorithm was employed through detection phase to eliminate redundant artifacts and to surpass optics-based aberrations. Background subtraction method was essentially applied to moving regions, and the object positions were automatically found after input images were compared with a background image. In this way, it is possible to detect and track multiple objects, too. In the scheme, the program considers the boundary of any moving region as an edge of the object.

After the edge is identified, the algorithm makes a circular approximation to the edge of the object and draws a circle around it. The diameter of this circle is taken as the diameter of the object, as well. The vision system was calibrated by calculating the ratio of the field of view and sensor size with the help of an Olympus Ronchi Ruling glass (100 lp/mm).

Before starting the experiments, external micro-pumping device (ISMACTEC high precision tubing pump) was connected to both side of the micro channel (inlet-outlet). The pump was used for the manipulation of flow speed and determination of flow direction in the capillary to make localization in the desired area depending on visual feedback. The identified cell region was used as a control parameter in order to provide coordination between the pump and the tracking software.

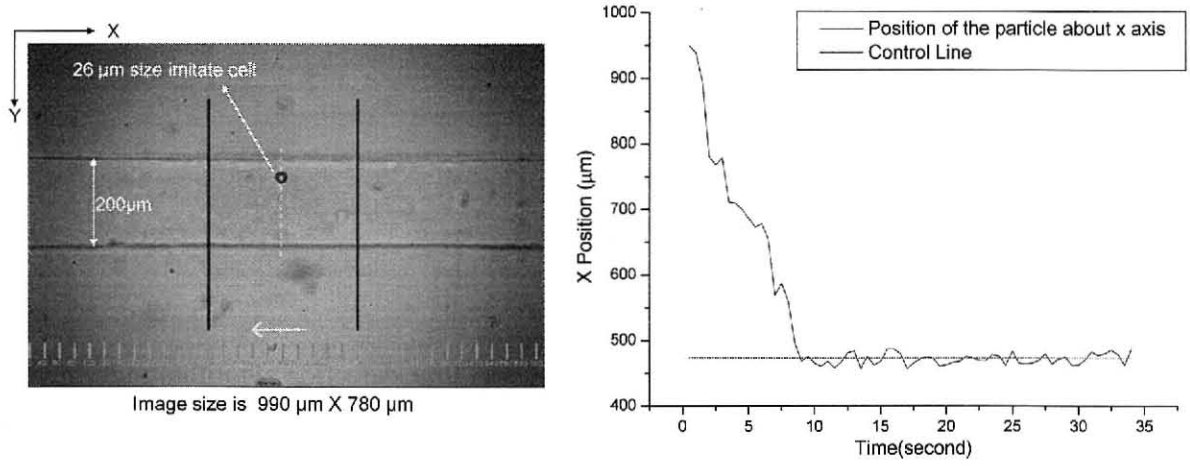

Figure 18, an example of the captured images. Cow donor cells (fibroblast) with sizes in the range 15 µm to 26 µm was simulated using microspheres (Duke Scientific "Latex - polymer" microspheres)

Using the integrated vision system, a number of experiments were performed to test the efficiency and feasibility of the integrated system. During experiments, the micro channel was illuminated by a collimated light as explained in section 2.4.3. It provided uniform illumination

over the micro channel. Moreover, the objective lens was covered properly by introduction of PDMS connector after the micro channel (see Figure 17). Negative effect of stray light caused by emission from an outside light source was effectively suppressed. Thanks to the fine illumination obtained, the threshold value, which was used in the background subtraction algorithm and determined experimentally, did not have to be changed for different experiments.

Figure 18 shows the captured image of ~26 μm particle. The position of the particles in the channel could be observed using the minimum enclosing circulation method, which is run in accordance with the information of image contours processed on the visual data. Results of the position records were updated simultaneously. At the final step, a continuous control operation was done by a simple P type controller fed by incoming cell data. Because of the dynamic environment in the micro channel, the formation of bubbles, which have shapes similar to those of test-particles decreased the total system efficiency. Since the system used a fixed objective distance, resolution was not very good and sometimes, it had detection difficulty. However, this can be easily circumvented using a variable objective or automated focusing mechanism. Even under the present circumstances, the tracking algorithm was successfully implemented for various tasks.

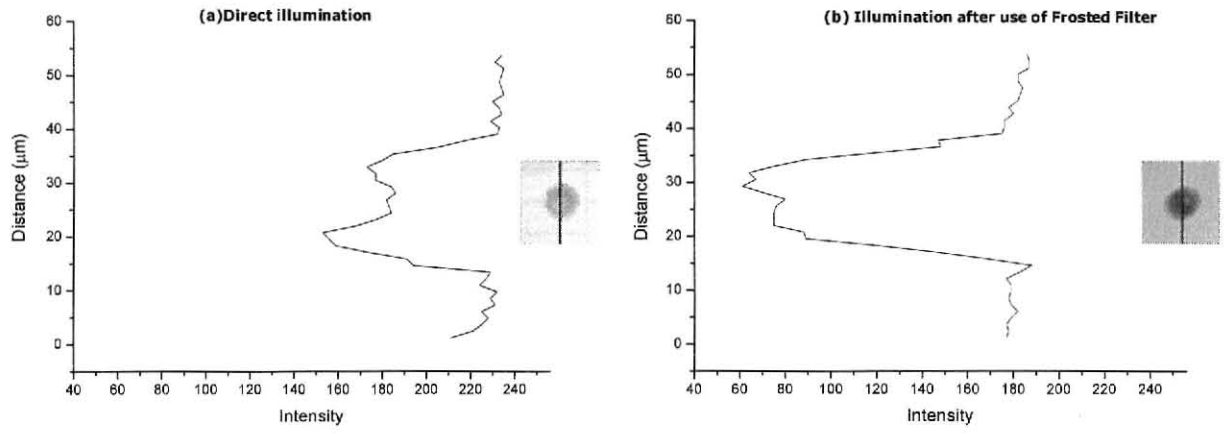

Figure 19, Single particle detection with (right) and without (left) the frosted filter

Since it is known that difference in the brightness of the particles and the background is an important factor determining the detection efficiency, experiments are performed using frosted filter to optimize the system. In Figure 19, we show the images taken with and without the frosted filter. Frosted filter allows a uniform distribution of brightness over the background. As it is seen, without the filter, there is a very bright field in the detected image causing subtle variations of intensity. This bright field was significantly suppressed with the introduction of the filter. In addition, it allowed a uniform illumination over the monitoring region resulting in an enhanced contrast factor.

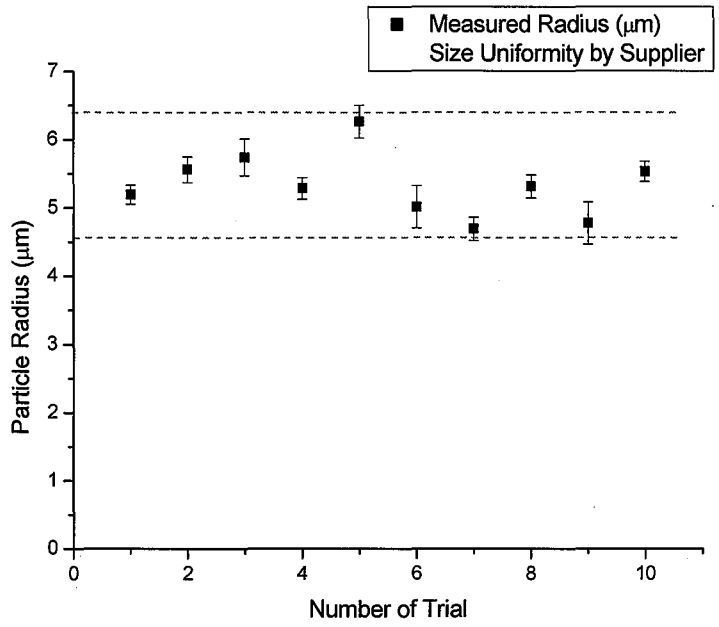

Figure 20, Estimated particle size using the constructed system. Each point in the figure is obtained by averaging 100 measurements with the error bars denoting the standard deviations. Horizontal red lines denote the real size uniformity provided by the supplier

Last experiment was performed to evaluate the system in finding the radius of the particles. The experiment was repeated for the particles of different sizes and good agreement was observed between the measured values and the values in the data sheet provided by the supplier. This experiment was performed using the Plumnet HandyMini camera with a 1/7 inch CCD. After

the fine calibration, the estimated the field of view is 0.96 mm by 0.73 mm (lateral 1 μm line is equal to 0.712 pixels). The results for the particles taken from the batch with average diameter of 11μm are shown in Figure 20. Experiments were carried out as follows: From the batch of 11μm particles, I randomly sampled 10. Then, each of the ten particles was transferred into the micro channel and let flow with an almost constant speed (43.8 μm/sec.). For the each particle I performed 100 measurements. From the captured images of the moving particles I calculated average radii and their standard deviations. As it is seen from the figure, the measured values lie within the range of possible particle size given in data sheet by the supplier who claims 18% size uniformity for the 11 μm batch.

2.2 Second Prototype based on Reflected Illumination

The second prototype system provides good image quality, allowing data on the oocyte and fibroblast cell to be extracted from the acquired images [56]. In this second version, the optical setup was changed and designed a task specific system which has a 1.5 mm monitoring area and light source on the same side as the CMOS camera connection. The specifications are given in Table 3.

Table 4, the specification of the second prototype system

Design wavelength	nm	587.6
Focal length (Objective lens)	mm	7.5
Effective aperture	mm	1.85
f/number		4.1
NA		0.123
Refractive index (Water)		1.3334
Depth of Focus	μm	25.8
Magnification		4.7

2.2.1 Design of Prototype System

This prototype can be placed and aligned on a chip with the aid of xyz micro stages[1]. As shown in Figure 21, the new system is small and can be combined with the microfluidic chips easily. This makes it possible to observe the cell container and microfluidic chip simultaneously in a short distance. Otherwise, as it is details given in next chapter, a user would have to use several commercial microscopes, which require a large workspace and the use of a long Teflon tube to connect the micro-glass tube to the inlet port of the PDMS chip.

[1] The detailed figures of lens system design are given in the Appendix Section

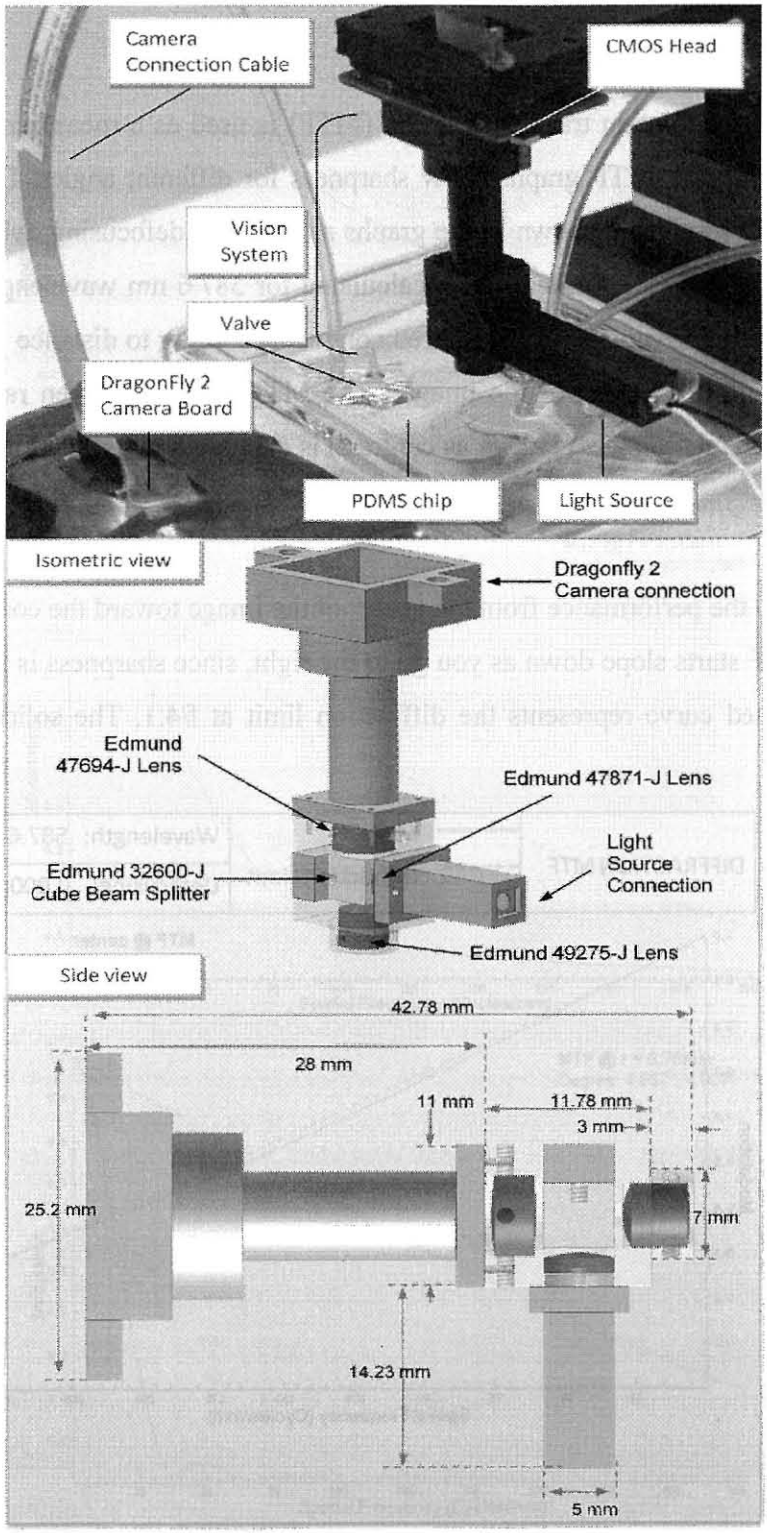

Figure 21, Compact Vision system design

2.2.2 MTF Test Results

In this study, the modulation transfer function (MTF) is used as a measurement parameter of optical quality [55][57]. MTF graphs show sharpness for different angles. Diffraction limited (perfect lens case) results are shown in the graphs as well and defocusing, which causes blurry image, set as 0.00. MTF performance was calculated for 587.6 nm wavelength. Four different MTF graphs plot the percentage of transferred contrast according to distance from the center of the objective plane (the center of the image). The MTF results at given radii, are shown in Figure 22. The modulation (also known as contrast) is expressed in terms of a percentage (1.0 = %100).

The graphs show the performance from the center of the image toward the corner (farthest from the center). MTF starts slope down as you go to the right, since sharpness is usually best in the center. The dashed curve represents the diffraction limit at f/4.1. The solid curves represent MTF.

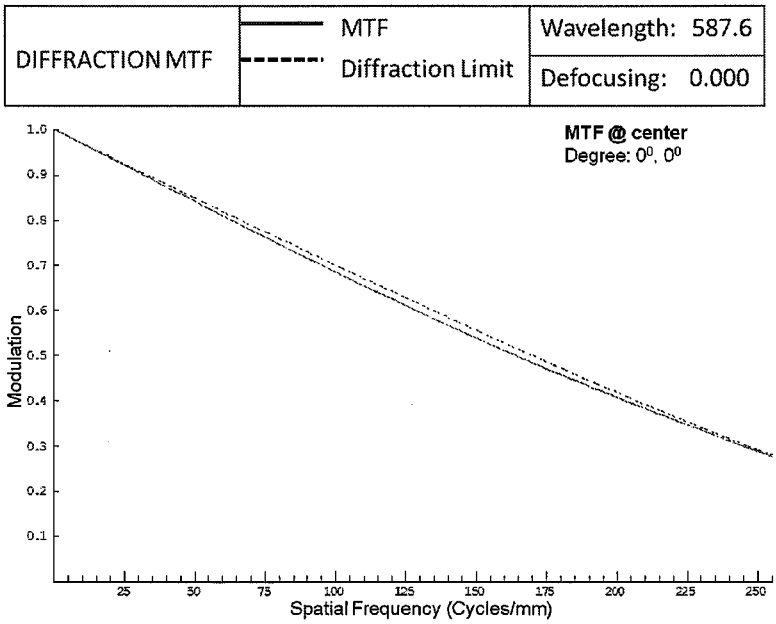

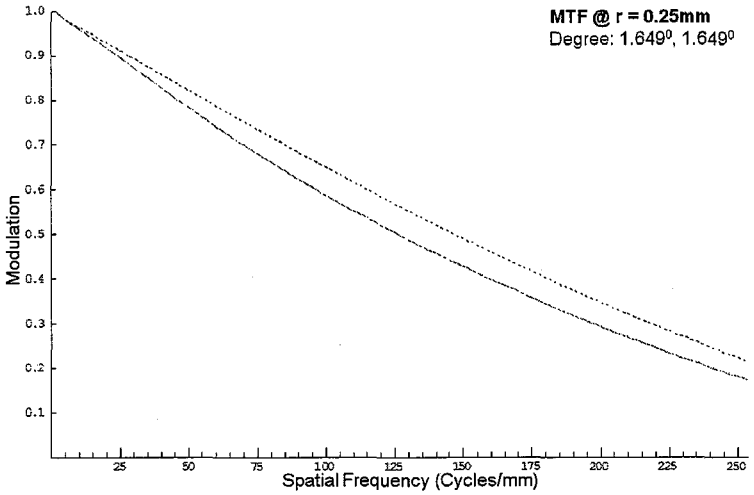

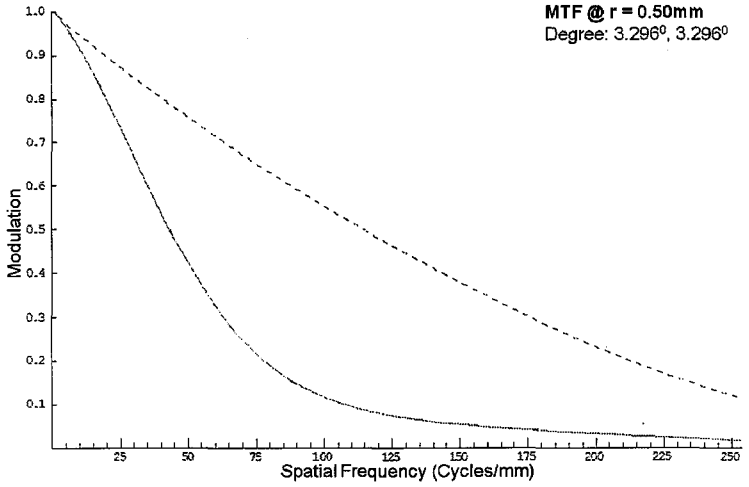

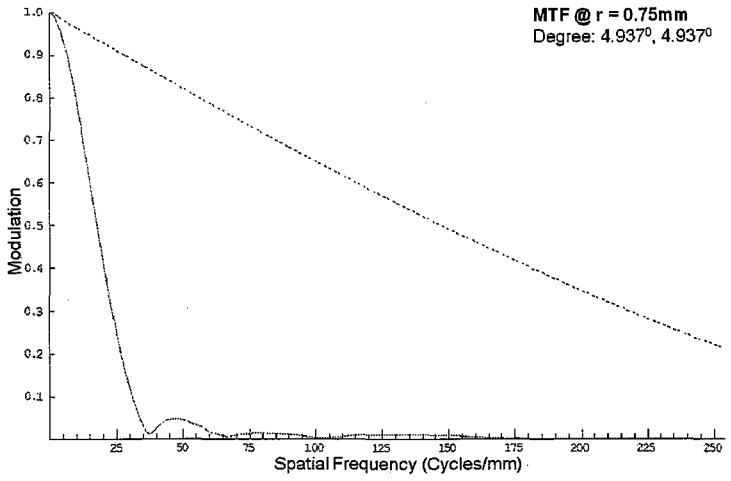

Figure 22, The MTF Results

2.3 Third Prototype based on Disposable Structure

The interest in dynamically tuning lens has attracted great attention to fabricate compact vision systems. Recently, a lot of efforts have been made by utilizing adjustable optical properties of polymer structures. Those are tunable photonic waveguide, miniature optical sensing and heat controlled microlens chip. The liquids themselves provide an attractive actuation mechanism. A tunable lens integrated with liquid pressure system is made to observe micro level objects such as living cells (fibroblasts or oocytes) in a PDMS micro-channel.

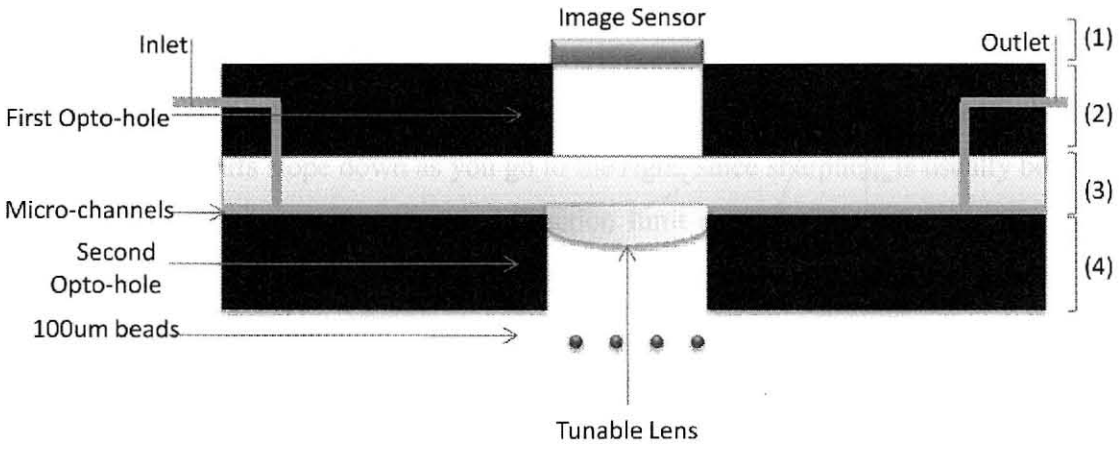

Figure 23, Schematic view of the "On-chip Disposable Compact Vision System". (1) Image Sensor, (2) First PDMS Melanin Layer, (3) Tunable Lens Layer, (4) Second PDMS Melanin Layer. Inlet and outlet parts are connected to pump. By applying pressure, lens membrane is deformed and it forms a tunable lens with variable focal length.

In this section, I discuss on fabrication and characterization of a simple, tunable, yet fully disposable, except imaging sensor, microfluidic-based optical device. The desired compact system is structured with PDMS. Tunable lens actuated by flow pressure (2mm in diameter) is controlled by a syringe pump. The contrast level is improved by introduction of Melanin cover between image sensor, lens and PDMS chip. With the advantage of tunably, an inaccurate monitoring of an object is eliminated by shifting focal plane.

Taking into account any microscopic system, the main parameters of an optical setup must be satisfied as image sensor (CCD or CMOS), lens setup and package (to stop stray light and enhance contrast). According to these parameters , in Figure 23, the proposed system using disposable polymer is illustrated. The CMOS image sensor is only non-disposable part. The all other parts are fabricated by using PDMS polymer. The vision system consists of 4 layers. The first layer is the image sensor holder. The second and fourth layers are opto-hole fabricated with mixture of Melanin and PMDS which provides opaque-hole, stops stray lights. Third PDMS layer forms the tunable lens.

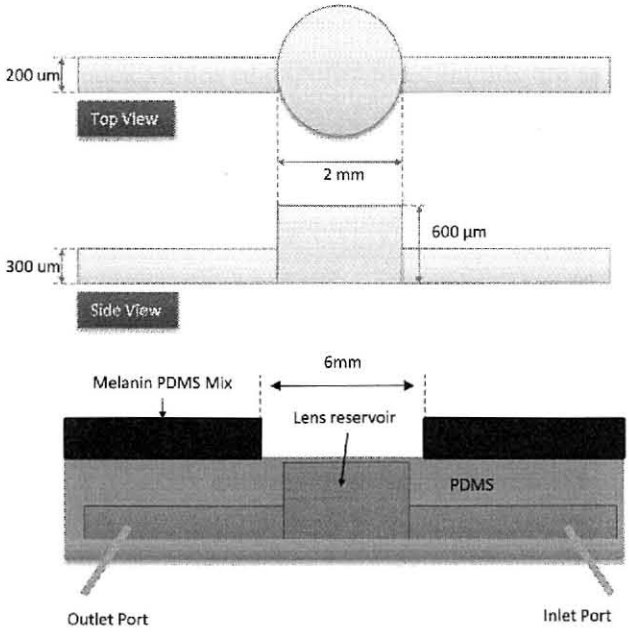

Figure 24, Schematics of the tunable lens system, which show position of inlet and outlet. Solid Melanin-PDMS layer is aligned with the lens layer under the microscope.

2.3.1 Vision System Design

2.3.1.1 Lens Structure

The molds of the tunable lens were patterned on a silicon wafer with the heights of 300µm and 600µm for channel and lens reservoir respectively, using SU8-based photolithography, which has been described elsewhere [58]. The PDMS material from Dow Corning [59]was used, as it

provides several excellent material properties for a tunable lens such as good transparency from 400nm to 1700nm, Young's modulus of 4.8 MPa, a maximum elongation of 420%. The refractive index of PDMS polymer is n = 1.415 at a wavelength of 532nm [60]. The plano-convex fluidic adaptive lens is consisting of PDMS fluidic lens reservoir and fluidic channels are connected two side of the tunable lens layer. The lens reservoir is in 600μm depth and 2mm in diameter. The PDMS lens reservoir and its membrane are fabricated together as shown in Figure 24.

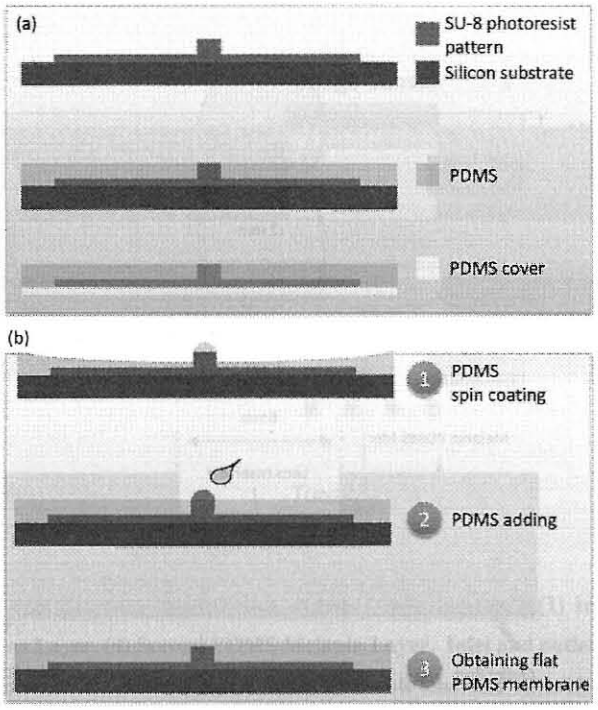

Figure 25, Resulting PDMS chip consists of a thin membrane layer. With this technique, additional membrane is not required. And also, it provides strong membrane structure as well as uniform lens formation.

The lens layer was fabricated with two steps process. In the beginning; the PDMS was spun coated on the mold 200 rpm for 100 second. Afterwards, the small amount number of PDMS was added on the lens reservoir and spun coated 10 sec 100 rpm. At the end, we obtain flat PDMS layer after repeating same operations several times (Figure 25). Finally, we cured PDMS at 60^0C oven and peeled off from the mold carefully and opened inlet and outlet ports.

2.3.1.2 Lens Liquids

The high refractive index liquids may leak from connection points of Teflon tube and PDMS inlet-outlet ports. Thus, the permeability limits the type of liquid which can be employed in the experiments. High diffusion rate liquids are small enough to diffuse through porous connection such as pure water or pure water and ethanol mixture (1:1). Liquids with low permeability, which characteristics are suitable for tunable lens, sometimes leak under the high pressure. Immersion oil and Sylgard 186 (without Catalyst) were found to not diffuse through the inlet or outlet ports easily. We used immersion oil for following experiments due to its better performance. The refractive index values of experimented liquids are as follows.

- Pure water: n = 1.33
- Pure water and Ethanol Mix (1:1): n = 1.35
- Sylgard 186 without Catalyst: n = 1.41
- Glycerol: n = 1.47
- Immersion oil (Cargille –Series A): n = 1.62

2.3.1.3 Melanin and PDMS Mixture

Melanin PDMS mixture was placed between tunable lens and micro-chip. Melanin (0.1gr) and PDMS (10gr) mixture solution was mixed roughly 10min. The spectrum analysis of the resultant combination is given in Figure 26. As shown in figure, using enough melanin, an opaque PDMS layer can be obtained. It stops any scattering or stray light under the visible light as improving contrast linked to resolution. This cured mixture was placed as opto-holes in the two layers of the MicroVision system. As the one was located between object and lens, the second one was located between CCD and lens.

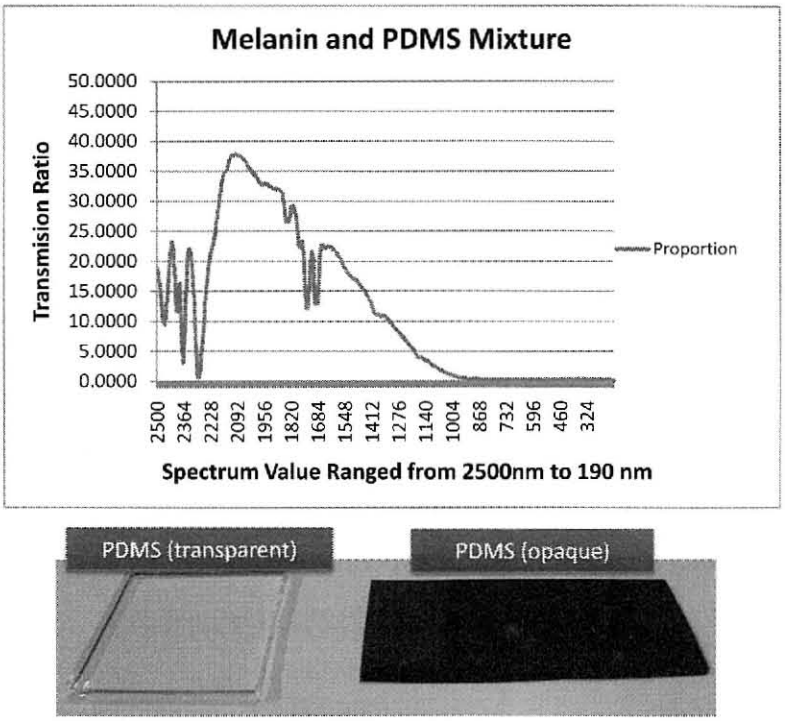

Figure 26, Spectrum graph of Melanin PDMS mixture. Transparent PDMS turns into opaque after adding the melanin.

2.3.1.4 Vision System Setup

The opaque PDMS layer is prepared and punched with 11mm and 2mm thickness to use as first and second opto-hole layers. The first one's hole size, which is between the tunable lens and CCD (Pointgrey Dragonfly 2 with external CCD board), is 6mm in diameter. Second opto-hole size, which is between lens and object, is 3mm in diameter. The second opaque PDMS layer is bounded irreversibly with the lens layer after plasma treatment. The first opto-hole layer is attached using silicon glue for reusability. For precise alignment of lens and CCD, first, the negative copy of CCD is taken via PDMS and then, the center of the negative mold is bounded on the opto-hole under the microscope. The Teflon tubes were connected to both side of the tunable lens layer and sealed using silicon glue around due to avoid unwanted leaking which causes decreasing inner pressure. At the end, the all setup is connected to micro-stage for fine adjustment of lens. The whole compact vision system is shown in Figure 27.

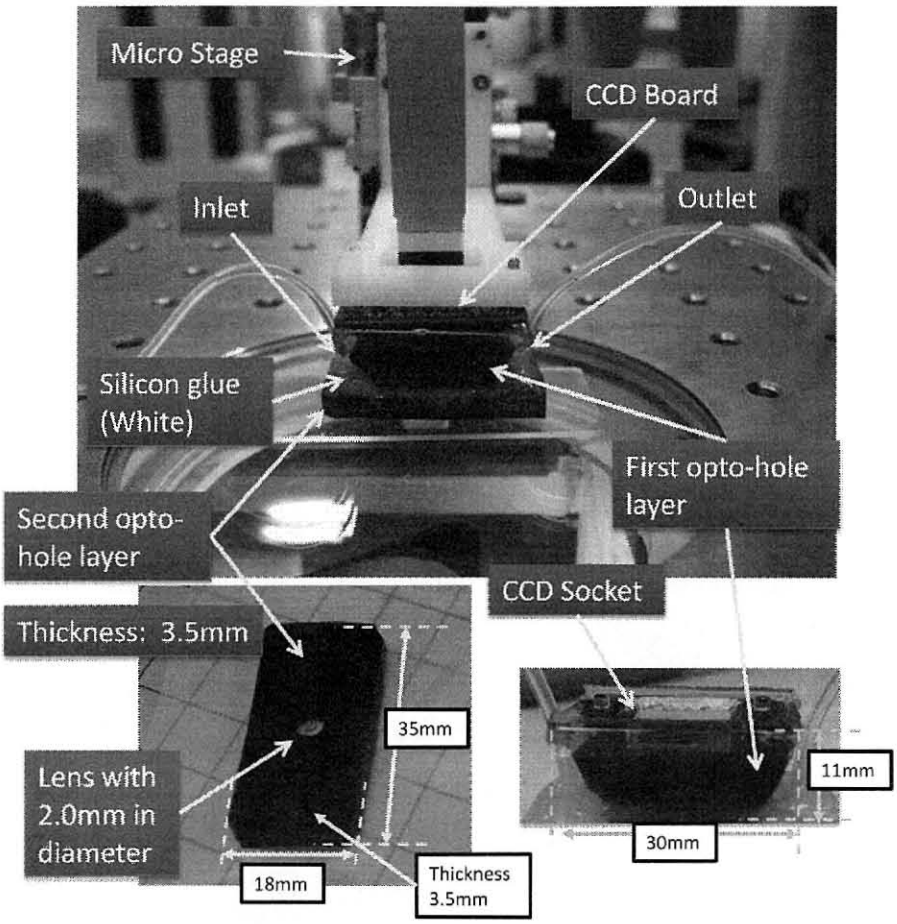

Figure 27, Disposable MicroVision system. Size: lengthxwidthxdepth (18mmX35mmX14.5mm)

2.3.2 Preliminary Experimental Results

The liquid forms body of the lens and provided membrane curvature creates shape of the lens. With different liquid pressure using the KDS pump (Kd-Scientific KDS270 micro-syringe pump), the curvature of the lens can be varied, as a result in changes of the focal distance. By varying the pressure from negative to positive, depended on KDS pump pressure, plano-convex lens may be formed (Figure 28). With fluid injection, the PDMS membrane is deformed elastically to a convex shape. If pressure level reduces, the radius of curvature of the PDMS membrane decreases, that causes the reduction of the focal distance. In fact that, negative pressure may form a concave lens, due to scope of this dissertation, it results are not discussed.

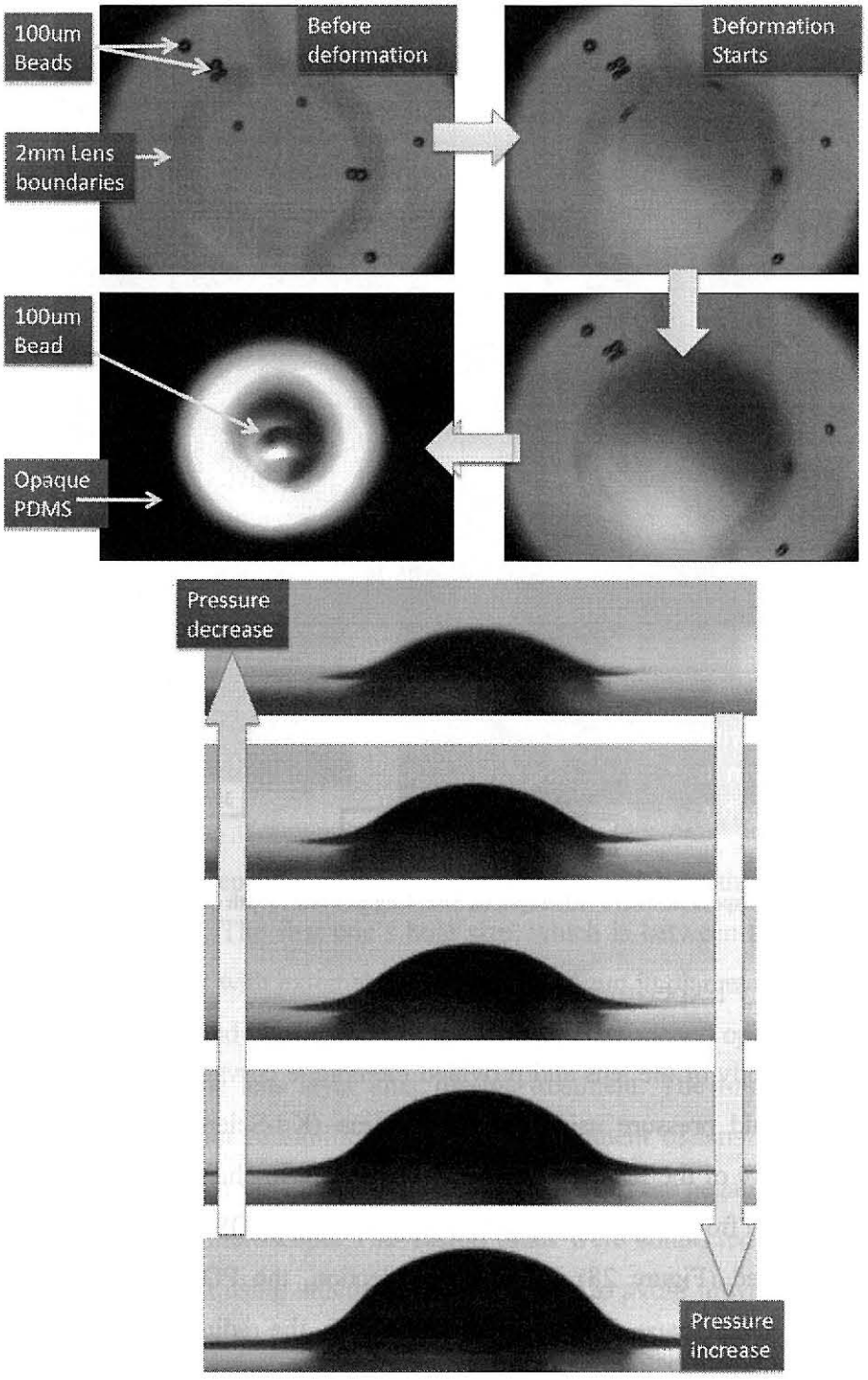

Figure 28, 100μm beads were monitored by microscope through the tunable lens in order to present lens deformation effect. Uniform membrane deformation was achieved with the advantage of the single level tunable lens layer (non-external membrane).

The focal length can be tuned freely by applying pressure through a fluidic channel. In terms of change in focal length, varied magnification levels were also achieved. Under the halogen light, the vision system was focused on 100μm beads and acquired images with 3 magnification levels which are shown in Figure 29. The lens performance was evaluated with transmission sinusoidal target pattern (Edmund Optics M-19-80, 2 to 256lp/mm) for fixed curvature. The results with 4 different MTF patterns are given Figure 30.

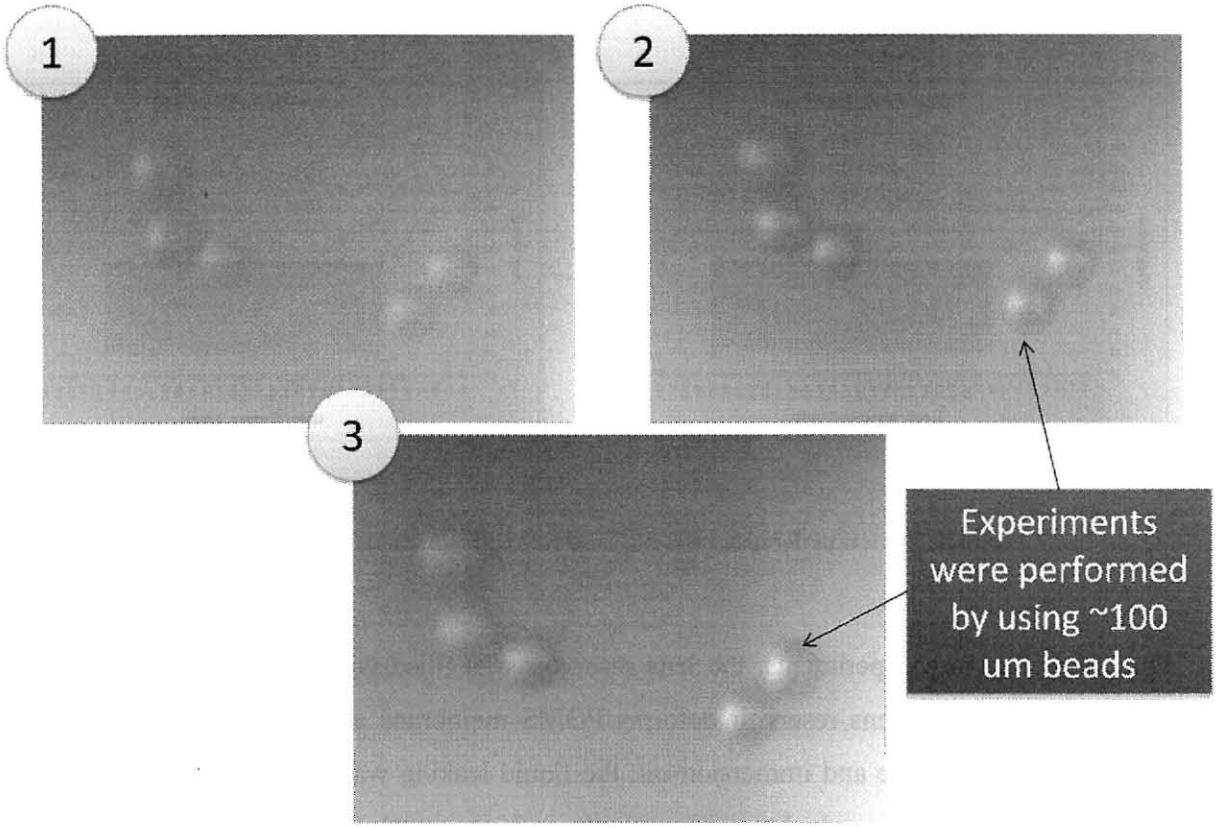

Figure 29, 100um beads are shown with different magnifications.

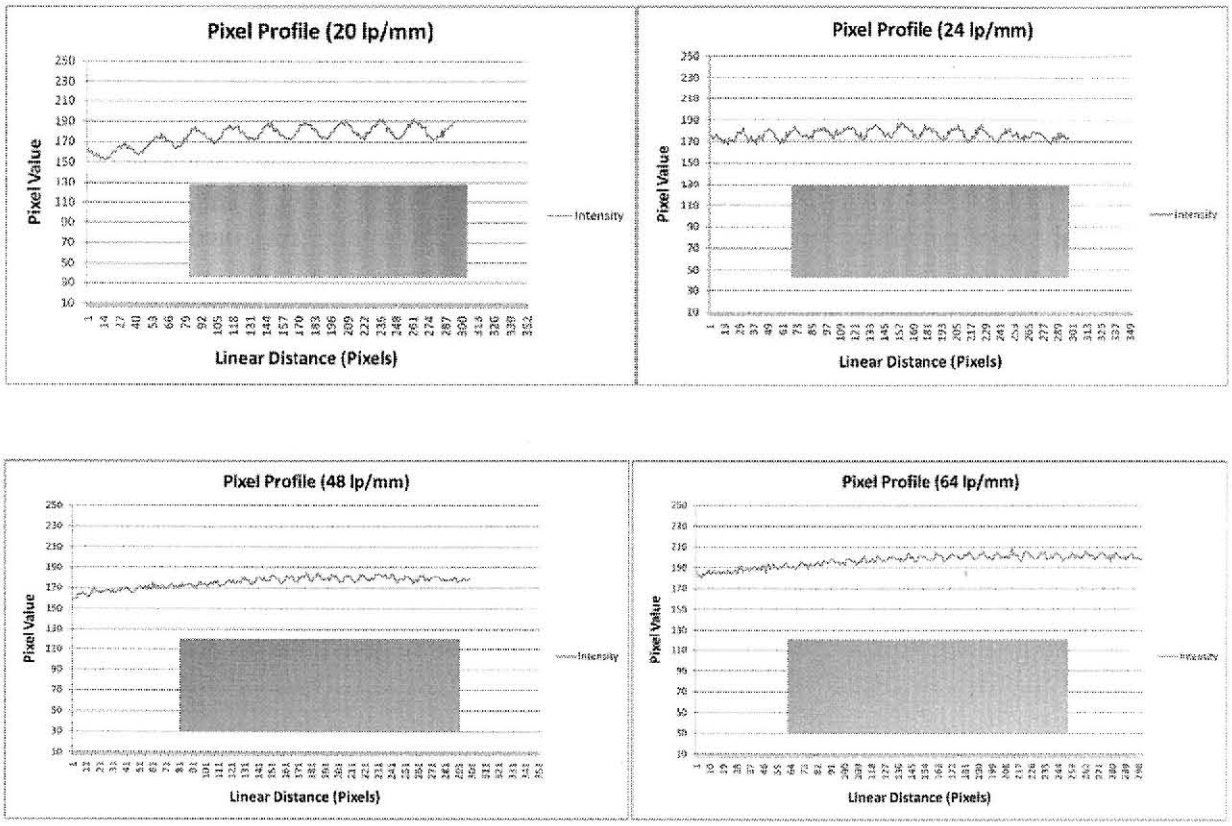

Figure 30, The lens performance was evaluated with transmission sinusoidal target pattern.

For the preliminary experiments, the lens reservoir was filled with immersion oil. Increasing liquid volume in the lens reservoir deforms PDMS membrane and shapes like a lens. Using non-external membrane and immersion oil, the liquid leaking was managed in micro-channel. However resulting images had some image aberrations, mostly caused by non-uniform light dispersion. Those aberrations, cloudy effects, decreased the contrast on the acquired image as it is seen in Figure 29. In the graphs of Figure 30, the vertical increments on intensity levels (pixel value) show that effect of light irregularity on the acquired images. Even if melanin introduction between layers increase the contrast, the aberrations happened, while transmitting inside the lens liquid. This aberration indeed reduces the real-time performance as well.

The future works may be concentrated on elimination such effects in order to obtain high contrast. For further experiments, the system will be improved for higher resolutions such as 10μm objects under the halogen light environment which is also related with the scope of Automated Cell Cloning project. In this project, monitoring mammalian oocyte and fibroblast cells of sizes in the range of 10μm to 100μm is a essential concept. With uniform light dispersion, the system will be associated with the detection/tracking and control program, which will be mainly programmed for single cell applications, explained in following chapters.

Chapter 3: Vision-based Single Cell loading and Supply

The gentle cell manipulation and loading into microfluidic chip one by one are the key steps of some cell based microfluidic applications. Because, in some cases such as cell cloning, any damage on cells could cause experimental failure.

Microfluidic methodologies, however, have suffered from limited means to manipulate fluids and cells. In conventional method, the single cell transfer and control from a container to in a PDMS microfluidic chip is carried out by the aid of a micropipette suction and manual on-chip stream manipulation by a pump. Biological cells must be picked up from the container one by one under the view of microscope and then, supplied into the microfluidic chip, where single cell operations are performed. For each single cell, an operator should go over the same method again until collecting desired number of cells. Even though this process is somehow relatively easy for big size cells (oocyte ~100μm), it is infeasible for small size cells (fibroblast ~15μm) for repetition of this process. A skilled operator is required for such kind of time consuming applications. Moreover, if the pump speed doesn't synchronize with every manual cell supply process, bubble formation could be observed in the flow stream, which is harmful for living cells. Once the desired number of cells is delivered into micro-channel, they need to be brought into the operation area one by one again. Besides, the distance between consecutive cells cannot be maintained in the micro-channel by manual methods. The principle behind the proposed solution is to accomplish all these functions (cell suction, transportation, on-chip position control, observation and cell supply) automatically with one integrated system.

The motivation in single cell loading and supply system is to support on-chip cell applications such as cell coupling or fusion. The cells must be aspirated precisely from a container. This needs micromanipulation and accurate positioning while approaching the target cell with micro-glass pipette (suction tip) attached to a micromanipulator. After that, a desired number of aligned cell group is stored in a dock. The snake-like shape PDMS docking zone is designed for

this purpose. Once cells are sorted, they are transferred to the next module or operation zone. To do this, "Y" character micro-channel is combined with the docking side and the pneumatic pressure valves are formed at the intersection of it. When the external pump infuses air in the valves, the membrane between layers deflects, closing the fluidic flow. Finally, the synchronization of valves and suction tip are handled via monitoring systems, which provides full automation and system integration. While intersection of PDMS chip is monitored a MicroVision system, the suction tip is monitored with a second MicroVision system. Instead of using two microscopic units, which requires long tube-connection between the suction tip and the microfluidic chip, MicroVision systems are integrated to the experimental setup as a non-destructive sensing method in order to enable high-throughput single cell transfer.

This chapter is divided into three main sections, (1) materials and methods, (2) experimental results (3) discussion and conclusion. In the first section, materials used to create the microfluidic chip and methods for preparing cells are briefly described. Secondly, an automated cell detection/tracking and controlling algorithm is presented along with its applications in the microfluidic chips, micro-manipulators and pumps. In the final section, experimental results indicating efficiency and usability of the total mechanism are described.

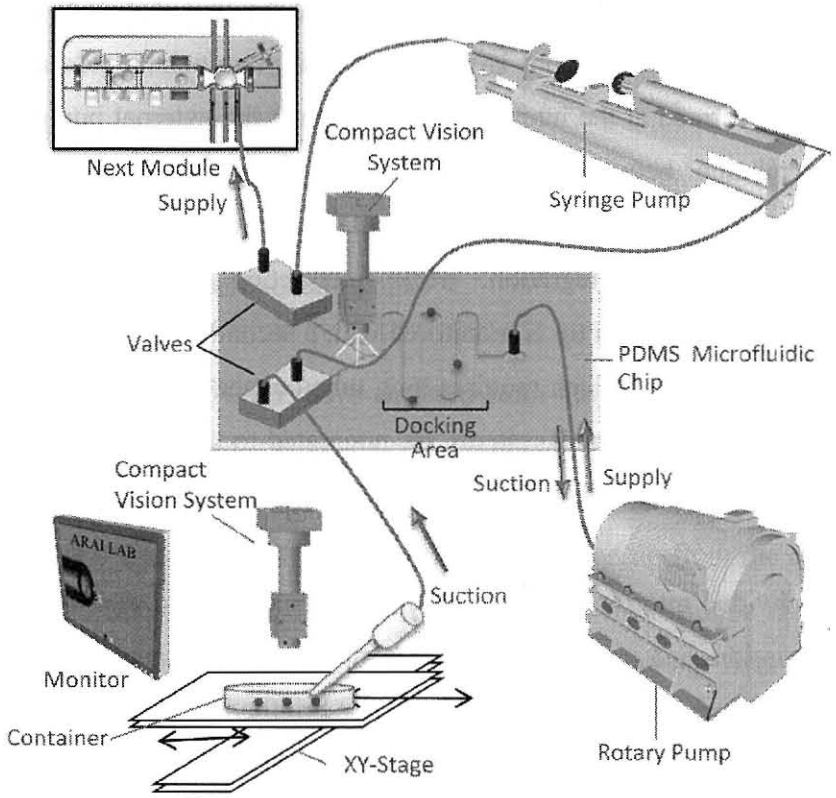

Figure 31, Schematic view of the "Vision-based Single Cell Loading and Supply System".

3.1 Materials and Methods

The proposed system is able to singly pick cells from a container and transport them to a microfluidic chip. The structure allows manipulating cells in microfluidic channels and docking them in desired locations at controllable numbers. However, due to the complex physical properties of oocyte and fibroblast cells, manipulating cells through a microfluidic chip poses certain challenges.

This system is comprised of the parts shown in Figure 31. External pumps, micro manipulators and camera systems are connected to a computer and run automatically based on a "Cell Detection/Tracking and Control" program. All experiments were performed at room

temperature and one microfluidic device was used several times, where the device was cleaned with filtered water after every experiment. Syringe filter (Sartorius-Minisart, hydrophilic) was attached to the end of a syringe to absorb impurities as the water passes through, while it stops contamination in the micro-channels.

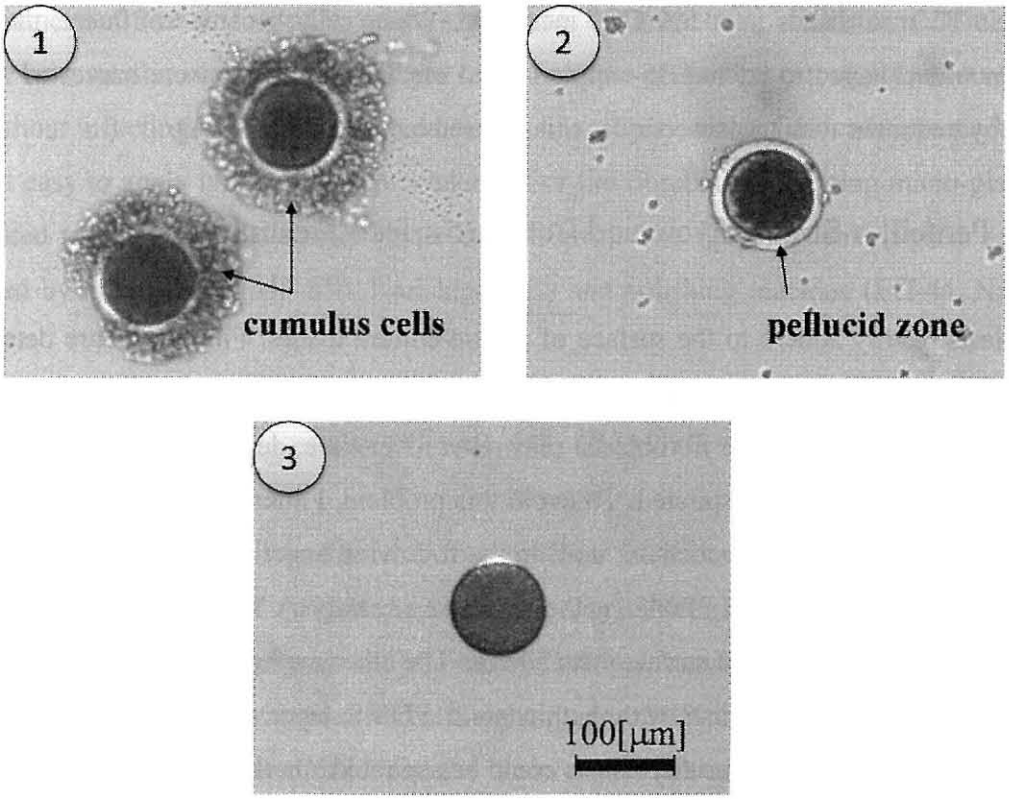

Figure 32, The pellucid zone of ova was removed by pronase treatment

3.1.1 Cell Types and Preparation

Experiments were performed using fibroblasts as fibroblast cells and oocyte cells as recipient cells. Oocyte cells were isolated from either cow or pig ovaries. Ova were cultured more than 24 hours after harvesting from the ovary. In order to detach cumulus cells from the harvested ova, cells were treated with hyaluronidase (Nacalai Tesque Inc.). The pellucid zone of ova was

removed by pronase treatment and near-circular oocyte cells isolated. The isolated oocyte diameter was 100-150μm (Figure 32).

Fibroblasts 10–30μm in diameter were isolated from female cow ears. The fibroblasts were cultured in Dulbecco's Modified Eagle's Medium supplemented with 10% Fetal Bovine Serum (FBS) in 35 mm dishes in a 5% CO^2 incubator. When cells became confluent, the culture medium was changed to 0.5% FBS-supplemented media. Fibroblasts were harvested from the dishes by treatment with trypsin- ethylenediaminetetraacetic acid (EDTA).

3.1.2 Penicillin-Streptomycin and Bottom Surface Treatment

Fibroblasts readily adhere to the surface of plastic culture dishes. Fibroblasts are detached by trypsin-EDTA (Wako Pure Cemical Ind, Japan) treatment [61], then waited over 30 minutes and attempted to aspirate the fibroblasts. However, over time, detached cells re-adhere to the culture dish and cannot be aspirated. To avoid this problem, I attempted two different methods to treat the culture dish. One method, used in the following experiments, was to paint the dish with a small amount of liquid PDMS (without the use of catalyst). This method is also known as siliconizing [62], ie. coating a surface with silicon. The other method was to pour PDMS (using a catalyst) and cover the dish with a thin solid PDMS layer. In the case of non-treated containers, less than half of the fibroblasts could be aspirated. On the other hand, the cells in the PDMS-coated dish were all easily aspirated. While the solid PDMS layer also aided fibroblast aspiration, there were irregularities in the PDMS surface, and additional time was also required.

3.1.3 Cell Suction System

In the acquisition process of a single cell, first of all, the rotary pump (ISMATech Inc.) was connected to the dock side of the PDMS chip via a Teflon tube [2](outer diameter 0.5mm - inner diameter 0.3mm). The main route starting from the dock side port (outlet port) to glass micro-

[2] Please see the Appendix for the detailed information.

glass tube was on the same line. Therefore, flow speed and flow direction in the micro-channel, as well as the speed on the tip of the micro-glass tube, were handled by this pump. During experiments, I recognized that small diameter tubes decrease the possibility of creating of cell stacks on the intersection point of the inlet port and the Teflon tube. Hence, the micro-glass tube and the cell delivery channel were connected using another Teflon tube (outer diameter 0.3mm - inner diameter 0.2mm). I used a micro-glass tube 0.30mm outer diameter, 0.18mm inner diameter as a suction mouth for the oocyte cells. A micro-glass tube can easily vacuum single cells without inflicting any damage. In addition, it has a noncomplex fabrication procedure that makes it easy to apply into common procedures. For the fibroblast, foregoing micro-glass tube was heated to decrease its diameter (inner dia. ~50μm). The tip of the micro-glass tube was processed by micro forge (MF-830, Narishige Inc.) and polishing machine (EG-44, Narishige Inc.).

3.1.4 The Manufacturing of the Microfluidic Chip

The microfluidic chip employed in this research has been designed to perform two main functions; aligning aspirated cells in docking area, and transferring them to the next module. The molds of the fluidic chip (main-mold), valves (2nd mold) and air-chamber (3rd mold) were patterned on a silicon wafer with different heights, using SU8-based photolithography, which has been described elsewhere [58]. On the main mold, channels for delivering cells were 200μm wide and 160μm deep, dimensions sufficient to contain an oocyte. It has a "Y" shape character and is completed with a snake-like dock which is shown in Figure 33.

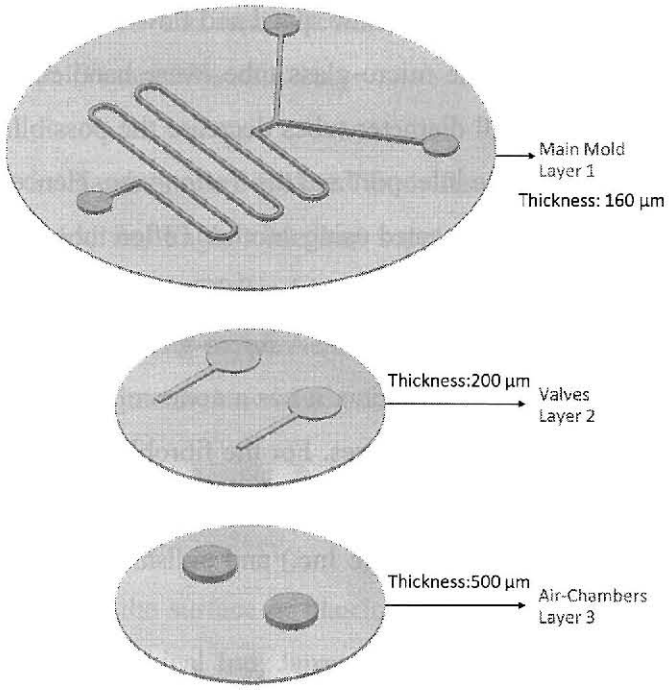

Figure 33, Three positive relief molds were fabricated with different heights to form the main fluidic channels and valves. The molds were created with a single photolithography step.

After preparation of the mold, the PDMS device and the valves were fabricated using conventional multilayer soft lithography technique. The entire chip is illustrated in Figure 34. Firstly, a thin layer of PDMS (thickness: ~300µm), the first layer, was spin coated on the main mold, then cured for less than 20 mins. at 100°C in an oven. The same method was repeated for the second layer, which also contained the valve. As incorrect placement of the second layer (thickness: ~250 µm), containing a thin membrane, may obstruct flow permanently, the first and second layers were carefully aligned together. The valve layer was completed by adding a PDMS slab containing an air-chamber (depth: 500µm). Then, the combined PDMS layers were treated by air plasma using expanded plasma cleaner for 1 minute together with a slide-glass rinsed in ethanol. The slide-glass was placed on the prosthesis and a pressure was applied until they were firmly bounded to each other. Finally, the total microfluidic chip was sealed with PDMS and cured a second time.

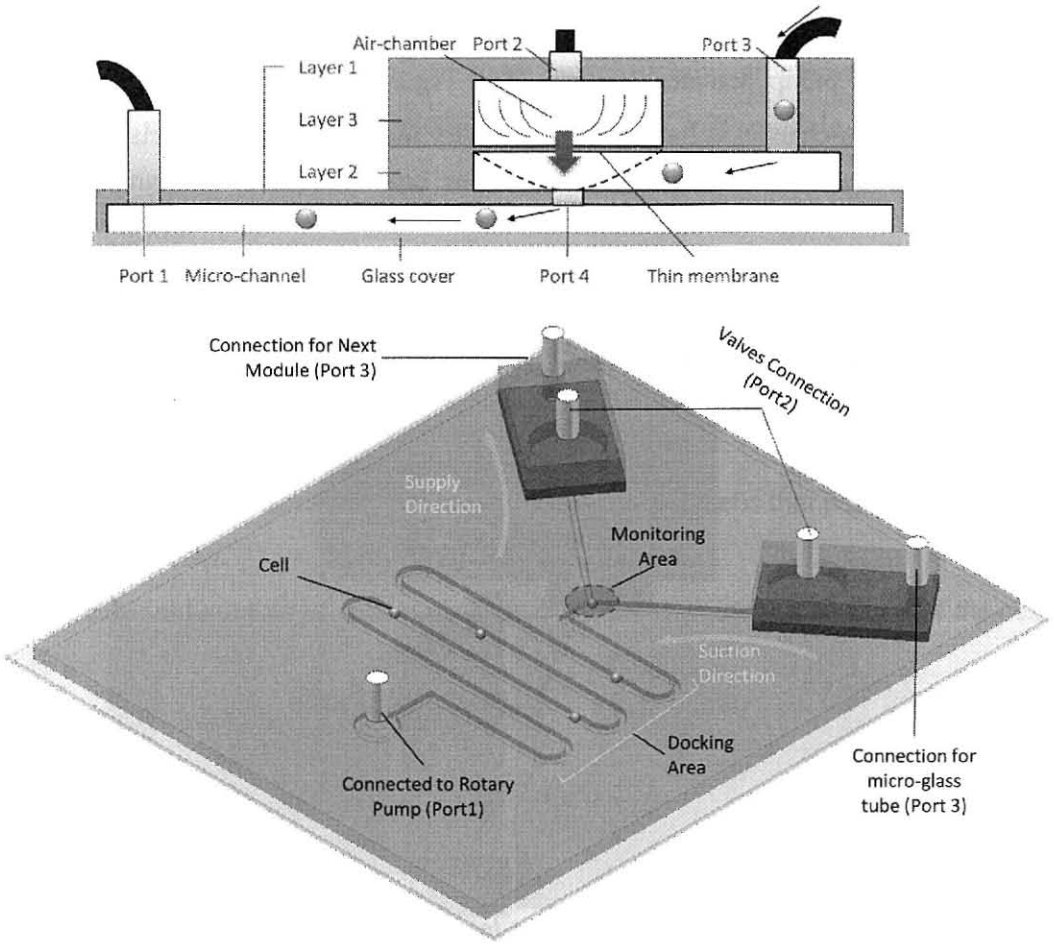

Figure 34, Port 1 is connected to a rotary pump that controls flow speed and direction in the fluidic channel. A thin PDMS membrane is actuated with Port 2 connected to syringe pump. When the air-chamber is filled with air, it closes the gate (Port 4) for the fluidic channel and stops cell flow from the loading inlet (Port 3). The "Y" character channel controls supply suction and supply directions by switching valves (indicated in green).

3.1.5 The Valve Control Principle

Within the PDMS chip (Figure 35.a), a valve region is pushed by applying air pressure to the air-chamber and obstructing the micro-channel. The air pressure control valves for "open" and "close" actions are activated by a syringe pump (Kd-Scientific KDS270). The syringe pump

links two valves so that one becomes "closed" if the other becomes "open" (Figure 35.b, Figure 35.c). In addition, the flow behavior of "Y" shape channel can be observed by use of color pigments, when the pump actuates (Figure 35.d, Figure 35.e). The control of the current direction in the micro-channel is handled by the rotary motion of a high precision rotary pump (ISMATech).

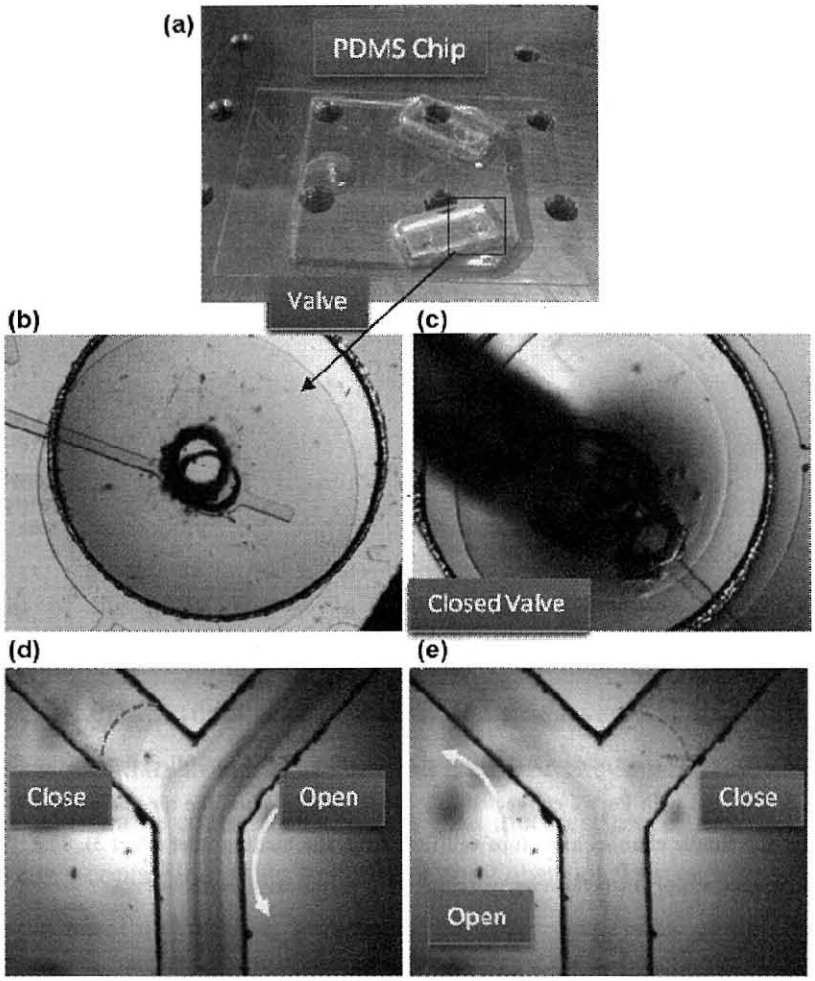

Figure 35, Valve Control Mechanism. (a) 3 Layer PDMS device with valves (b) Valve structure (c) Closed Valve activated by air pressure (d-e) Color pigments movements while the chip is in the suction or the supply mode at the speed of 40µl/min.

3.2 Cell Detection/Tracking and Control Program

The detection/tracking and control program was mainly programmed for single cell applications[3]. It can control several modules including TCP/IP module, camera module, and image processing module, pump and micro-stage controllers. Its execution steps can be described as follows:

a. Start the first camera and detect the position of single cells in the cell container.
b. Align the micro-glass tube to the cell position and begin suction (ISMATech rotary pump).
c. Toggle to the second camera and count the number of cells that pass the cross section in the PDMS chip.
d. If the desired number of cells passes the cross point, switch valves and let the cells flow to the next module.
e. Switch valves (KDS Pump) and cameras if a second group of cells are required.
f. Transfer cells to cell-coupling module
g. Track a single cell in cell-coupling module.

A background subtraction algorithm was employed throughout the detection phase in order to eliminate redundant artifacts and to surpass optics-based aberrations. The background subtraction method was essentially applied to moving regions, and the object positions were automatically found after input images were compared with a background image. In this way, it is also possible to detect and track multiple objects. After the edge is identified, the algorithm makes a circular approximation to the edge of the object and draws a circle around it, which is taken as the diameter of the object.

[3] For other techniques used in this program, please look at Appendix

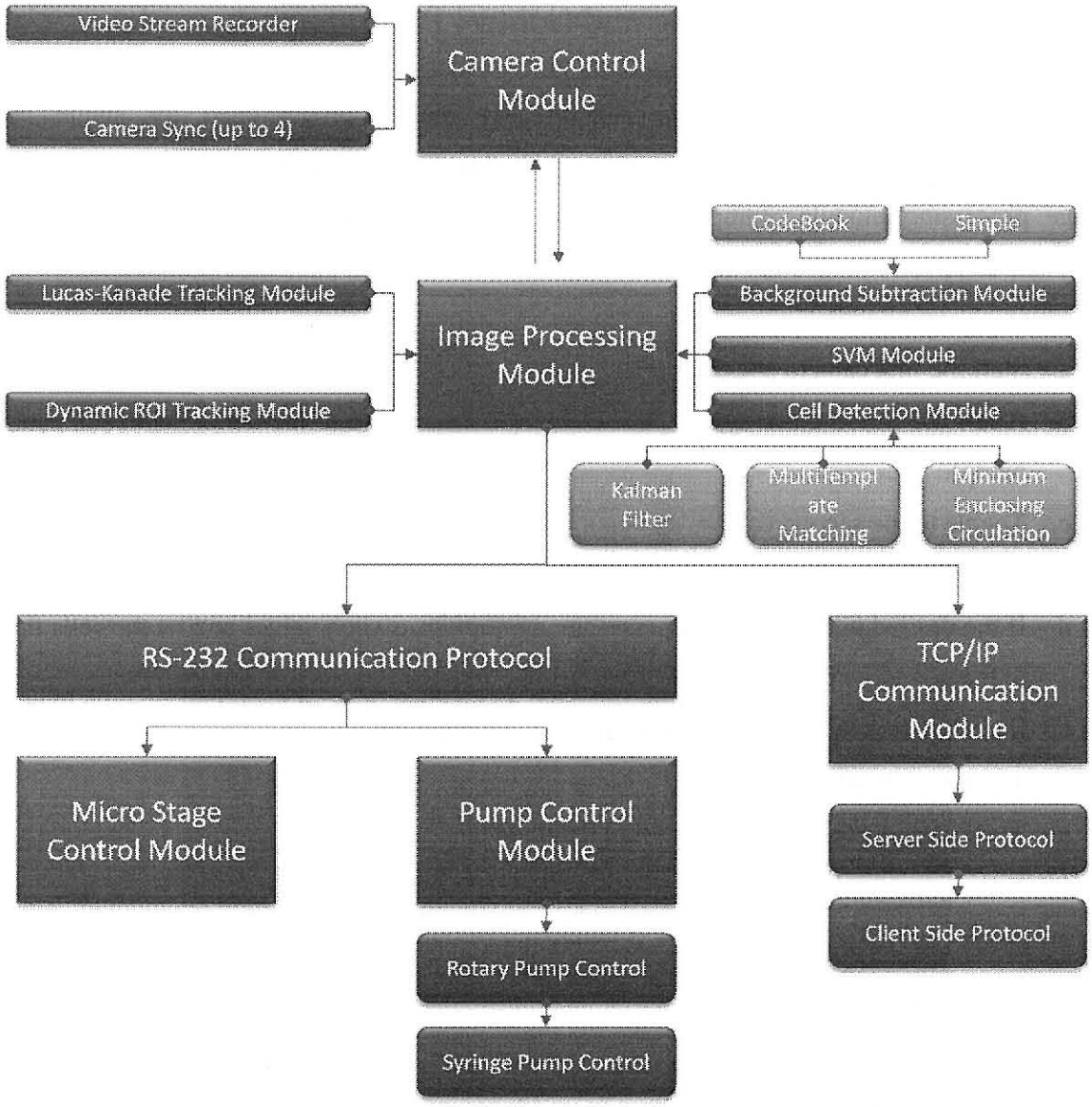

Figure 36, The Cell Detection/Tacking and Control Program modules. Each modules works based on data acquired by synchronized cameras. All camera units are connected to same image processing algorithm to find cell positions. Image processing algorithm utilizes Multi-template matching accompanied by Support Vector Machine (SVM), kalman filter and minimum enclosing circulation to detect single cell position and automatically initialize tracking. For different cases, 2 tracking methods are applied: Dynamic Region Of Interest (ROI) and Lucas-Kanade Tracking.

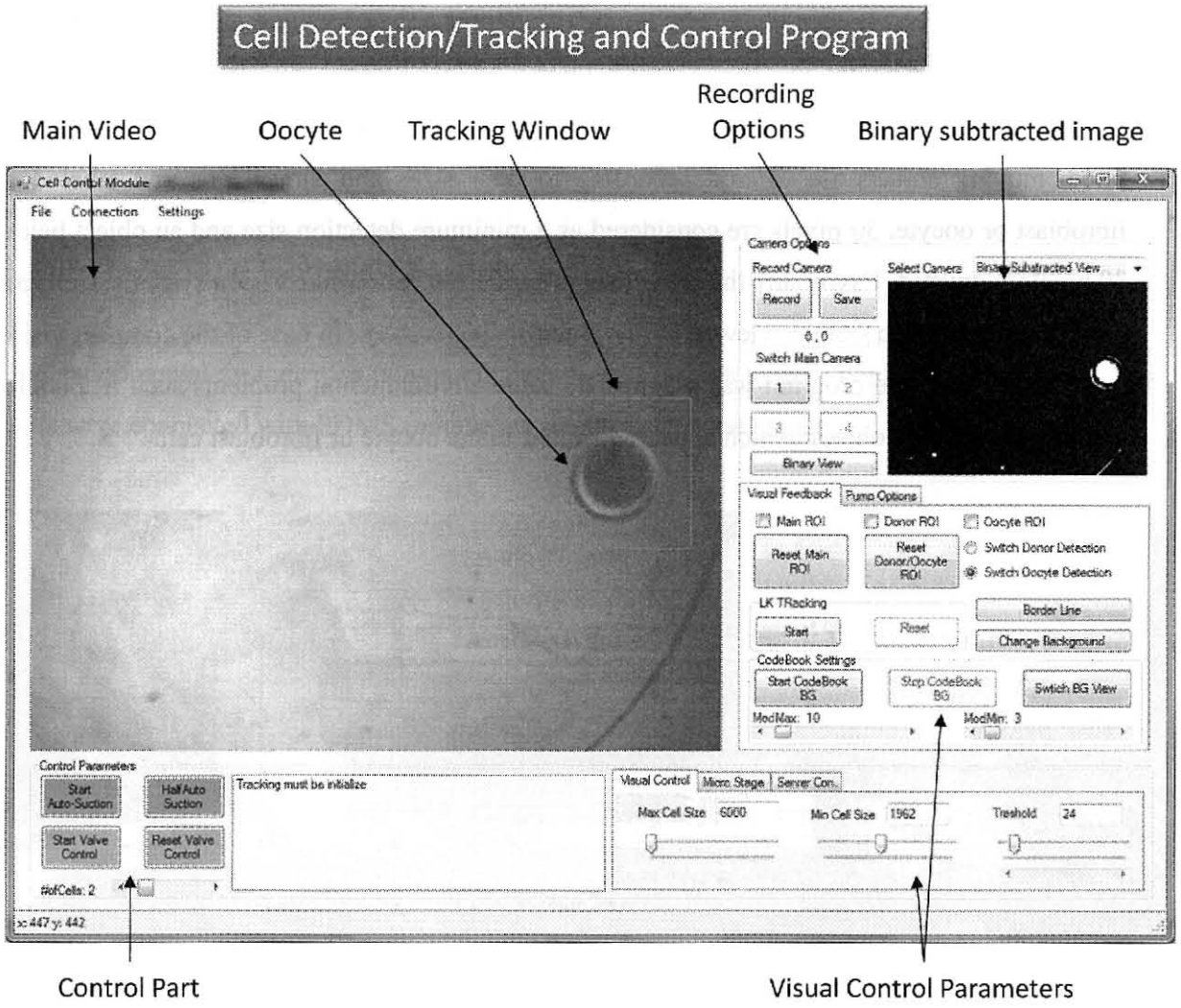

Figure 37, the program was written by Managed Visual C++. Visual programming method made control of different modules easier. All different setups for each modules and visual camera feedback were placed on the same form. The program supports 4 different camera systems at the same time and allows to real-time video recording either raw or compressed. A user can selected a desired number of cells and start whole process.

It is important to note that the relative size of each pixel in a digital image is very important. To determine accurate diameter, ratio between single cell image reconstructed on image sensor and corresponding total pixel number must be calculated. The pixel ratio for each cell was calibrated

by Olympus Ronchi Ruling glass (100 lp/mm). A fibroblast cell ~15 μm corresponds to about 30 pixels. In addition, the program consider the boundary of any moving region as an edge of the object, because cells always come into the observation area one by one. Once background is fixed, moving objects are filtered according to their sizes and dimensions and labeled as fibroblast or oocyte. 30 pixels are considered as a minimum detection size and an object below 30 pixels is omitted. Essentially the same idea is applied to both MicroVision systems. Cells are only floating in the container viewed by the microscopic camera. In case of the compact vision system, however, the program was plagued by some environmental problems such as bubbles and other redundant objects which appeared similar to the oocyte or fibroblast cell.

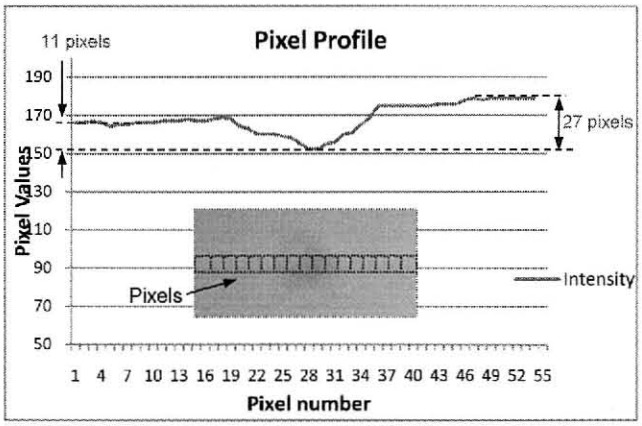

Figure 38, Pixel intensity changes according to pixel number to extract fibroblast cell from background. Minimum intensity change is used as default threshold value.

As oocyte cells are ~10 times bigger than fibroblast cells, requiring a deep channel depth (150 μm), the fibroblast cells can easily go out of focus range and hence the image becomes blurred. Furthermore, the fibroblast cell is very transparent under visible light. Even though its shape is near circular, because of the light conditions, in most cases, it is complicated to extract its features from the background (Figure 38). After entering the micro-channel, due to light dispersion over the fibroblast cell, high density parts become darker, while bright areas frequently converge to the background color. Although the system could often capture the

edges of the fibroblast cell through consecutive frames, in some cases, for the reasons explained above, the system could not locate the edges of the fibroblast cell.

3.3 Experimental Results

3.3.1 Oocyte and Fibroblast Suction

The experimental system with pumps microstage and camera system is given in figure 37. All parts were connected with PDMS module and controlled by computer.

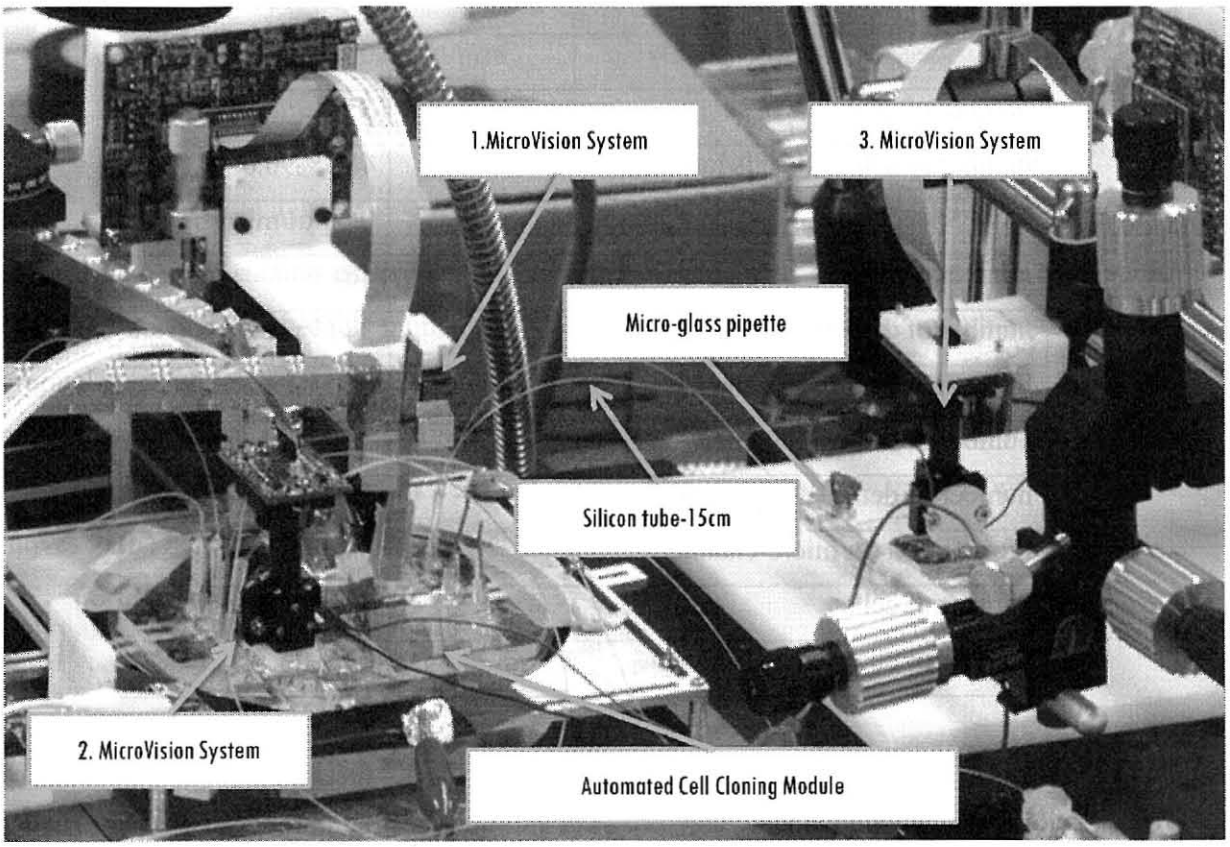

Figure 39, Experimental Setup

After a number of treatments explained in the previous section, the oocyte and the fibroblasts were dispersed in random manner in different containers (Figure 40). Before dispersion, the required flow-speed must be defined in order to stabilize cell detection. In case of the fibroblasts, the ideal flow speed is determined by changing the rotary pump speed as in Table 5.

Table 5, Fibroblast cell detection ratios for different speed of flow.

Flow Speed (in micro-channel)	0.39 µl/min.
number of cells	55
number of detected cells/ratio	55 / %100
Flow Speed (in micro-channel)	0.50 µl/min.
number of cells	53
number of detected cells/ratio	48 / %90.6
Flow Speed (in micro-channel)	0.60 µl/min.
number of cells	46
number of detected cells/ratio	34 / %74
Flow Speed (in micro-channel)	0.65 µl/min.
number of cells	50
number of detected cells/ratio	22 / %44
Flow Speed (in micro-channel)	0.80 µl/min.
number of cells	50
number of detected cells/ratio	0 / %0

After deciding the optimum speed, user program an initial desired number of cells for suction and the program searches for the cells in the container (Figure 41.a). As soon as the program detects a cell or a cell group, it takes the position of the cells, draws circles around each detected cell, and displays their positional information (Figure 40). The suction mouth of the micro-glass

tube aligns with the nearest cell on the bottom surface, which is numbered as "0", and then the rotary pump starts the flow. From the tip of micro-glass tube to node "A" on the microchip, the required absorption time is given in Table 6:

Table 6, Approximate absorption time for one cell from the cell container to the microchip.

Glass Tube Volume	(0.09X 0.09 X π) X 20 = 0.508 µl
Silicon Tube Volume	(0.15 X 0.15 X π) X 200 = 14.130 µl
Micro-channel Volume	(0.15 X 0.2 X 20)= 0.600 µl
TOTAL	15.238 µl
Min rotary pump speed/min	**10 µl/min**
Approximate absorption time	**91.42 sec**

In case of oocyte suction experiment, 10µl/min was chosen as an initial suction flow speed. Once the suction of the cell numbered "0" is completed, the suction mouth returns to the original starting point, takes off from the surface to "safe height" and carries on suction of the medium without cells. After 6 seconds (an experimentally calculated delay used in order to put a specific distance between each cell) the suction mouths return to the bottom surface and moves to the next cell, numbered as "1".

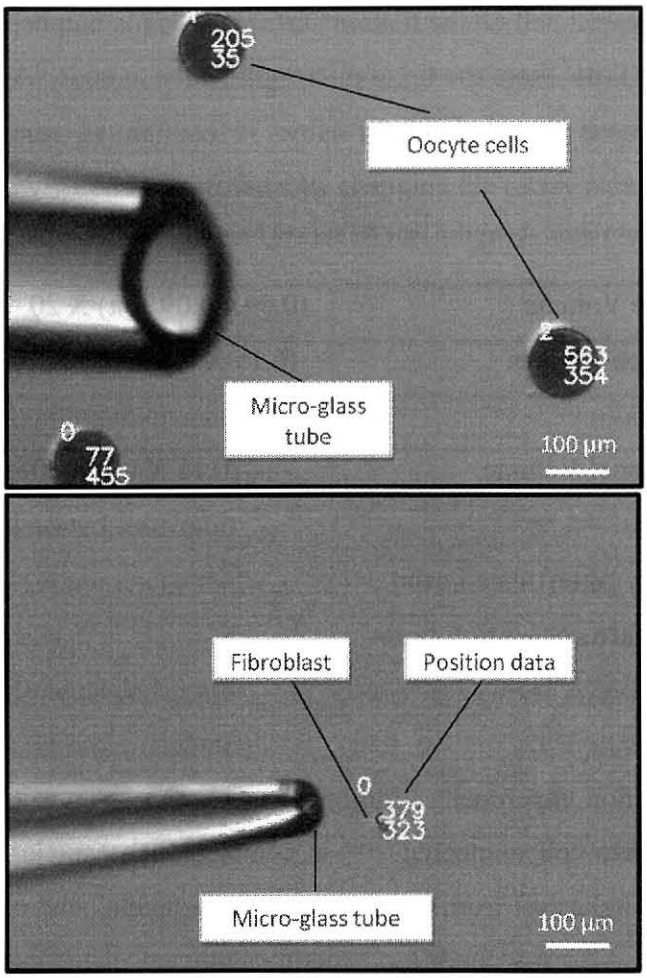

Figure 40, Fibroblast and oocyte suction from a container. The tip size of the glass tube for the fibroblast is approximately 50 µm, and for the oocyte approximately 180 µm. The detection algorithm locates the cells and aligns the micro-glass tube with them.

This procedure repeats until the last cell is vacuumed from the screen view. If the program reaches the total number of desired cells, it stops searching, moves to the "safe height" and continues with the suction, even if there are still some cells on the screen. The aspirated cells are batched in the docking area with a specific distance. The time interval between two connected cells is given in Figure 41.b in both cases of suction mode and supply mode. Although approximate absorption time for one cell until reaching to node A, was calculated as 91.41 sec., the experimental elapsed time was measured as 100 sec. The delay occurred due to the drag resistance of cells as they move through the continuous fluid flow.

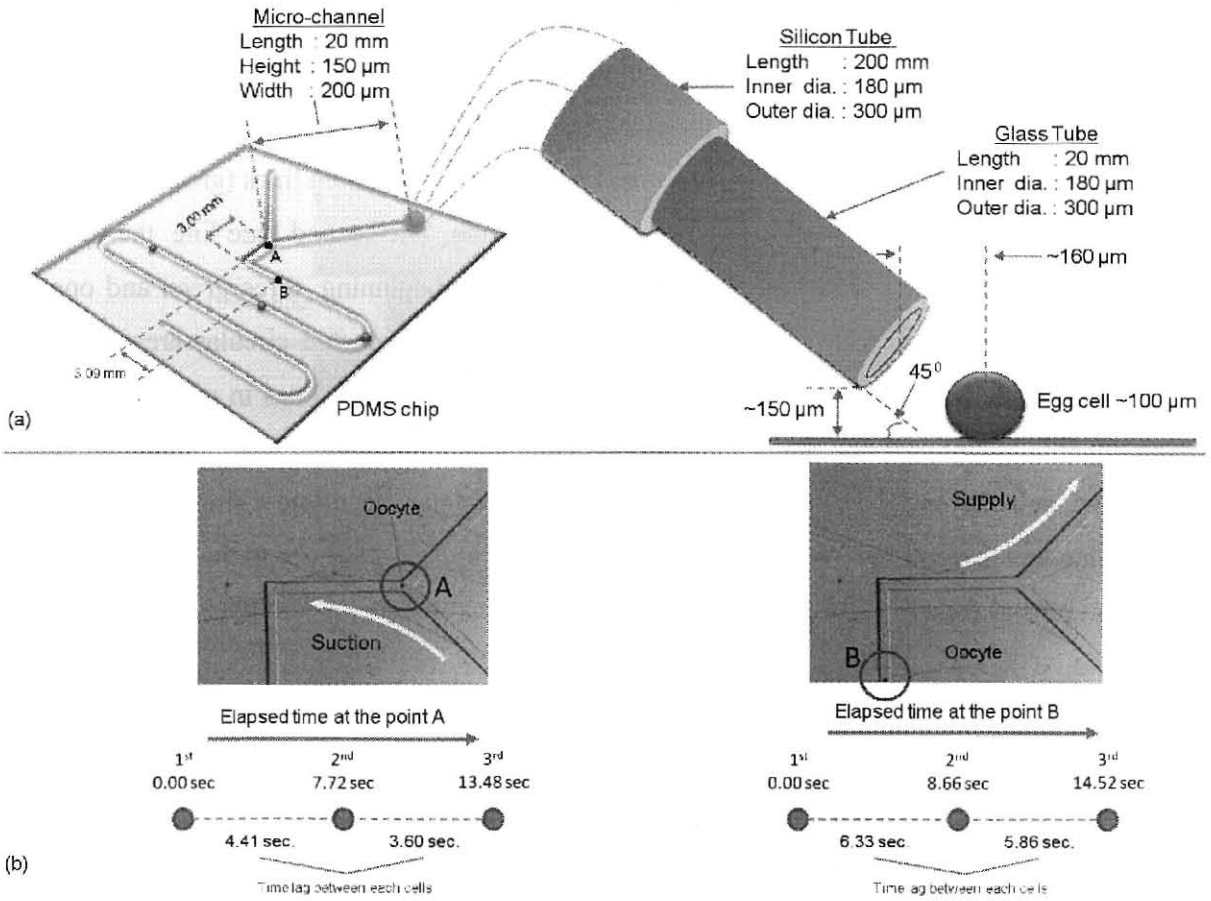

Figure 41, (a) The cell suction system. The micro-glass tube bended 45^0 approaches approximately ~160 µm to an oocyte and vacuum it. (b) After dispersion, time lag between two consecutive cells at the point A and B.

3.3.2 Direction Control

Once the aspiration of the desired number of cells is completed, the camera system on the cell container is toggled to the compact vision system placed on the cross section of the "Y" character micro-channels (Figure 42). The task of the compact system is, by switching the valves, to ensure that the collected cells are gathered at the dock and transported to the next module.

When a new cell shows up from the upper-right hand corner, the program detects cells and starts tracking. To avoid environmental failure in the PDMS chip and to maintain efficiency, four control parameters are added to the "Cell Detection/Tracking and Control" program. These parameters are shown on the screen as sequential lines. The first three lines (green color) are for confirming that a detected cell safely passes to dock side. The second blue line, the upper-left hand side, counts the number of cells transferred. In the beginning, three green and one blue parameters toggle as "false". As soon as the center of the detected circular area of the cell passes a single line, it toggles to "true". After it passes three green lines in order, the program counts this as one cell and waits for a second cell. When the desired total number of cells is reached, cells in the dock are transported to the next module. Each time a single cell passes the blue line this is recorded for the final confirmation. To start cell transfer to the next module, the system runs as follows:

a. The rotary pump connected to the end of the "Y" shape channel stops the flow.
b. The syringe pump applies pressure to the right pneumatic valve (infusion) while releasing the left valves (withdraw). In experiments, time elapsed during valve switching was measured to be approximately three seconds.
c. The main flow direction is reversed.
d. The rotary pump starts running again and transfers cells in the batch to the micro-channel on the left.

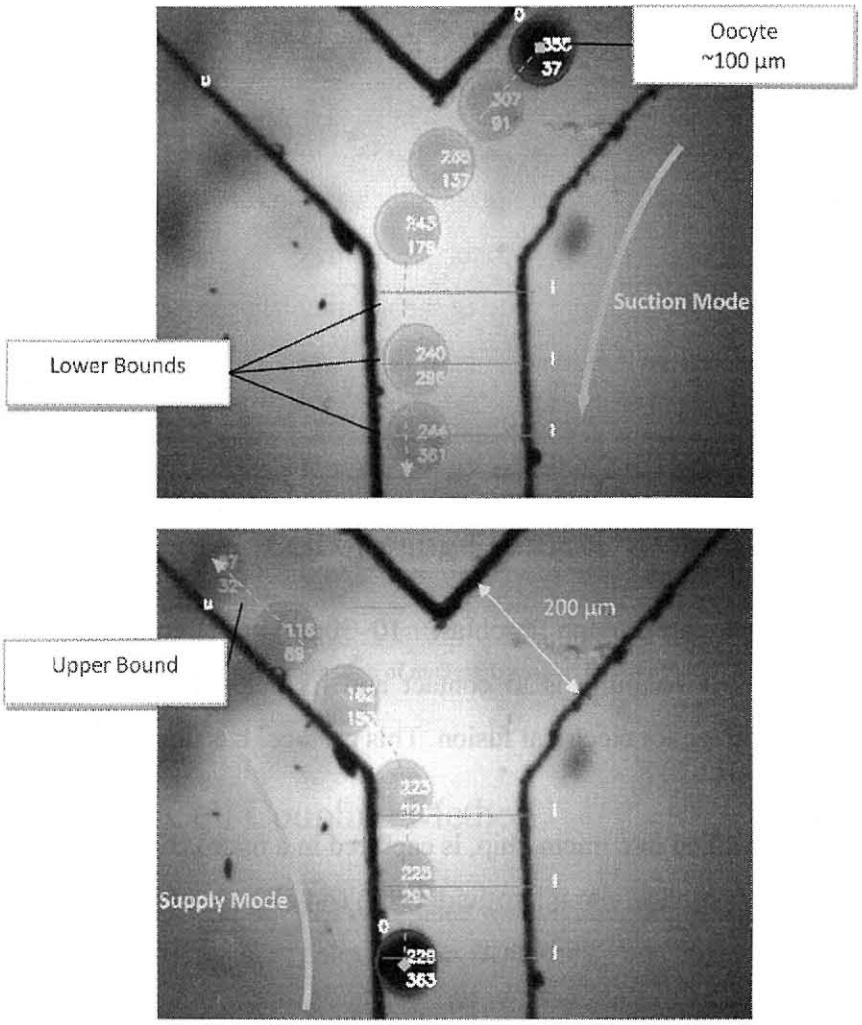

Figure 42, Experimental result for tracking and controlling an oocyte in the microfluidic chip. The images were taken by the compact vision system. Dashed lines with transparent oocyte figures for both images show trajectories in case of suction and supply modes.

Chapter 4: Cell Coupling

The cell coupling is a critical task of somatic cell cloning process (Figure 43), which are currently performed with bulky laboratory equipments, micromanipulators and microscopes. In conventional way, an experienced operator is required to achieve complex steps of cell coupling. By using the advantages of state of the art microfluidic technology, here, a novel on-chip cell coupling system is reported. Figure 1 demonstrates the cell coupling and fusion sequence in the whole cell cloning protocol. For the best of our knowledge, there exists no successfully implemented microfluidic device for the somatic cell coupling.

For realizing the cell coupling on a chip, two kinds of cells, egg cell (bovine oocyte: 100~150μm) and donor cell (bovine fibroblast: 10~30μm) are cultured since they are suitable for this application. The coupling is to contact and fix cells (fibroblast and oocyte) before impressing the DC voltage for electrical fusion. This protocol has three main functions:

1. An oocyte, supplied into micro chip, is captured in a micro channel
2. A fibroblast is supplied into microfluidic chip and aligned with immobilized oocyte
3. The new oocyte and fibroblast are coupled via brief period of AC voltage (dielectrophoresis).

In order to couple an oocyte with a fibroblast, both cells must be moved to the same location (operation zone). The cell movements are controlled with vision-based on-chip manipulation techniques as dielectrophoresis (DEP) and fluid-flow which are scope of this dissertation. Flow speeds of different micro-channels are controlled by external pumps.

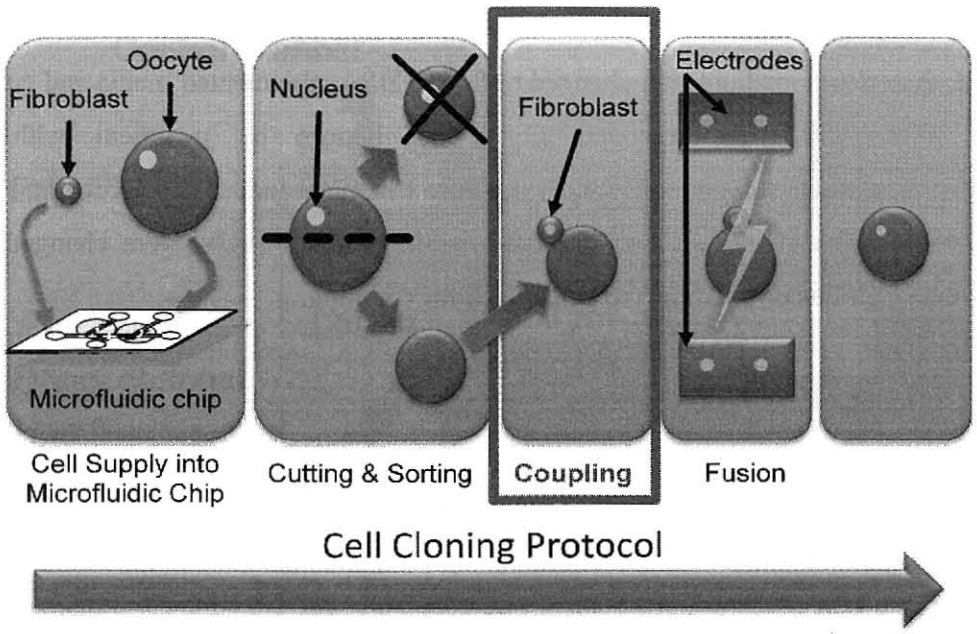

Figure 43, This protocol is suitable for the automation of nuclear transplantation process with microfluidic technology

4.1 Materials and Cell Coupling Method

Two kinds of cell (fibroblast and oocyte) were used for cell coupling process. Experiments were performed at the room temperature.

4.1.1 Cell Types and Treatment

Oocytes were harvested from bovine ovaries and cultured 22-24 hours in medium 199 (Gibco) with 10% Fetal Bovine Serum (FBS) in a 5% CO2 incubator. In order to detach cumulus cells around oocyte, oocytes were treated with an appropriate amount of hyaluronidase (Nacalai Tesque) according to a protocol. The zona pellucida of oocyte was removed by pronase (Wako Pure Chemical Industries) treatment. The oocyte after treatments is 100-150μm orbicular shape. In these experiments, other chemical treatment for cutting and nucleus detection and cutting procedures were omitted in order to simply the process. Fibroblasts (10-30μm) were isolated from female bovine ears. Fibroblasts were cultured in Dulbecco's Modified Eagle's Medium

supplemented with 10% FBS in 35mm dishes in a 5% CO2 incubator. When cells became confluent, the culture medium was changed to 0.5% FBS-supplemented media and cultured for 5 days. Fibroblasts were removed from dish bottom by treatment with trypsin-ethylenediaminetetraacetic acid (EDTA, Wako Pure Chemical Industries) according to Wako's protocol and harvested. Before coupling, the medium of both cells were changed to ZFM (Zimmerman Cell Fusion Medium) to be suitable for coupling.

4.1.2 Cell Coupling Module

The illustration of the microfluidic chip for cell coupling is shown in Figure 44. In order to couple an oocyte with a fibroblast, user has to capture the both cells and move them in a same location. However it is a difficult task to built mechanical structures into a micro channel. The designed microfluidic chip utilizes fluidic power and dielectric migration. Figure 45 demonstrates the workflow of on-chip cell coupling protocol. In this protocol, firstly, an oocyte is supplied from oocyte channel. By the flow from the control channel, the oocyte is led to narrow channel (operation zone) between both of electrodes. Liquid suction from handling channel fixes the oocyte at the narrow channel (Figure 45.a). After that, a fibroblast is supplied from donor channel. The fibroblast is led to narrow channel in the similar manner as the oocyte. Both flow from oocyte channel and control channel are controlled by external pumps, and the fibroblast slowly comes into contact with the immobilized oocyte (Figure 45.b). At the end, the oocyte is coupled with the fibroblast and then the fused cell is released (Figure 45.c).

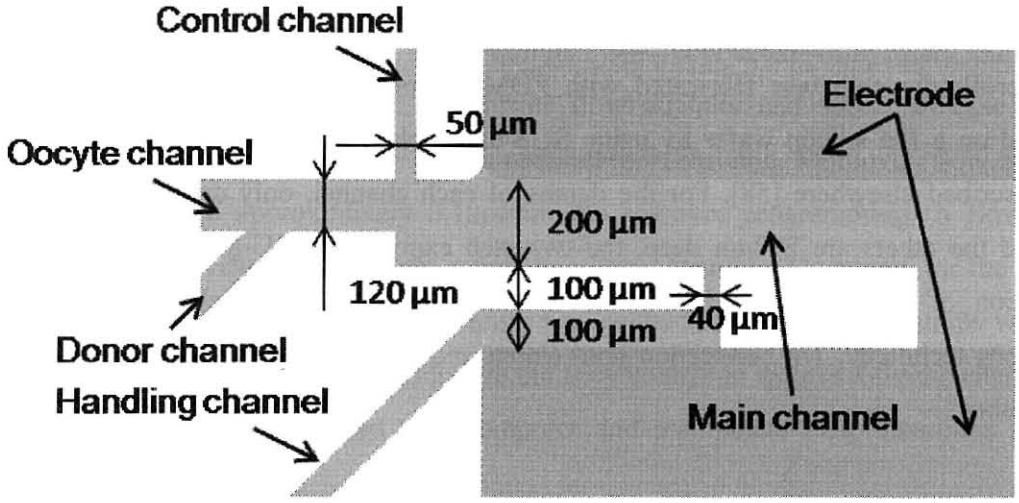

Figure 44, Schematic view of cell coupling system.

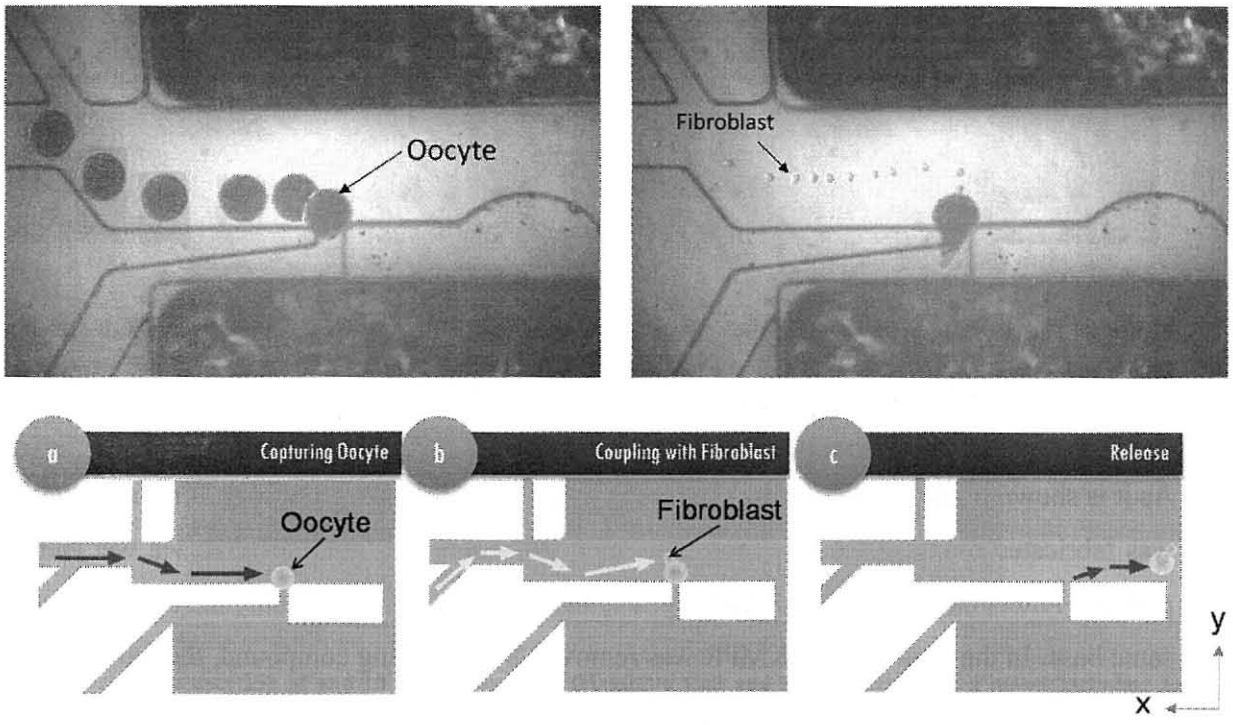

Figure 45, Workflow of cell coupling. (a) Capture oocyte. (b) Coupling with fibroblast. (c) Release.

4.1.3 Fabrication of the Microfluidic Chip

The microfluidic chip was fabricated with PDMS. First, the mold of the fluidic chip was patterned on a flat silicon wafer by using SU8-based photolithography technique, which has been described elsewhere [58]. For the depths of each channel, only donor channel is 50μm deep and the others are 200μm deep, the two step exposure of SU-8 was carried out. After preparation of the mold, the PDMS device was fabricated using classic multilayer soft lithography technique. The connection ports (inlets and outlets) were punched and connected to silicon tubes.

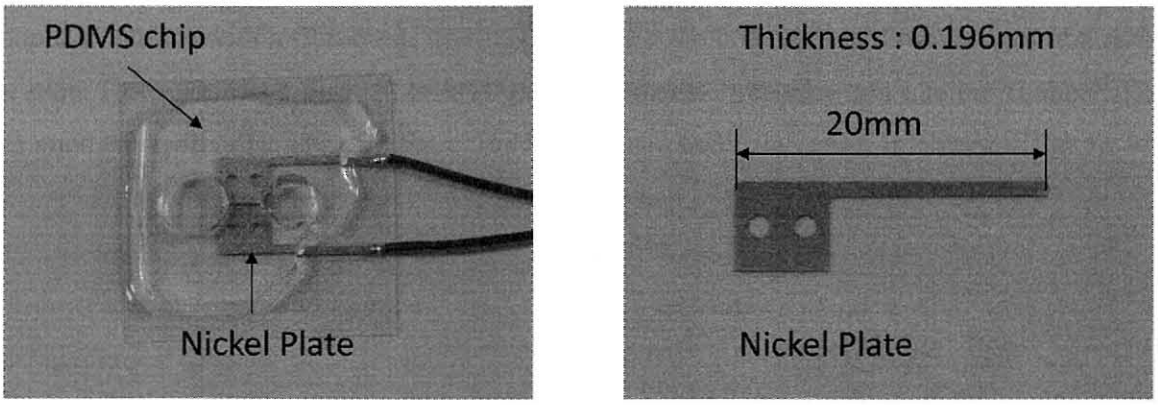

Figure 46, The electrodes were made by using Ni coating. The length of nickel plate is 20mm and thickness is 0.196mm. 200μm wide micro-channel is sandawiched by two nickel plate.

As it is shown in the Figure 46, the electrodes were made by using Ni coating. Cr-Au sputtering was fabricated onto a glass base, and patterning for wiring was manufactured via wet etching process. After that, the mold for coating was made by thick film photoresist (KMPR) on the same base. In the final step, as KMPR was removed by separating compound, the fabrication of electrodes was completed. The microfluidic chip was completed by placing the PDMS and electrodes on a glass cover-slip.

The inlet and outlet ports of the micro channels were connected with pumps through tubes. For oocyte channel and donor channel, each terminal was connected with rotary pump (high precision tubing pump ISMATech). It controls flow quantity and speed. In case of inner diameter (ID): 0.19mm, flow quantity can be reduced to 0.39μl/min. Moreover, flow quantity is able to be reduced to approximately 0.10μl/min by software programming. A flow control program was also developed to achieve more exact flow quantity. Moreover, for the handling channel and the control channel, each terminal was connected with syringe pumps which had good response and high resolution to improve the flow control in the microfluidic channel [63]. Syringe pumps are also connected to a computer and manipulate flow directions and flow speed.

Commercial syringe pump (KDS-2; KD Scientific Co.) was generally used in the experiments. This pump had highly-accurate flow control and the automatic cell cutting experiment succeeded; however, there was a 0.2 sec delay between each command. However, this syringe does not have a sufficient response and flow rate. Therefore, in the experiments, a home-made pump (Figure 47) was constructed to get high resolution and high-speed response [30].

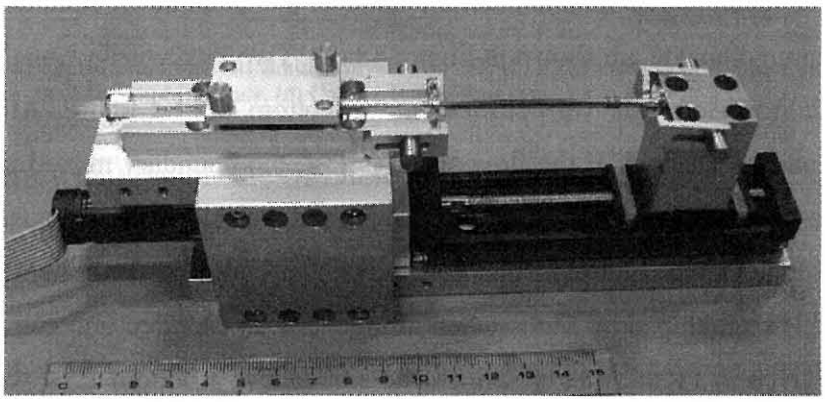

Figure 47, Pump uses 250 μl and 10 μl microsyringes (Hamilton Co.) and is integrated with a motor including an installed gearbox and encoder (Maxon Motor Co.).

A 10μl Hamilton microsyringe for aspiration was used. The inside diameter of the syringe is about 480μm. The pitch of the ball screw is 1mm, and the reducing ratio of the gearbox is

1/374. This means that the distance of one rotation of the motor is about 2μm, the quantity of water pushed from the syringe by one rotation is 0.35x10-3μl, and the flow rate of aspiration is 0.2μl/min. Therefore, if the motor could be controlled at less than 570rpm, it would be suitable for aspiration. The minimum rotation speed of this motor is about 0.1rpm, so it is sufficient for the purposes. Each pump was connected to a computer and can operate it through a PC. It also provided automation for future experiments.

4.2 Experimental Results

4.2.1 Fluid Analysis

For successful coupling process of an oocyte with a fibroblast, supplied cells have to be captured in the central narrow channel. Thus, we attempted to manipulate the movement of a cell by coordinating flow of the liquid in a microfluidic channel. In the microfluidic channel, flow from oocyte channel and control channel mainly affected the flow in main channel. Therefore, the change the basin width ratio for the flow quantity (or flow speed) ratio from two channels were inspected. The fluid simulation result of the basin in the state of no cell and the state of one captured oocyte are shown in Figure 48.a-b. Two kinds of flow made the boundary. The cell came from left side was pushed in the bottom of the figure. After that, it was transferred to narrow channel. If the flow speed is fast, the boundary moved to bottom of the picture (Figure 48.a-b). Besides, In case the flow speed was slow, the boundary between two flows was unstable. These indicated that cell movement could be controlled by change flow quantity ratio. The on-chip flow status when an oocyte was captured and comparison of flow rates are also given in Figure 48.c-d. Unlike the simulation, a bottom flow was strong in the experiment and some oocytes could be captured with this flow. The basin width (y/(x+y)) for the flow quantity ratio (b/(a+b)) was approximately linear. Therefore, In the light of linear ratio, the cell movement may be controlled without confliction with upper flow. However, in the state of oocyte captured, there is a boundary which is near where the oocyte is captured. Hence, an oocyte and a fibroblast may not be coupled even if a fibroblast is moved by the flow quantity

ratio. Since the flow is sensitive, even a little difference of pressure of channel's terminal area may cause failure because this field is very small. Thus, other force to assist the contact an oocyte with a fibroblast is required, that is dielectrophoresis force.

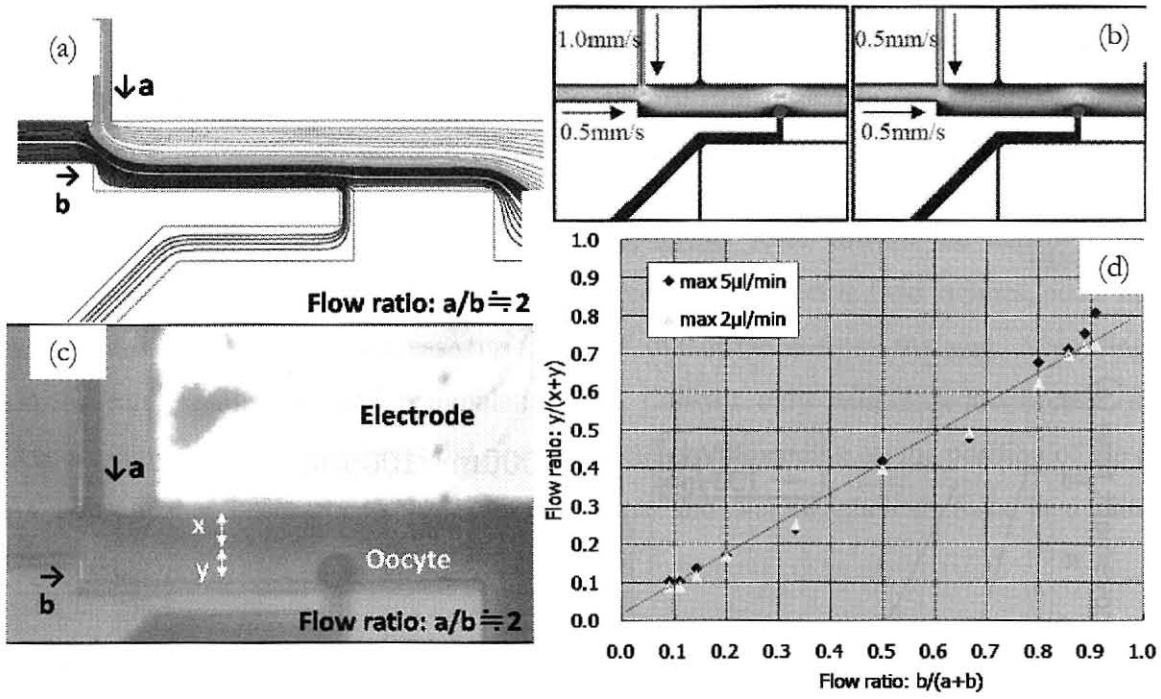

Figure 48, Fluid analysis. (a) Fluid analysis simulation with no cell. (b) FEM analysis of the flow velocity in the micro channel. (c) Real flow in oocyte captures state. (d) Comparison of flow rate

4.2.2 Frequency Characteristic of Dielectrophoresis

As illustrated in Figure 49, electric field is easily grown so that two electrodes sandwich main channel. The dielectrophoresis is the phenomenon that forces acts on by the difference between polarizability of solution and objects under heterogeneous interchange electric field. And, dielectrophoresis power (F_{DEF}) was expressed in an expression below,

$$\mathbf{F}_{DEP} = 2\pi\varepsilon_m a^3 \mathrm{Re}\left[\frac{\underline{\varepsilon}_p - \underline{\varepsilon}_m}{\underline{\varepsilon}_p + 2\underline{\varepsilon}_m}\right]\nabla|\mathbf{E}|^2$$

F_{DEF} is in proportion to clause $\nabla|E|^2$ of the electric field incline, and damps with distance. For the application of dielectrophoresis, we attempted optimization of the frequency by a method to measure oocyte movement time by the dielectrophoresis under the constant voltage (Figure 49). Oocytes did not move at the frequency less than 100kHz. It seems that this comes from that oocytes stuck to bottom surface. When frequency increased in a range of 100kHz - 5MHz, dielectrophoresis force increased too. In case of over 5MHZ, circuit impedance became the false setting and the electrode voltage increased. Because of the resonance phenomenon, the real applied voltage is uncertain. Therefore, 1-5MHz was selected for dielectrophoresis from these results.

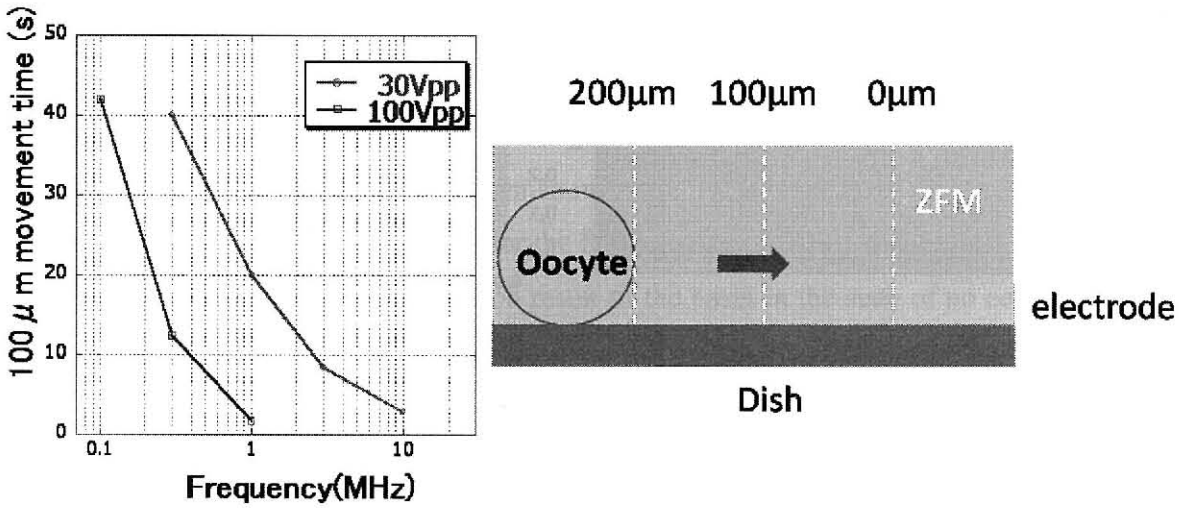

Figure 49, Frequency characteristic of dielectrophoresis

4.2.3 Electric Field Analysis

By demanding dielectrophoresis force acting on an oocyte and its terminal velocity in liquid from electric field analysis, the terminal velocity can be derived from Stokes' law,

$$V_s = \frac{2}{9}\frac{(\rho_p - \rho_f)}{\mu} g R^2$$

Figure 50 demonstrated the result in case of applied alternating voltage: $1V_{rms}$ ($2.8V_{pp}$), 1MHz. These results indicated that when the dielectrophoresis force toward the narrow channel occurred, an oocyte could be controlled and captured. But the electric field inclines, occur in the narrow channel, suddenly decrease in terms of the distance from the gap. According to experimental results, the cell manipulation was difficult only with dielectrophoresis force because enough power sometimes did not act efficiently, depending on the position of the cell. As a result, it is necessary to use both fluid force and dielectrophoresis force in a suitable condition for cell movement and manipulation.

Next, analyses of fibroblasts were proceeded on the similar manner. In this case, analyses were carried on as an oocyte was already captured in the narrow channel (Figure 51). It was seen the oocyte surface creating a heterogeneous electric field when alternating voltage was impressed in the state of oocyte captured. The strong part of the electric field intensity was distributed in a belt over the equator of the oocyte, and dielectrophoresis force worked as to attach fibroblasts on the oocyte neighborhood. These results indicated that the fibroblast which is approached to oocyte neighborhood by liquid flow is capable to couple with the oocyte surface when the voltage of frequency that produces equilateral dielectrophoresis force is impressed from the electrodes. In addition, heterogeneous electric field occurs on the narrow channel, and the oocyte strongly bound to the narrow channel.

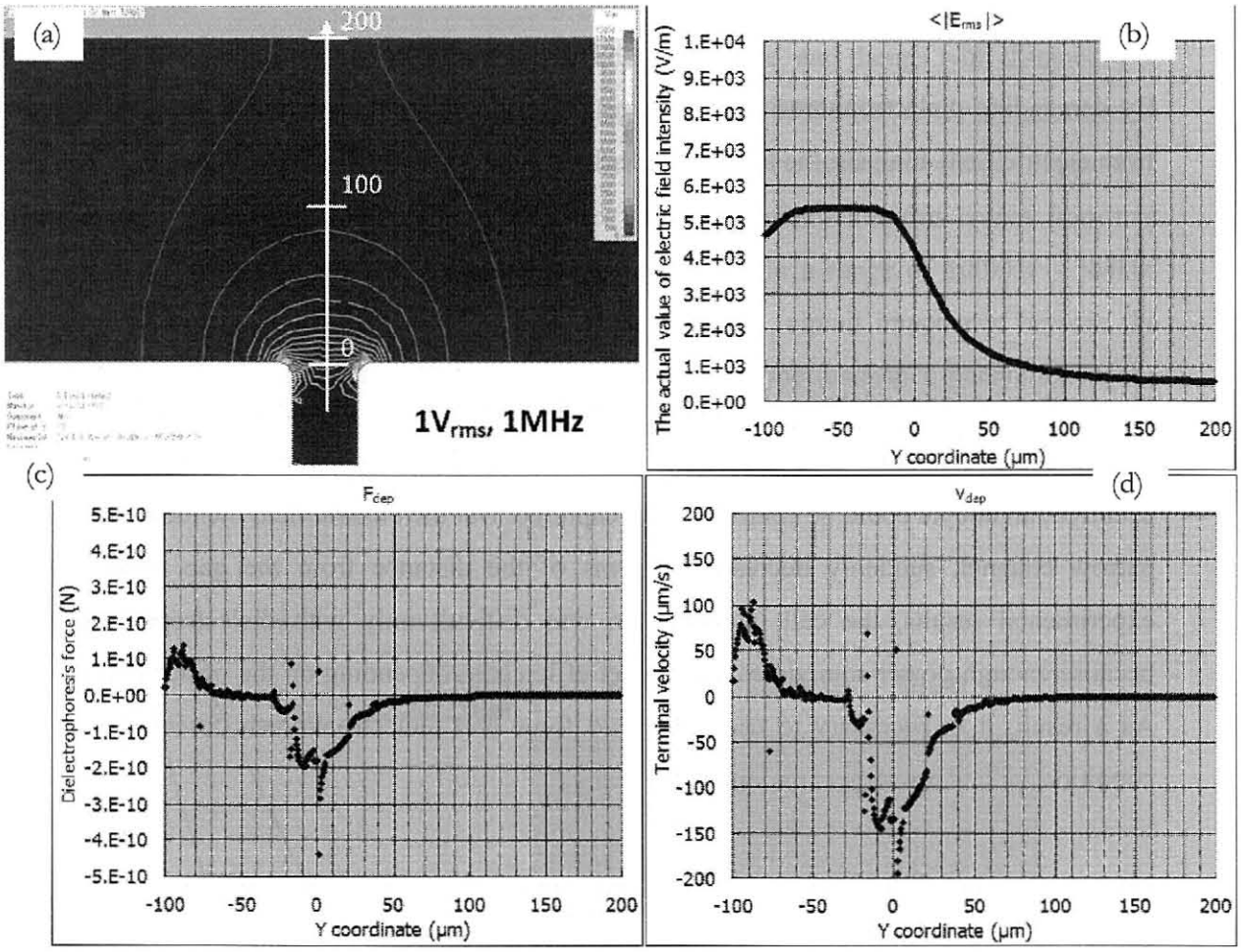

Figure 50, Electric field analysis and force to oocyte. (a) Electric field. (b) Electric field intensity. (c) Dielectrophoresis force. (d) Terminal velocity.

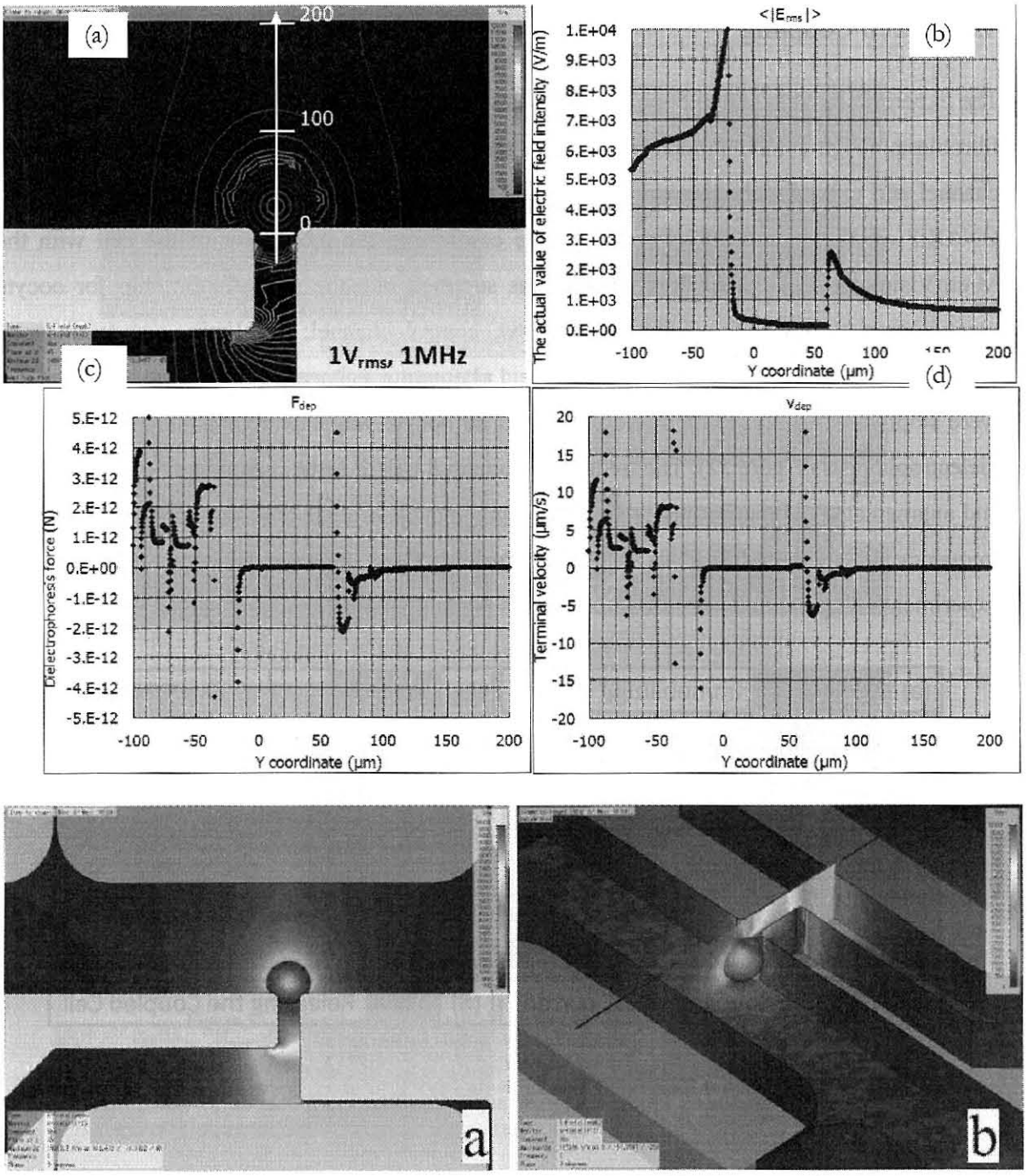

Figure 51, Electric field analysis and force to fibroblast. (a) Electric field. (b) Electric field intensity. (c) Dielectrophoresis force. (d) Terminal velocity. Colored figure of (a-b) Electric field of vertical direction.

4.2.4 Cell Coupling

The experiments of the coupling operation were performed by using bovine oocyte and bovine fibroblasts (Figure 53). Pumps were connected with oocyte, fibroblast, control, handling channel and exit of main channel. The system was operated with change pump direction and ON/OFF of the electric power supply while confirming the movement of the cell with the MicroVision camera. At first, an oocyte was supplied into the microfluidic chip for oocyte capture process. Each pump speed is follow, control channel; 0.4μl/min, oocyte channel; 0.1μl/min, exit of main channel; 0.5μl/min, and alternating voltage is $30V_{pp}$, 5MHz. All pumps were stopped when an oocyte came close, and an oocyte was captured in narrow channel by dielectrophoresis (Figure 52). The frequency domain for DEP force is from 100 kHz to 10 MHz and augmentation of the frequency leads to augmentation of dielectrophoresis force. While the frequency is less than 100 kHz, an oocyte does not move through the control channel. The experiments are performed at 3 MHz. Results is given in Table 7.

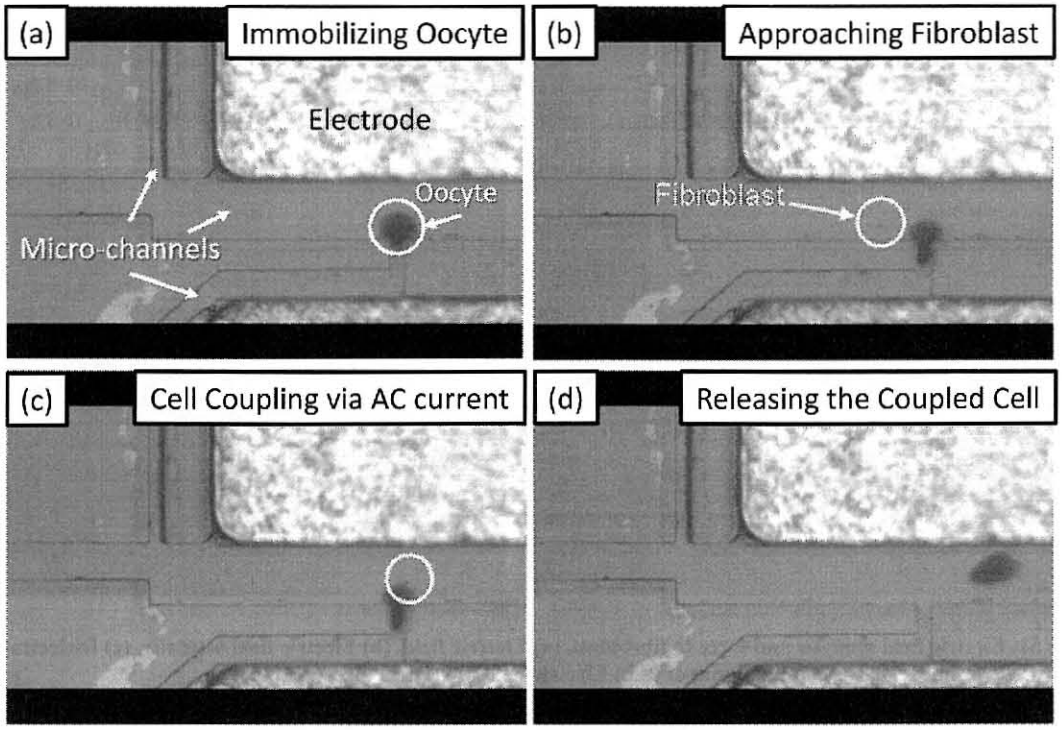

Figure 52, Each process of cell coupling. (a) Oocyte capture. (b) Guidance of fibroblast. (c) Coupling. (d) Release.

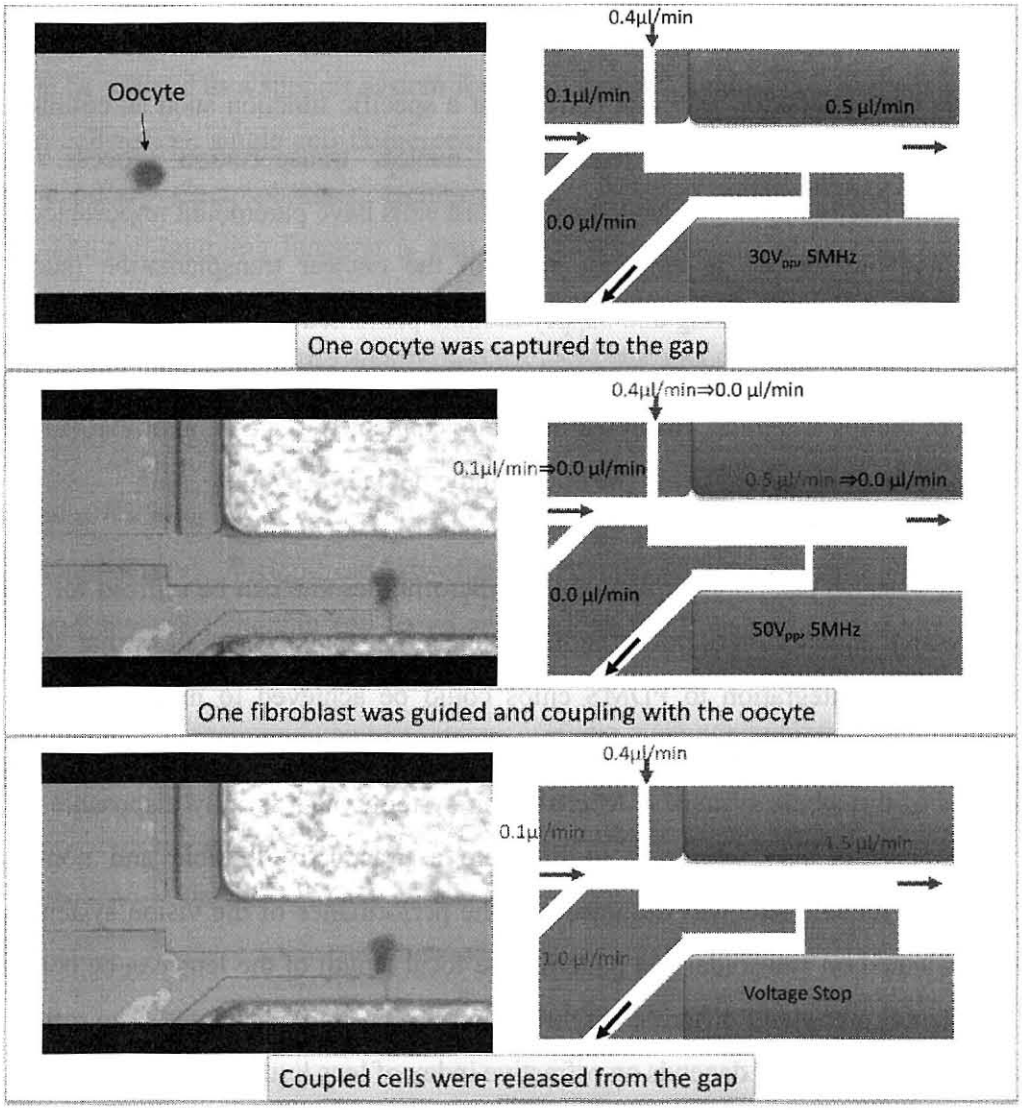

Figure 53, Channel speeds and voltage change for each phase of cell coupling

Table 7, Success Ratio of cell coupling. It shows that a fibroblast can be attached on an oocyte via DEP force.

	Num. of cells	Sensor Detection [%]	Cell Capturing [%]	Successful Coupling [%]
Oocyte	16	16/16 (100%)	15/16 (94%)	12/16 (75%)
Fibroblast	39	23/39 (59%)	-	

Chapter 5: Conclusion

Each module of the Desktop Bioplant carries out a specific function such as cutting, sorting, filtering, positioning, and fusing required in nuclear transportation process. Real-time observation and manipulation of oocyte or fibroblast cells have paramount importance for these operations, and are needed in essential steps of the nuclear transplantation (such as cell coupling). The single cell loading and supply module presented in this thesis allows individual cells to be aspirated from a container and transferred to other modules. The components, comprising of pumps and micro manipulators, were connected to a computer that automatically controlled all functions carried out in the microfluidic device.

MicroVision Systems can be incorporated into microfluidics and can be utilized for the instant and non-invasive observation of microfluidic channels. The experiments show that MicroVision systems and their integration to PDMS chips could be achieved to meet crucial practical considerations such as high resolution within a short distance while maintaining the compactness of the whole system. A MicroVision system which is fully disposable except the CCD sensor part is also fabricated to illustrate a practically feasible and non-expensive alternative. The tunable lens was designed and the performance of the vision system with this lens was evaluated on sinusoidal test pattern. The focal length of the lens can be controlled by using an external pump and different magnification levels can be achieved. The resolution can go down to 40lp/mm which depends on refractive index of lens liquid.

In this study, the potential applications of vision-based on-chip cell manipulation were also demonstrated, the automation of nuclear transplantation, by singly transporting oocyte and fibroblast cells and cell coupling. The pneumatic pressure valves were successfully applied onto the microfluidic chip. Experimental results showed that the synchronized MicroVision modules together with a computer vision algorithm can handle pumps, valves and micro-manipulators simultaneously. The information extracted from the data sets of the acquired images was used to manipulate the particles in micro-channels. Furthermore, the performance of the algorithm was

tested with different parameters, and its capability of detecting different cell sizes was demonstrated. The results also show that the "vision-based single cell loading and supply" system can be utilized as a support system for various on-chip single cell analysis systems such as on-chip cell fusion, single cell fluorescent microscopy, cell encapsulation with microfluidic droplets, capillary electrophoresis, techniques for chemical analysis, and on-chip micro-injection. The cell coupling function is also an important example of on-chip embryonic cell operation by using fluid-flow force and dielectrophoresis force. The simulations and experiments about fluid dynamics and the electric field analysis demonstrated the success of the on-chip cell coupling process.

In conclusion, "Vision-based On-chip Cell Manipulation" tasks were successfully realized on Lab-on-a-chip devices. Vision-based on-chip cell manipulation can realize mammalian cell coupling and any other on-chip cell-based applications via ""vision-based single cell loading and supply" system.

REFERENCES

[1] T. T. Vilkner, D. Janasek and A. Manz, "Micro total analysis systems. Recent developments", Anal. Chem., vol.76, no.12, pp. 3373-3386, 2004.

[2] A. Unger, H. P. Chou, T. Thorsen, A. Scherer and S. R. Quake, "Monolithic microfabricated valves and pumps by multilayer soft lithography", Science, Vol. 288. no. 5463, pp. 113 – 116, April 2000.

[3] E. W. H. Jager, O. Inganäs and I. Lundström, "Microrobots for micrometer-size objects in aqueous media: potential tools for single-cell manipulation", Science, Vol. 288. no. 5475, pp. 2335 – 2338, June 2000.

[4] *G.M. Walker, H.C. Zeringu and, D.J. Beebe*, "Microenvironment design considerations for cellular scale studies", Lab Chip, vol. 4, pp. 91-97, 2004.

[5] Ramesham, R.; Ghaffarian, R., "Challenges in interconnection and packaging of microelectromechanical systems (MEMS) Electronic," Components and Technology Conference 50th , pp. 666-675, (2000).

[6] YC Lee, BA Parviz, JA Chiou, S Chen, "Packaging for microelectromechanical and nanoelectromechanical systems," IEEE Trans. on Advanced Packaging, vol. 26, no. 3, pp 217-226, (2003).

[7] Y. Cui, Q. Wei, H. Park C. M. Lieber, "Nanowire nanosensors for highly sensitive and selective detection of biological and chemical species", Science 293, 1289-1292 (2001).

[8] M. A. Schwarz and P. C. Hauser, "Recent developments in detection methods for microfabricated analytical devices", Lab Chip 1, 1-6 (2001).

[9] F. Arai, D. Andou, T. Fukuda, Y. Noda, T. Ota: Micro Manipulation Based on Micro Physics -Strategy Based on Attractive Force Reduction and Stress Measurement-Proc. Int. Conf. on Intelligent Robotics and Systems(IROS), Vol. 2, pp. 236-241,1995.

[10] F. Arai, D. Andou, Y. Nonoda, T. Fukuda, H. Iwata, K. Itoigawa: Micro Endeffector with Micro Pyramids and Integrated Piezoresistive Force Seneor, Proc. Int. Conf. on Intelligent Robotics and Systems(IROS), Vol. 2, pp.842-849, 1996.

[11] Youlan Li, Colin Dalton, H. John Crabtree, Gregory Nilsson and Karan V. I. S. Kaler, "Continuous dielectrophoretic cell separation microfluidic device", Lab Chip, Vol: 7, pg: 239 - 248, 2007

[12] Song-Bin Huanga, Min-Hsien Wub and Gwo-Bin Leea, "A tunable micro filter modulated by pneumatic pressure for cell separation", Sensors and Actuators B: Chemical, vol. 142, no. 1, pg. 389-399, October 2009

[13] Abhay Vasudev, Ashish Jagtiani, Li Du and Jiang Zhe, "A low-voltage droplet microgripper for micro-object manipulation", vol.17, no 7, June 2009

[14] Andrea Adamo and Klavs F. "Microfluidic based single cell microinjection", Lab Chip, vol. 8, pp. 1258-1261, 2008.

[15] Sakuma, S., Onda, K., Yamanishi, Y., Arai, F., "On-chip detection and separation of micro-particles using magnetized microtools driven by focused magnetic field", ICRA '09. IEEE International Conference on Robotics and Automation, Kobe -Japan pg.1820 - 1825, May 2009

[16] Neuman KC, Nagy A., "Single-molecule force spectroscopy: optical tweezers, magnetic tweezers and atomic force microscopy" Nat Methods. 2008 Jun;5(6):pg.491-505.

[17] Mehmet Toner, Daniel Irimia, "Blood-on-a-chip", Annual Review of Biomedical Engineering, August 2005, Vol. 7, Pages 77-103.

[18] Umehara S, Wakamoto Y, Inoue I, Yasuda K, "On-chip single-cell microcultivation assay for monitoring environmental effects on isolated cells", Biochem Biophys Res Commun, Vol.305, pp. 534-540, 2003.

[19] Enger J, Goksör M, Ramser K, Hagberg P, Hanstorp D., "Optical tweezers applied to a microfluidic system", Lab Chip, vol.4, pp.196 - 200, 2004.

[20] R. A. Flynn, A. L. Birkbeck, M. Gross, M. Ozkan, B. Shao, M. M. Wang, and S. C, "VCSEL arrays as optical tweezers", Sens. Actuators Vol.87, pp. 239-243, 2002.

[21] A.L. Birkbeck, R.A. Flynn, M. Ozkan, D. Song, M. Gross, S.C. Esener, "Cells in microfluidic devices", Journal of Biomedical Microdevices, vol.5, no.1, pp.47-54, 2003.

[22] Manfried Dürr, Jörg Kentsch, Torsten Müller, Thomas Schnelle, Martin Stelzle, "Microdevices for manipulation and accumulation of micro- and nanoparticles by dielectrophoresis", Electrophoresis, vol.24, no.4, pp.722 - 731, 2003.

[23] Y. Huang, S. Joo, M. Duhon, M. Heller, B. Wallace, X. Xu, "Dielectrophoresis of charged colloidal suspensions", Anal. Chem., vol.74, pp.3362, 2002.

[24] J. Voldman, M.L. Gray, M. Toner, M.A. Schmidt, "A microfabrication-based dynamic array cytometer", Anal. Chem., vol. 74, pp.3984, 2002.

[25] C. Chou, M. Morgan, F. Zenhausern, C. Prinz, R. Austin, "Electrodeless Dielectrophoretic Trapping and Separation of Cells". microTAS, pp. 25–27, 2002.

[26] F. Arai, A. Ichikawa, M. Ogawa, T. Fukuda, K. Horio and K. Itoigawa, "High Speed Separation System of Randomly Suspended Single Living Cells by Laser Trap and Dielectrophoresis", Electrophoresis , vol.22, no. 2, pp. 283-288, 2001.

[27] J. J. Hawkes, R. W. Barber, D. R. Emerson, and W. T. Coakley, "Continuous cell washing and mixing driven by an ultrasound standing wave within a microfluidic channel," Lab-chip, vol. 4, pp. 446, 2004.

[28] O. Manneberg, B. Vanherberghen, B. Önfelt and M. Wiklund, "Flow-free transport of cells in microchannels by frequency-modulated ultrasound", Lab Chip, 2009, 9, pp. 833 – 837.

[29] J. Nilsson, M. Evander, B. Hammarström, T. Laurell , "Review of cell and particle trapping in microfluidic systems", Analytica Chimica Acta vol. 649, pg. 141–157, (2009)

[30] Akihiko Ichikawa, Tamio Tanikawa, Kazutsugu Matsukawa, Seiya Takahashi, Koutaro Ohba," Fluorescent Monitoring using Microlfuidic chip and Development of Syringe Pump for Automation of Enucleation to Automate Cloning", ICRA '09. IEEE International Conference on Robotics and Automation, Kobe –Japan, 2009

[31] G.T.A. Kovacs, Micromachined Transducers Sourcebook,McGraw-Hill, New York, 1998, Chapter 4, pp. 357–528.

[32] S. Devasenathipathy, J.G. Santiago, S.T. Wereley, C.D. Meinhart, K. Takehara, "Particle imaging techniques for microfabricated fluidic systems", Experiments in Fluids, 34 pp.504–514, (2003).

[33] Koschwanez, J., et al., "Identification of budding yeast using a fiber-optic imaging bundle.", Review of ScientificInstruments, 75(5): pp. 1363-1365, (2004).

[34] Webster JR, Burns MA, Burke DT, Mastrangelo, "Monolithic capillary electrophoresis device with integrated fluorescence detector", Anal Chem 73:1622–1626, (2001).

[35] Roulet JC, Volkel R, Herzig HP, Verpoorte E, de Rooij NF, Dandliker R, "Performance of an integrated microoptical system for fluorescence detection in microfluidic systems.", Anal Chem 74:3400–3407, (2002).

[36] Jeffrey R. Krogmeier, Ian Schaefera, George Sewardb, Gregory R. Yantza and Jonathan W. Larsona, "An integrated optics microfluidic device for detecting single DNA molecules", Lab Chip, (2007).

[37] Scho¨nholzer, F., D. Hahn, B. Zarda, and J. Zeyer. "Automated image analysis and in situ hybridization as tools to study bacterial populations in food resources, gut and cast of Lubricus terrestris", Journal of Microbiological Methods, vol. 48, no. 1, pp. 53-68, 2002.

[38] Elfwing, A., Y. LeMarc, J. Baranyi, and A. Ballagi., "Observing growth and division of large numbers of individual bacteria by image analysis.", Applied and Environmental Microbiology, vol. 70, no. 2, pp. 675-678, February 2004.

[39] Changqing Yia, Cheuk-Wing Lia, Shenglin Jia and Mengsu Yang,"Microfluidics technology for manipulation and analysis of biological cells." Analytica Chimica Acta, vol 560, issue 1-2, pp 1-23, February 2006.

[40] Alison M Skelley, Oktay Kirak, Heikyung Suh, Rudolf Jaenisch and Joel Voldman, "Microfluidic control of cell pairing and fusion", Nature Methods, vol. 6, pp. 147 – 152, January 2009.

[41] T. Arai, T. Tanikawa, F. Arai, M. Sato, H. Aso and S. Takahashi, "Automated Embryonic Cell Manipulation Using Micro Robotics Technology", International

Conference on Intelligent Robots and Systems, Workshop, IEEE IROS 2007, USA California, San Diego, October 2007.

[42] A. Meissner and R. Jaenisch, "Mammalian Nuclear Transfer", Developmental Dynamics, vol. 235, pp. 2460-2469, 2006.

[43] Briggs, R, King, T. J, "Transplantation of living nuclei from blastula cells into enucleated frogs' eggs", Proc. Natl. Acad. Sci. USA, vol.38, pp. 455-463, 1952.

[44] J. Gurdon, "The developmental capacity of nuclei taken from intestinal epithelium cells of feeding tadpoles", J. Embryol. Exp. Morphol. vol. 10, pp. 622-640, 1962.

[45] S. M. Willadsen, "Nuclear transplantation in sheep embryos", vol. 320, pp. 63-65, Nature 1986.

[46] R. S. Prather, F. L. Barnes, M. M. Sims, J. M. Robl, W. H. Eyestone, N. L. First, "Nuclear transplantation in the bovine embryo: assessment of donor nuclei and recipient oocyte", Biol. Reprod, vol. 37, pp. 859-866, 1987.

[47] R. S. Prather, M. M. Sims, N. L. First, "Nuclear transplantation in early pig embryos", Biol. Reprod, vol. 41, pp.414-418, 1989.

[48] I. Wilmut, A. E. Schnieke, J. McWhir, A. J. Kind, K. H. Campbell, "Viable offspring derived from fetal and adult mammalian cells", Nature, vol. 385, pp. 810-813, 1997.

[49] T. Wakayama, A. C. Perry, M. Zuccotti, K. R. Johnson, R. Yanagimachi, "Full-term development of mice from enucleated oocytes injected with cumulus cell nuclei", Nature, vol. 394, pp. 369-374, 1998.

[50] Y. Kato, T. Tani, Y. Sotomaru, K. Kurokawa, J. Kato, H. Doguchi, H. Yasue, Y. Tsunoda, "Eight calves cloned from somatic cells of a single adult", Science, vol. 282, pp. 2095-2098, 1998.

[51] I. A. Polejaeva, S. H. Chen, T. D. Vaught, R. L. Page, J. Mullins, S. Ball, Y. Dai, J. Boone, S. Walker, D. L. Ayares, A. Colman, K. H. Campbell, "Cloned pigs produced by nuclear transfer from adult somatic cells", Nature, vol. 407, pp. 86-90, 2000.

[52] [31] T. Arai, T. Tnikawa, F. Arai, O. Satoh, H Asouh, and S. Takahashi, "Automated Embryonic Cell Manipulation Using Micro Robotics Technology", International Conference on Intelligent Robots and Systems, Workshop, IEEE IROS 2007

[53] Jun Wang, Chang Lu, "Microfluidic cell fusion under continuous direct current voltage", APPLIED PHYSICS LETTERS 89, 234102, (2006).

[54] Anette Strömberg, Anders Karlsson, Frida Ryttsén, Maximilian Davidson, Daniel T. Chiu and Owe Orwar, "Microfluidic Device for Combinatorial Fusion of Liposomes and Cells", Anal. Chem., 73 (1), 126 -130, (2001).

[55] Warren J. SMITH's, "Modern optical engineering: the design of optical systems", McGraw-Hill , 3rd ed., ISBN 0071363602, (2000).

[56] Huseyin Uvet, Tatsuo Arai, Yasushi Mae, Tomohito Takubo and Masato Yamada, "Miniaturized Vision System for Microfluidic Devices ", Advanced Robotics, vol. 22, no. 11, pp. 1207-1223, 2008.

[57] Sidney F. Ray, "Applied Photographic Optics", Focal press, 3rd ed., pp. 163-165, 2002.

[58] Zhang J., Tan K. L., Gong H. Q., "Characterization of the poly-merization of SU-8 photoresist and its applications in micro-electro-mechanical systems (MEMS)", Polymer testing, Vol. 20, No6, pp.693–701, 2001.

[59] DowCorning, Product Information SYSGARD 186 (Silicone Elastomer). DownCorning: Midland, 2005.

[60] Piruska A, Nikcevic I, Lee SH ...., The autofluorescence of plastic materials and chips measured under laser irradiation, Lab Chip 2005, 5:1348-1354

[61] Rocky S. Tuan and Cecilia W. Lo, "Methods in Molecular Biology. Developmental Biology Protocols. Vol III" Humana Press, vol 137, pp. 422-423, 2000.

[62] Gunnar P. H. Dietz and Mathias Bähr, "Synthesis of Cell-Penetrating Peptides and Their Application in Neurobiology",Book: Methods in Molecular Biology, vol.399, pp. 181-186, February 2008.

[63] A. Ichikawa, T. Tanikawa, S. Akagi, K. Ohba, "Automatic cell cutting and nucleus detection", IEEE International Conference on Robotics and Biomimetics, submitted.

Appendix

1. Single Particle Suction

Controlling flow in microfluidic chip channel by external pump pressure is a convenient way due to its quick response of flow and invasive for living cells. Here, I discussed different techniques which helped me for reliable oocyte cell aspiration from a sample reservoir to tubing connected to PDMS chip without liquid leaking.

In order to find out the system capability and limitation for reliable oocyte cell suction, experiments were also performed with ~97μm beads,

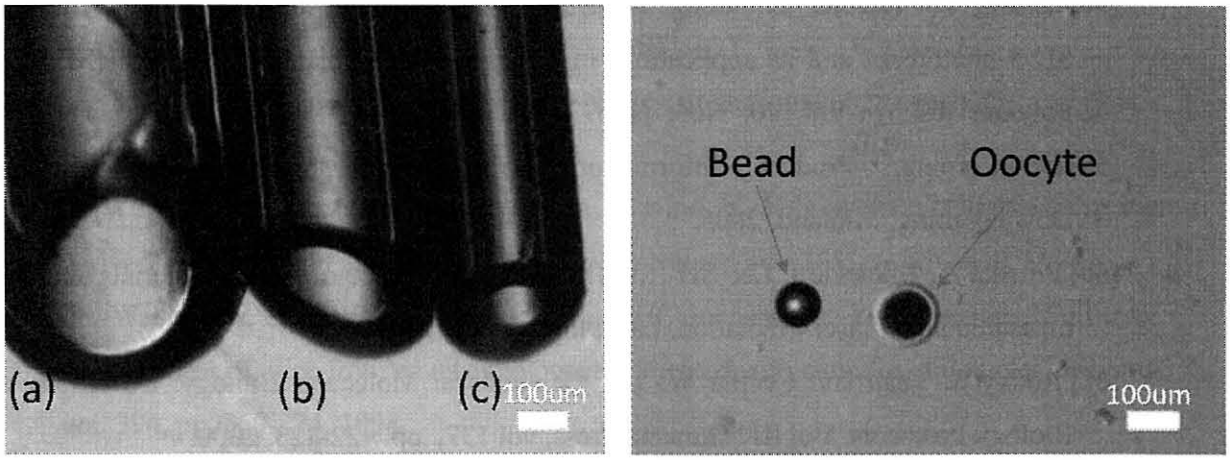

Figure 54, (Duke Scientific Corporation, research and test particles, catalog number: 7602A). Following results show the efficient tubing options for the single cell suction

I use different kinds of tubing options as φ300×500 μm, φ200×400 μm and φ100×300 μm (**Error! Reference source not found.**). The tubes connected both sample reservoir and PDMS inlet part. Connections require extra attention and must be done under the microscope. PDMS side of connection can be done as follows:

Tubing Preparation (Figure 55)

1. Cut a plastic pipette tip from its end about 1 cm length.

2. Hold the end of the tube and cut the top it with very fine razor. This provides smooth connection to PDMS.

3. Place tube into pipette tip and glue with any silicon glue. Tube must be leave approximately 2-3 mm out from the pipette end

PDMS Inlet Preparation (Figure 56)

1. Punch a small hole on PDMS with 45^0 angle.

2. Place 1mm inner diameter silicon tube into this hole

3. Fix with PDMS. To quick fix with PDMS, curing time is important. Because of that, a external heater can be used for this purpose for example soldering machine could be good option.

Insertion of tubing is quite easy. Once holding the end of tubing glued with pipette tip, it carefully insert through 1mm silicon tube under the microscope view. It must be noted that the fine connection of tubing and micro- channel is really important and should be confirmed under the microscope view. Any bad connection causes cell stuck on the intersection of micro-channel and tube, and experimental failure. After preparing tube and PDMS inlet, the tube is connected to the micro-channel as shown in

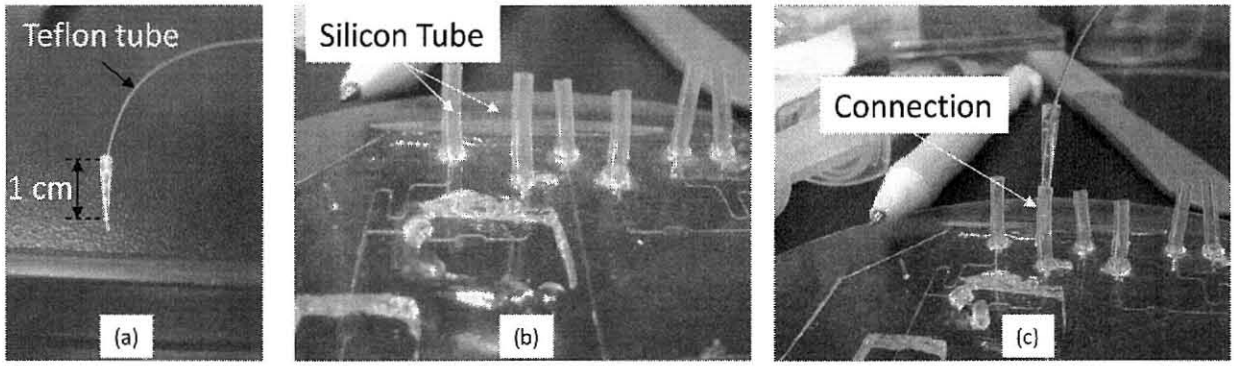

Figure 55

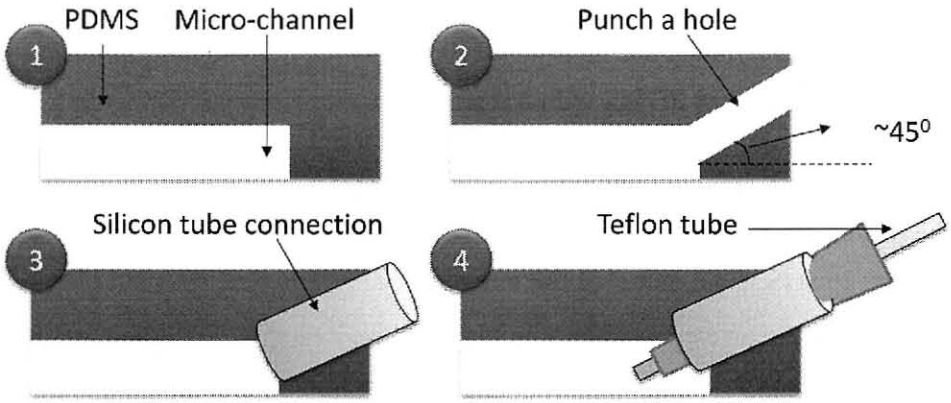

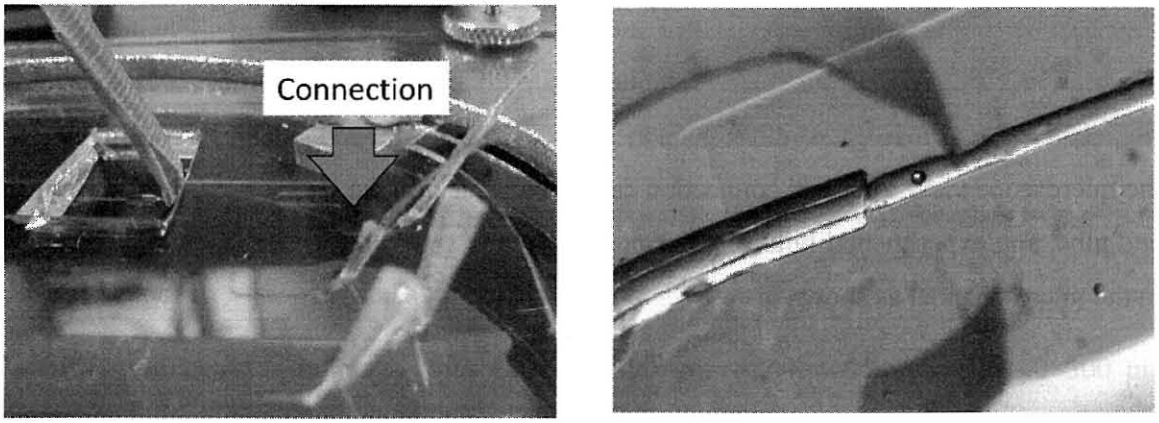

Figure 56

2. Detection Algorithms

2.1 Kalman Filter

In the coupling phase, oocyte (egg cell) and fibroblast (donor cell) must be aligned before DEP force. To recognize that cell coupling successfully achieved, both cells are needed to track while approaching each others. Because of the fact that the oocyte size 10 times bigger than the fibroblast cell and needs high depth of PDMS channel, the fibroblast cell can easily goes out of focus range and become blurry. Furthermore, the fibroblast cell is very transparent under the visible light. Once gliding into micro-channel, according to organelle distribution in cell cytoplasm, light dispersion over it might change. While high dense parts become darker, bright area converge to background color. Although its shape is near to circular, it is complicated to extract features from the background. Hence, in this project, the compact vision system accompanied by a combined algorithm includes particle filtering and active contour model, was implemented on such LOC devices. The final results will enhance automation of cell coupling of fibroblast and oocyte in order to complete fusing process successfully (See Figure 57 and Figure 58).

In this application, The program assumes that the oocyte does not move during experiments. To associate tracking with only one cell, a toleration box is added the algorithm. Once cell is detected, the system has to lock on the fibroblast cell until it reaches to the oocyte. Formerly, following to grab one frame, contour clusters were found as a consequence of background subtraction. Afterwards, active contour function is performed in order to acquire x and y coordinates of each contour clusters.

Advantage of active contour model is capture cell boundaries by its elastic curves. Inside of these boundaries, the program can easily locate object area and arc length as well. By giving upper and lower bound, the area information is able to be employed as a filter to surplus redundant objects, gliding in micro-channel, from the fibroblast cell. For each frame, correct cluster that refers to the locked fibroblast cell must be selected. However, to achieve accurate

selection, an only area based filtering is not enough so that Kalman filter were used to improve robustness. (See Figure 59). Kalman filter essentially predict position for posterior 3rd frame each time, once measurements were passed into the Kalman function. According to three estimations, the algorithm generates a toleration box as a matter of fact that where the fibroblast cell could be. Whenever each x and y was measured, it selects the best candidate and eliminates the others. Afterward, selected x and y values becomes new measurements of the locked fibroblast cell and again passes to Kalman filter function until it stick onto oocyte at the end.

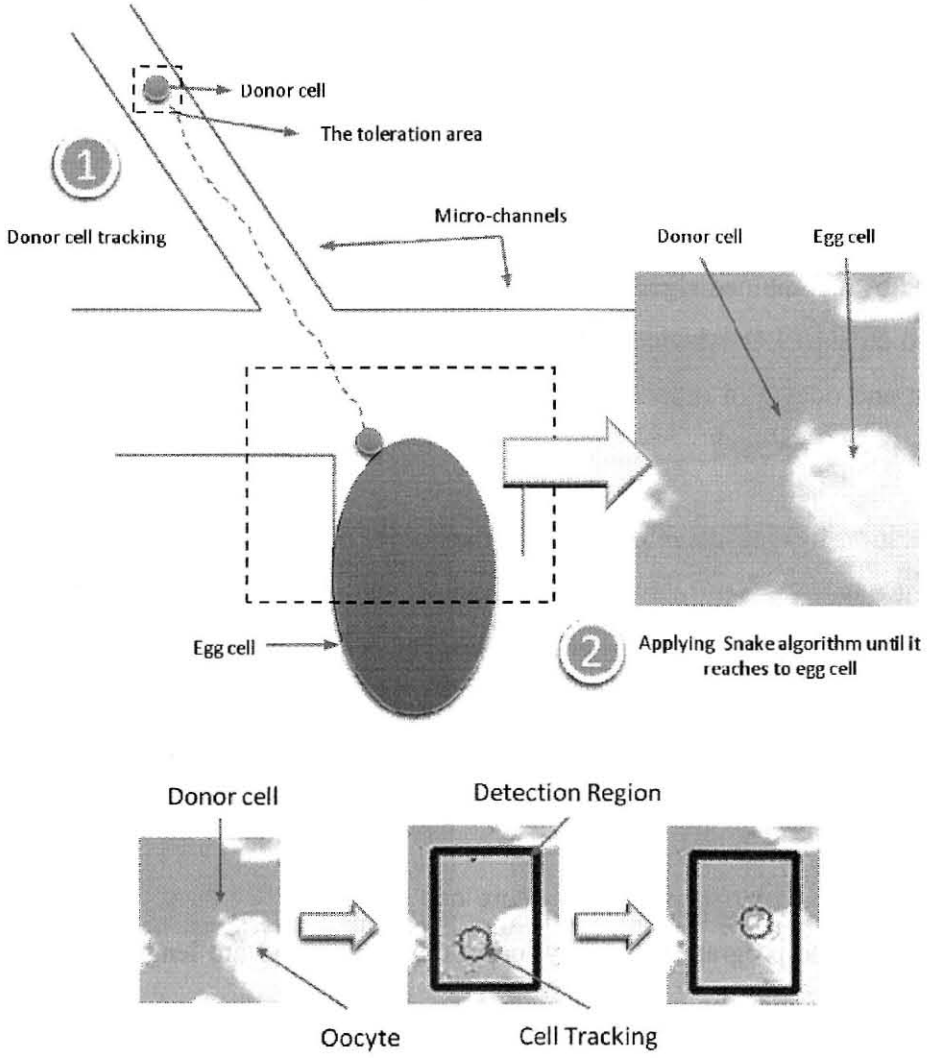

Figure 57

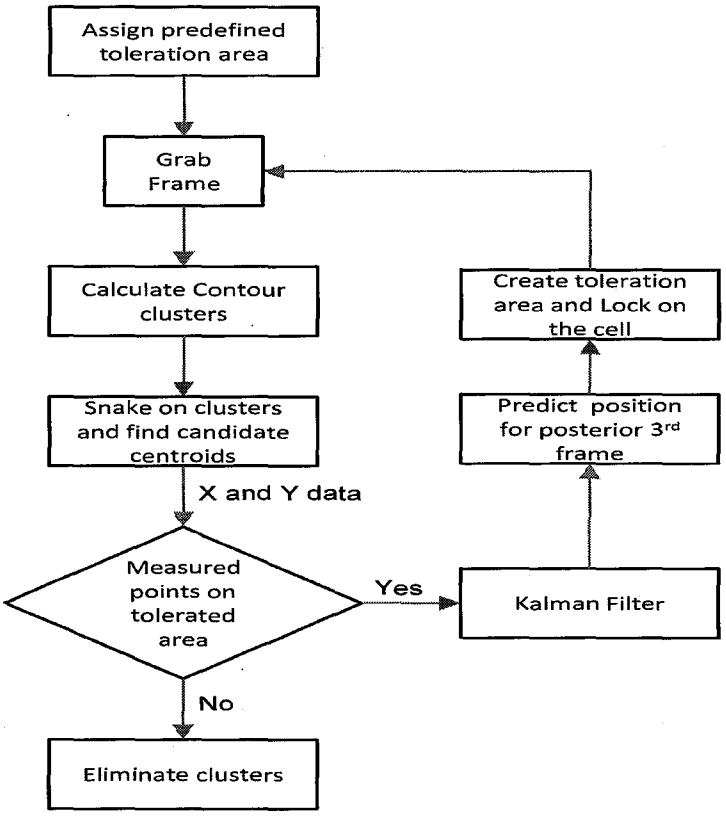

Figure 58

In the experiments, kalman filter was applied using OpenCV library which is an open source and available for a board range of platforms as Windows, Linux and Max OS. The kalman filter works in following sequence:

1. Prediction with (cvKalmanPredict)

2. Data Association with measurements

3. Correction Kalman prediction by using the measurements (cvKalmanCorrect)

At the each step, the kalman filter function was needed to associate with measurement from active contour function. Three measurements were evaluated. For each measurement, previous

prediction were picked to estimate posterior location in the next frame. After three predictions, the toleration area was formed and virtually drawn around tracked fibroblast cell. The experimental performance was shown in figure 8.

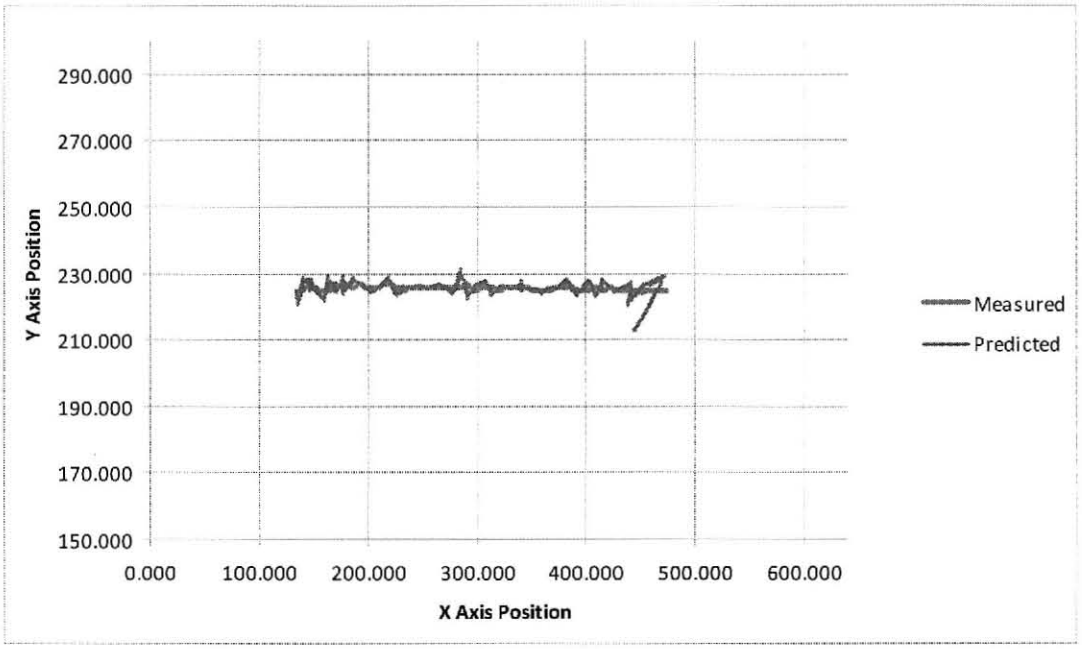

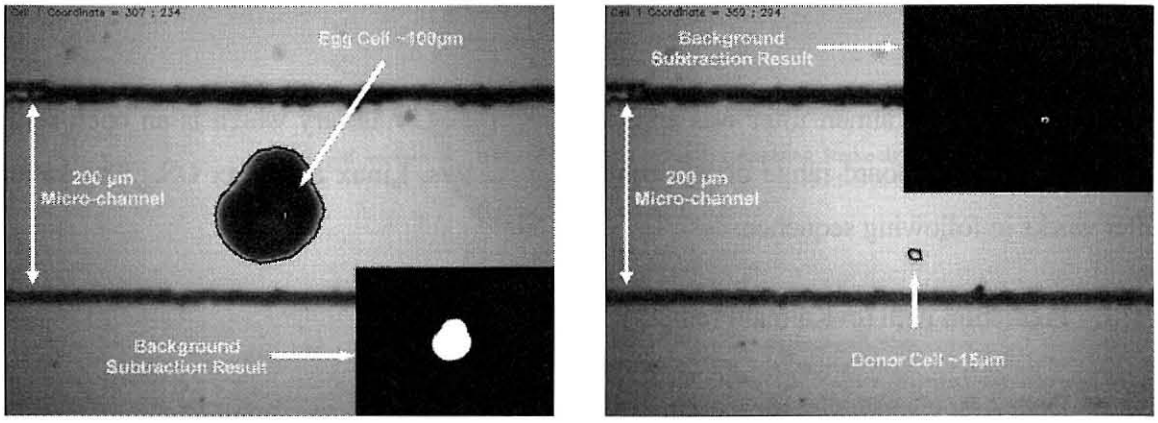

Figure 59

2.2 Multi Template Matching (MTM) and Support Vector Machine (SVM)

Template matching is one of the image comparison techniques. It is widely used to find the existence and location of a particle within a captured image. In this research, an efficient auto-detection of fibroblast cells using a multi-template matching and support vector machine techniques were combined. In many cases, the run time of template matching applications is dominated by repeating the similarity calculation, locating multi-templates, and exploring of the optimum result. In this approach, SVM algorithm was also added for the final decision Figure 60.

In the experiments, the particle detected by MTM sends to SVM function. Two templates find the best candidates according to its correlation value. The candidates are evaluated by pre trained SVM function. The experiments show that more training of SVM function provides better results. However, because of the slow speed of MTM function, this technique could not be used in the experiments. The proposed techniques results are given Figure 61.

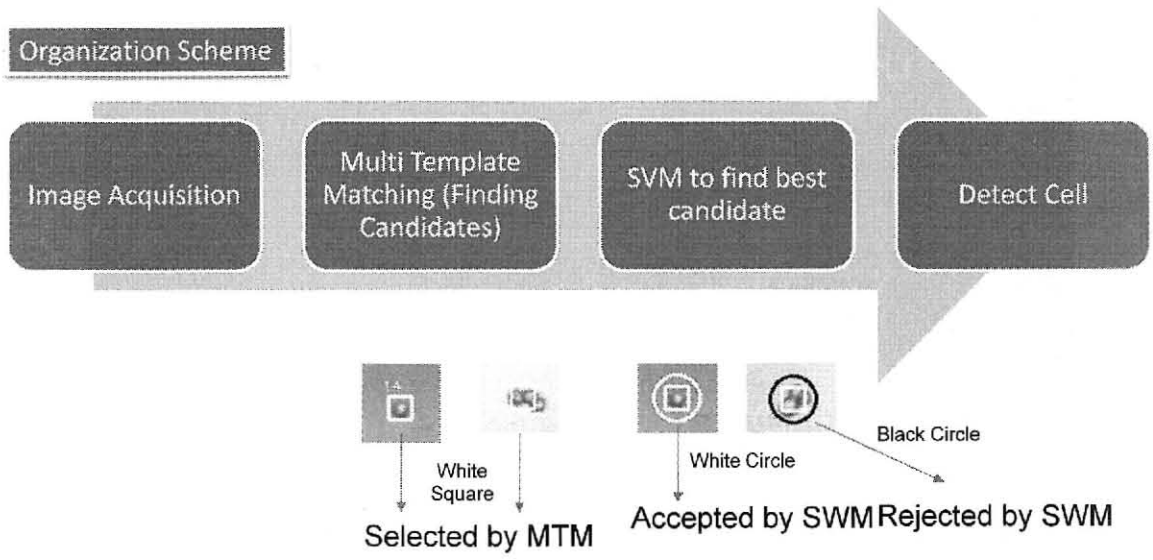

Figure 60

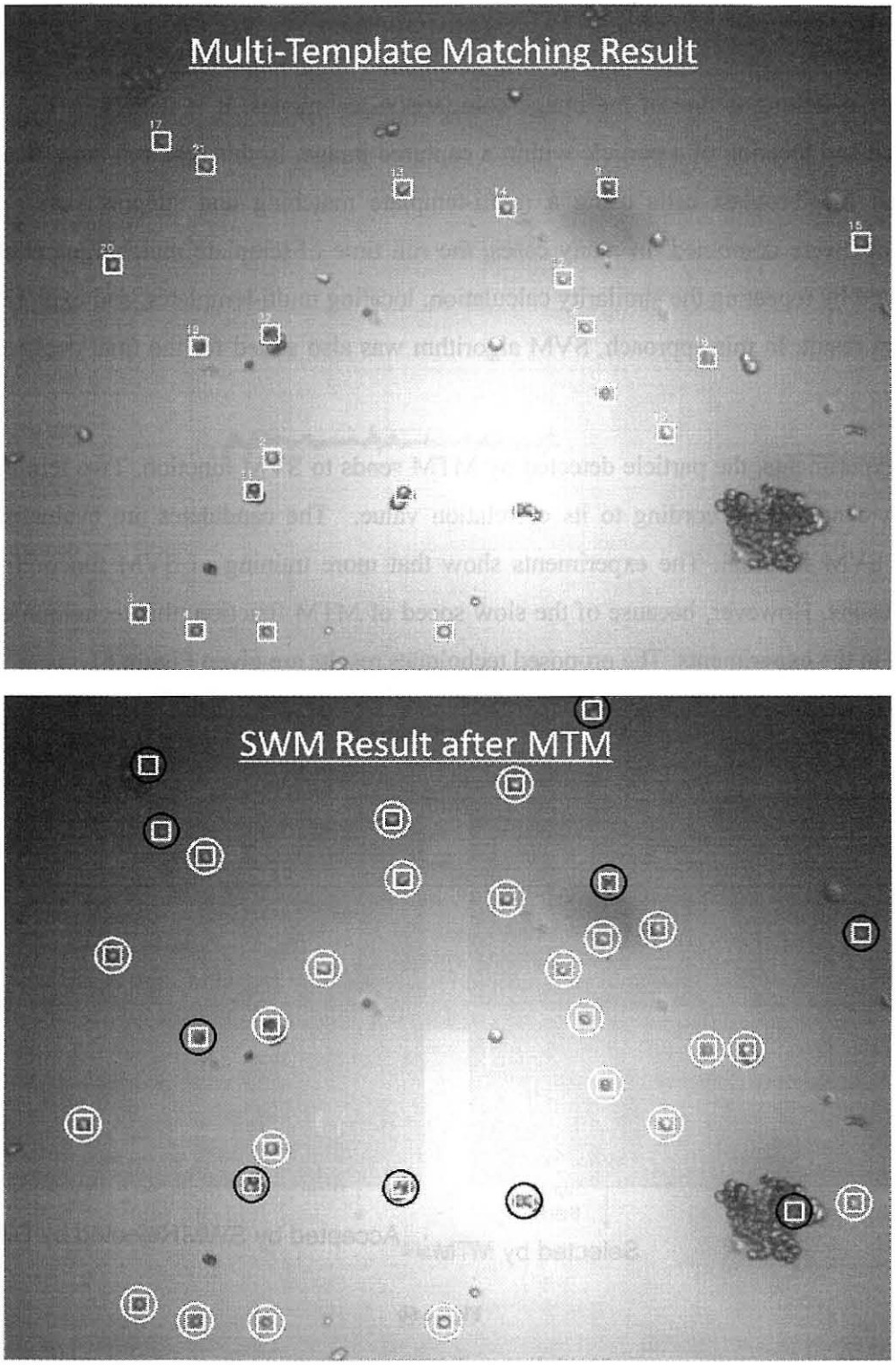

Figure 61

2.3 Background Subtraction Method with Dynamic ROI Approach

During experiments, the MTM+SVM or Lucas Kanade tacking and detection algorithms were failed due to some environmental difficulties caused by microfluidic chip structures. In micro level visual sensing under visible light, fibroblast cell color profile is very close to PDMS spots formed during fabrication of microfluidic chips. As shown in Figure 62, it is really hard distinguish those spots via sophisticated algorithm.

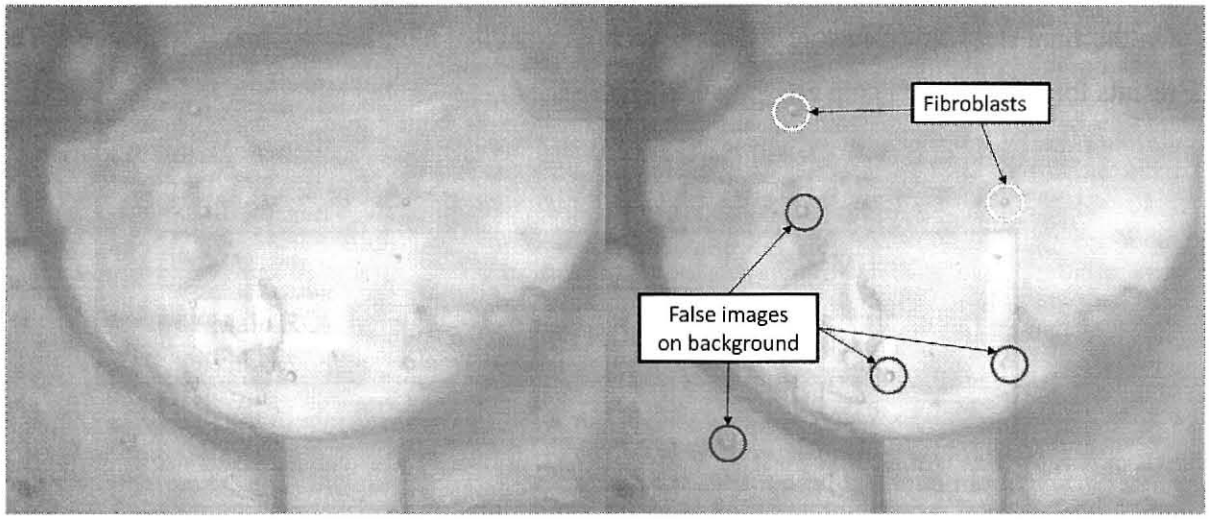

Figure 62

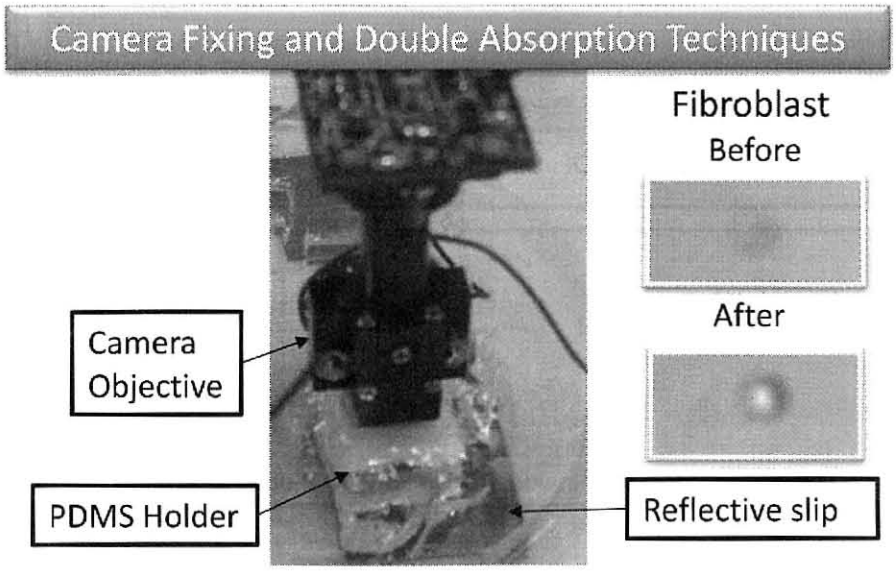

Figure 63

A simple approach was developed to overcome this problem. First of all the MicroVision camera was attached on a chip as it is shown in Figure 63. By this way, the back ground was fixed and any unwanted objects were cleared on the screen by background subtraction. After that, resolution was improved by introducing a reflective sheet right under the MicroVision camera. Double absorption technique increased the contrast of fibroblast and provided high detection rate.

On the final steps, the dynamic ROI approach was applied as it is illustrated in Figure 64. The results for cell coupling chip are shown in Figure 65.

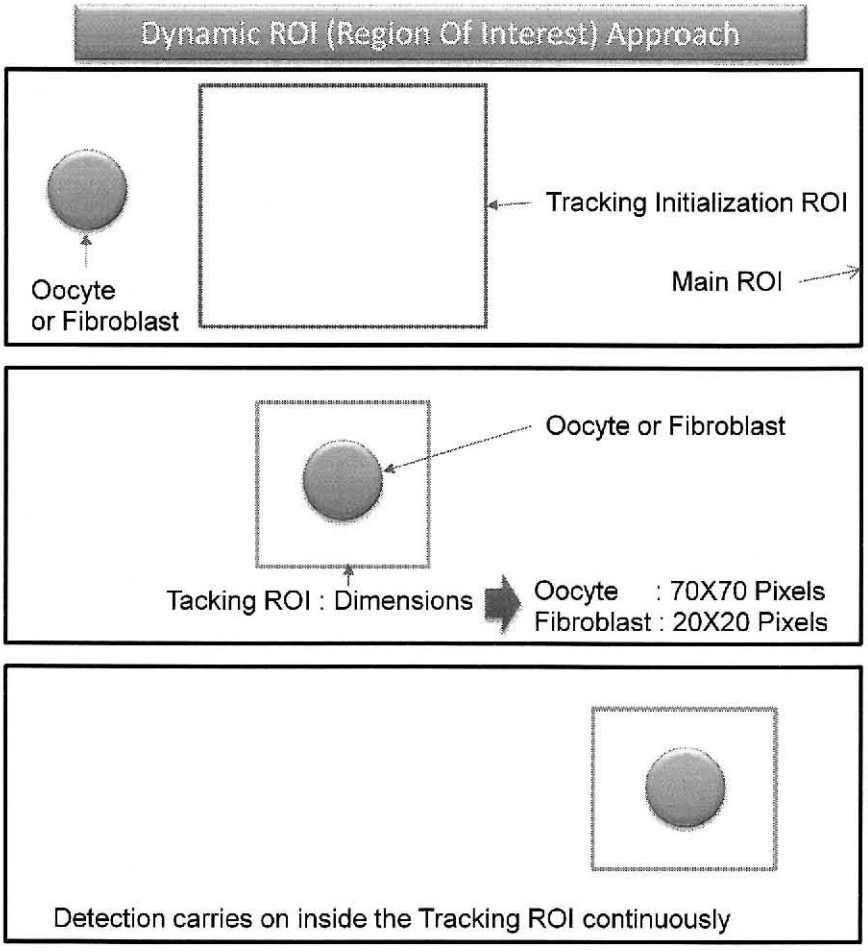

Figure 64

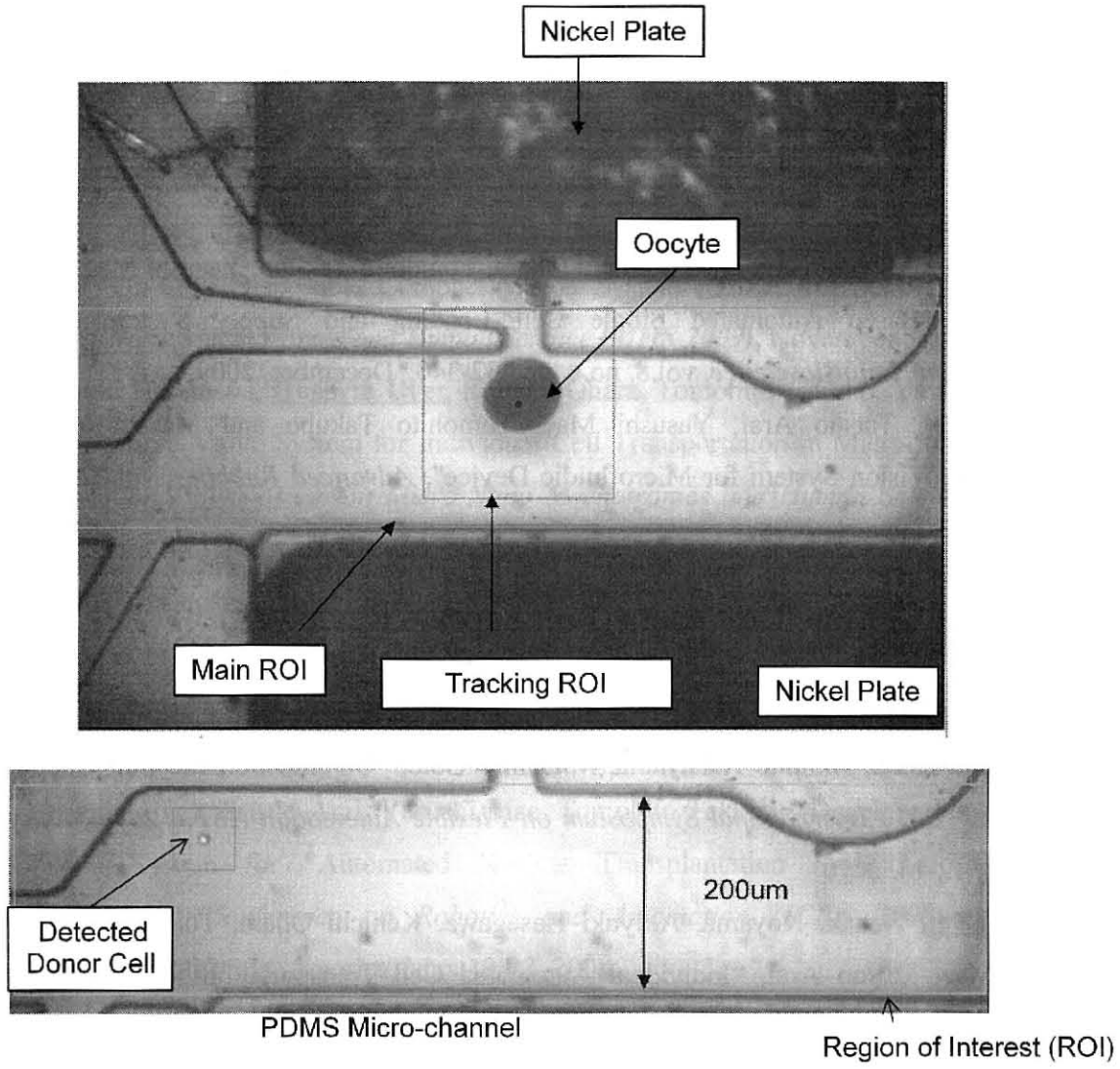
Nickel Plate
Oocyte
Main ROI
Tracking ROI
Nickel Plate
200um
Detected
Donor Cell
PDMS Micro-channel
Region of Interest (ROI)

Figure 65

LIST OF PUBLICATION

Journals

- **Huseyin Uvet**, Akiyuki Hasegawa, Kenichi Ohara, Tomohito Takubo, Yasushi Mae, Tatsuo Arai, "Vision-Based Automated Single Cell Loading and Supply System", ***IEEE Transaction on NanoBioscience***, vol.8, no.4, pp.332-340, December, 2009.
- **Huseyin Uvet**, Tatsuo Arai, Yasushi Mae, Tomohito Takubo and Masato Yamada, "Miniaturized Vision System for Microfluidic Device", ***Advanced Robotics***, vol.22, no.11, pp.1207-1222, January, 2008.

International Conference Papers (Full Paper – Reviewed)

- **Huseyin Uvet**, Akiyuki Hasegawa, Kenichi Ohara, Tomohito Takubo, Yasushi Mae, Tatsuo Arai, Osamu Satoh, Akihiko Nakayama, Mitsuhiro Goto, "On-chip Somatic Cell Coupling and Fusion", *2010 International Symposium on Flexible Automation* ***(ISFA 2010),*** Tokyo, Japan, July 12-14, 2010
- **Huseyin Uvet**, Naoaki Koyama, Akiyuki Hasegawa, Kenichi Ohara, Tomohito Takubo, Yasushi Mae, Tatsuo Arai, "Individual Automated Cell Transportation for Microfluidic Applications", *2010 International Symposium on Flexible Automation* ***(ISFA 2010),*** Tokyo, Japan, July 12-14, 2010.
- Akiyuki Hasegawa, **Huseyin Uvet**, Kenichi Ohara, Tomohito Takubo, Yasushi Mae, Tatsuo Arai, "Cell Coupling System for Somatic Cell Cloning Using Microfluidic Chip", *IEEE International Conference on Robotics and Biomimetics* ***(ROBIO 2009)***, December 19-23,2009.
- Akiyuki Hasegawa, **Huseyin Uvet**, Kenichi Ohara, Tomohito Takubo, Yasushi Mae, Tatsuo Arai, "Automatic Cell Transfer Module", *IEEE International Conference on Robotics and Biomimetics* ***(ROBIO 2009)***, December 19-23,2009.

- **Huseyin Uvet**, Akiyuki Hasegawa, Kenichi Ohara, Tomohito Takubo, Yasushi Mae, Tatsuo Arai, "Self-Controlled Cell Selection and Loading System for Microfluidic Systems",*The IEEE/RSJ International Conference on Intelligent Robots and Systems* ***(IROS 2009)***, St. Louis, MO, USA, October 11-15, 2009.
- **Huseyin Uvet**, Akiyuki Hasegawa, Kenichi Ohara, Tomohito Takubo, Yasushi Mae, Tatsuo Arai, "On-Chip Disposable Compact Vision System", *IEEE International Symposium on Micro-Nano Mechatronics and Human Science* ***(MHS 2009)***, November 8-11,2009.
- Akiyuki Hasegawa, **Huseyin Uvet**, Kenichi Ohara, Tomohito Takubo, Yasushi Mae, Tatsuo Arai, "Micro Valve System for Individual Cell Transportation in Microfluidic Chip", *IEEE International Symposium on Micro-Nano Mechatronics and Human Science* ***(MHS 2009)***, November 8-11,2009.
- Akiyuki Hasegawa, **Huseyin Uvet**, Kenichi Ohara, Tomohito Takubo, Yasushi Mae, and Tatsuo Arai, "Self-controlled Cell Supply System for Somatic Cloning Work in Microfluidic chip", *The 13th International Conference on Miniaturized Systems for Chemistry and Life Sciences* ***(microTAS 2009)***, November 1-5, 2009.
- **Huseyin Uvet**, Tatsuo Arai, Yasushi Mae, Tomohito Takubo: "Development of a Compact Vision System for "Automated Nuclear Transplantation Project", *2008 IEEE/RSJ International Conference on Robotics and Automation* ***(ICRA 2008)***, pp.3106-3111, Pasadena, California, America, May 19-23, 2008.
- **Huseyin Uvet**, Tatsuo Arai , Kenji Inoue, Tomohito Takubo, Sadaaki Kunimatsu, "Compact Vision System Design and Application on a PDMS Chip", *IEEE International Conference on Nano/Micro Engineered and Molecular Systems* ***(IEEE-NEMS 2007)***, pp.719-pp.724, January 16 - 19, 2007, Bangkok, Thailand.
- **Huseyin Uvet**, Tatsuo Arai, Kenji Inoue, Tomohito Takubo, Saadaki Kunimatsu, "Compact Vision System on a Chip Application", *17th IEEE International Symposium on Micro-NanoMehatronics and Human Science in 2006* ***(MHS 2006)***, Nov.11-Nov.14, 2006, Nagoya, Aichi, Japan.

Domestic Conference Papers

- **Huseyin Uvet**, Akiyuki Hasegawa, Kenichi Ohara, Tomohito Takubo, Yasushi Mae, Tatsuo Arai, "Automated Cell Supply Module Cell Detection and Control in a Micro-chip", *The Robotics and Mechatronics Conference* ***(ROBOMEC 2009)***, Fukuoka, Japan, May 24-26, 2009.
- **Huseyin Uvet**, Tatsuo Arai, Yasushi Mae, Tomohito Takubo "Cell Coupling Detection in a Capillary by Using Compact Vision System", *26th Annual Conference of the Robotics Society of Japan* ***(RSJ 2008)***, Kobe, Japan, September 9-11, 2008.
- **Huseyin Uvet**, Tatsuo Arai, Tomohito Takubo, Yasushi Mae, Masato Yamada, "Vision Based Sensing for Microfluidics Devices ", *25th Annual Conference of the Robotics Society of Japan* ***(RSJ 2007)***, Chiba, Japan, September 13-15, 2007
- **Huseyin Uvet**, Tatsuo Arai, Kenji Inoue, Tomohito Takubo, Saadaki Kunimatsu, "A Vision System for Cell Manipulation Process", *The Robotics and Mechatronics Conference* ***(ROBOMEC 2006)***, Tokyo, Japan, May, 2006.

Awarded Papers

Best Conference Paper Award ROBIO 2009 (IEEE International Conference on Robotics and Biomimetics) for the paper entitled *"Automatic Single Cell Transfer Module"*.